

Design of a minimally invasive surgical instrument set

*for an innovative Titanium Implantable
Vertebral Augmentation Device*

Master Thesis
Double Master's Degree
Integrated Product Design & Biomedical Engineering
Dennis Sarwin



Design of a minimally invasive surgical instrument set

for an innovative titanium implantable vertebral augmentation device

By

Dennis Sarwin

in partial fulfilment of the requirements for the degree of

Double Master of Science

in Integrated Product Design & Biomedical Engineering

at the Delft University of Technology,
to be defended publicly on Tuesday, July 6th, 2021, at 14:00.

Supervisors:	Dr. ir. J. F. M. Molenbroek	TU Delft, IDE
	Dr. Y. Song	TU Delft, IDE
	Dr. J. Zhou	TU Delft, 3mE
Thesis committee:	Dr. T. Horeman	TU Delft, 3mE
	ir. S. Aarts	Amber Implants



An electronic version of this thesis is available at <http://repository.tudelft.nl/>.

Table of contents

Abbreviations	10
Abstract	11
Preface	12
1. Introduction	14
1.1 Context	14
1.2 Medical relevance	15
1.3 Problem definition	15
1.4 Goal	17
1.5 Scope	17
1.5 Research questions	19
1.6 The Company	19
1.7 Design Process	19
2. Analysis	21
2.1. Theoretical Research	21
2.1.1 Spine anatomy	21
2.1.2 VCF cause, incidence, and consequences	23
2.1.3 VCF device competitors	24
2.1.4 Surgical instruments of VCF device competitors	29
2.2. Empirical Research	30
2.2.1 Interviews	30
2.2.2 Surgery analysis	31
2.2.3 List of requirements	33
3. Development of concepts	34
3.1 Development process introduction	34
3.2 Overview of concepts	35
3.2.1 TIVAD Inserter – Concept 1	35
3.2.2 TIVAD Inserter - Concept 2	36
3.2.3 TIVAD Inserter - Concept 3	37
3.2.4 TIVAD Expander	38
3.2.5 Handle concepts	39
3.3 Selection of best concept	40
3.3.1 Harris profile – TIVAD Inserter	40
3.3.2 Fulfills function	41
3.3.3 Locking feature	41
3.3.4 Visibility	41
3.3.5 Ergonomic handle	41
3.3.6 No interference	41
3.3.7 Mechanical performance	41
3.3.8 Connection speed	41
3.3.9 Connection success rate	42
3.3.10 Price	42

4. Experimental evaluation	43
4.1 Experimental tests	43
4.1.1 Performance test: insertion & expansion torque	43
4.1.2 Test setup	44
4.1.3 Specimen BMD	45
4.1.4 Stage 1 – TIVAD Insertion Torque Results (SBS)	46
4.1.5 Stage 2A – TIVAD Insertion Torque Results (CVB) & QIA Results	47
4.1.6 Stage 2B – TIVAD Expansion torque results (CVB)	51
4.1.7 Usability test results	52
4.1.7.1 Usability test results	53
4.2 Risk assessment	58
5. The embodiment	62
5.1 Material selection	62
5.1.1 TIVAD Inserter	63
5.1.2 TIVAD Expander	64
5.1.3 TIVAD Inserter & Expander handle	64
5.2 Manufacturing technique	66
5.2.1 TIVAD inserter & expander shaft	67
5.2.1.1 Manufacturing steps TIVAD inserter	67
5.2.1.2 Manufacturing steps TIVAD expander	68
5.2.2 TIVAD handle	69
5.2.2.1 Manufacturing steps TIVAD inserter & expander handle	69
5.3 Cost price	70
6. Final design	71
6.1 Description	71
6.2 Discussion	75
6.2.1 Stage 1, 2A & 2B	75
6.2.1.1 TIVAD insertion into CVB – stage 2A	75
6.2.1.2 TIVAD expansion screw failure – stage 2B	75
6.2.1.3 Test environment	75
6.2.1.4 TIVAD Expansion results	76
6.2.1.5 Quantitative Image Analysis	76
6.2.1.6 Additional features	76
6.3 Recommendations	77
6.4 Conclusion	79
References	81
Appendix 1 – Stakeholders	87
Appendix 2 – Design methods	88
Appendix 3 – Surgical instruments of existing VCF devices	90
3.1 Balloon Kyphoplasty (BKP) SIS (2nd generation)	90
3.2 Vertebral body stenting (VBS) SIS (3rd generation)	92
3.3 Spine Jack SIS (3rd generation)	93
Appendix 4 – Interviews	94
Appendix 5 – List of requirements TIVAD SI	95

Appendix 6 – FEM Analysis concepts	99
6.1 FEM analysis – TIVAD connection design	99
6.2 Methods	100
6.2.1 FEM Analysis settings	100
Appendix 7 – Concept generation process	102
Appendix 8 – Physical ergonomics end user	106
Appendix 9 – Experimental tests (Torque measurements & usability)	107
9.1 Methods	107
9.1.1 Experimental tests setup	107
CVB Fracture creation	110
9.1.2 Calibration Torque sensor	111
9.2 Materials	112
9.2.1 Essential surgical instruments	112
9.2.2 Non-essential surgical instruments (for stage 1)	112
9.2.3 Non-essential surgical instruments (for stage 2a & 2b)	112
9.2.4 Implants	112
9.2.5 Torque sensor	113
9.2.6 Samples/specimens	113
Appendix 10 – Experimental tests (Quantitative Image Analysis)	114
10.1 Methods	114
10.2 QIA Calibration	117
10.3 Materials	118
Appendix 11 – Risk assessment (general)	120
Appendix 12 – CES Edupack engineering solver plug-in	123
Appendix 13 – Cost price	125
Appendix 14 – Technical drawings	127
Appendix 15 – Surgical technique	129

Table of Figures

Figure 1 Vertebral Compression Fracture (AO, 2006).....	14
Figure 2 Car Jack Principle.....	16
Figure 3 TIVAD implant in closed (upper) and open (lower) position.....	16
Figure 4 Thesis scope overview.....	18
Figure 5 In-situ situation of implanted and expanded TIVAD implant.....	18
Figure 6 Post-TIVAD surgery situation. Lateral (left), AP (middle), transverse (right).....	19
Figure 7 Reader's guide of design phases, process, and applied design methods.....	20
Figure 8 Spine anatomy overview, spine regions (left), vertebral body shape per region (right) (Frost et al., 2019).....	21
Figure 9 microCT VB, transverse plane (left), lateral view (right) (Frost et al., 2019; Zhao et al., 2009).....	22
Figure 10 Relation between T-score and number of VCFs (Cranney et al., 2007).....	24
Figure 11 Pedicle screw system with external rod fixation.....	25
Figure 12 Vertebroplasty (1 st generation) (Jay & Ahn, 2013).....	25
Figure 13 Balloon kyphoplasty steps (Medical Advisory Secretariat, 2004).....	26
Figure 14 Vertebral Body Stenting procedure (DePuy Synthes, 2016).....	27
Figure 15 Spinejack procedure (Premat et al., 2018).....	28
Figure 16 Non-essential & essential TIVAD surgical instrument overview.....	30
Figure 17 C-arm during spine surgery.....	32
Figure 18 TIVAD Connection interface.....	35
Figure 19 TIVAD Inserter Concept 1.....	35
Figure 20 TIVAD Inserter Concept 2.....	36
Figure 21 TIVAD Inserter Concept 3.....	37
Figure 22 TIVAD Expander Concept.....	38
Figure 23 Transparent view TIVAD Expander Concept: 2-in-1 approach.....	39
Figure 24 TIVAD inserter handle (left), TIVAD expander handle (right).....	39
Figure 25 TIVAD (left), Pedicle screw (right).....	44
Figure 26 Torque sensor setup: laptop, signal amplifier & DAQ unit (left). TIVAD adapter, torque sensor & Handle concept (right).....	44
Figure 27 TIVAD Inserter during stage 2A experimental test.....	45
Figure 28 Insertional torque in SBS.....	46
Figure 29 Insertional Torque in CVB (thoracic region, cadaver 1).....	50
Figure 30 Insertional Torque in CVB (lumbar region, cadaver 1).....	50
Figure 31 Insertional Torque in CVB (lumbar, cadaver 6).....	51
Figure 32 Expansion Torque in CVB (cadaver 5: T7, T9; cadaver 6: L1).....	52
Figure 33 T-shaped handle (left) vs. straight handle (right).....	53
Figure 34 Handle dimensions tests with different hand size.....	54
Figure 35 TIVAD Inserter (Concept 3) during experimental test.....	55
Figure 36 TIVAD Inserter (Concept 3) & Expander (Concept 1, still with straight handle) in action.....	55
Figure 37 TIVAD expansion screw (left), inside TIVAD implant (right).....	56
Figure 38 Wrist position.....	57
Figure 39 TIVAD Inserter (front) & Expander (back) Exploded view.....	66
Figure 40 Turning machine (left), Broaching machine (middle), 3-axis CNC (right).....	67
Figure 41 TIVAD Inserter shaft.....	68
Figure 42 TIVAD Expander shaft.....	68
Figure 43 Final TIVAD Inserter & Expander design.....	72
Figure 44 TIVAD inserter and expander in use.....	73
Figure 45 TIVAD Inserter (left) & Expander (middle) in context (lumbar spine: L1-L5), patient in a prone position (lateral view), the dilator is not shown in this figure. TIVAD will stay behind in restored fractured VB (right).....	74
Figure 46 Experimental test with TIVAD Inserter and CVB in a horizontal position.....	75
Figure 47 Stakeholder overview.....	87
Figure 48 BKP SIS.....	90
Figure 49 VBS SIS.....	92
Figure 50 Spine Jack SIS.....	93
Figure 51 Preliminary FEM analysis results.....	99

Figure 52 Results preliminary FEM analysis	101
Figure 53 TIVAD Inserter connection interface sketches	102
Figure 54 TIVAD Expander connection interface	103
Figure 55 TIVAD Inserter & Expander features sketch	104
Figure 56 TIVAD Inserter & Expander handle idea sketches.....	105
Figure 57 DINED information on how much torque a human can apply with two hands.....	106
Figure 58 Hand measurement instruction.....	106
Figure 59 CVB fracture creation process	110
Figure 60 Torque sensor calibration graph	111
Figure 61 TIVAD Inserter (top), Expander (middle), 2-in-1 approach (bottom).....	112
Figure 62 TIVAD implant prototype.....	113
Figure 63 microCT machine (left), microCT settings (middle), microCT preview (right).....	114
Figure 64 scanIP threshold setup	115
Figure 65 scanIP mask creation.....	115
Figure 66 scanIP HA Phantom properties setup.....	116
Figure 67 Calibration graph phantom.....	117
Figure 68 Phantom calibration graphs.....	118
Figure 69 HA Phantom	118
Figure 70 CES Edupack Engineering plug-in, TIVAD inserter shaft	123
Figure 71 CES Edupack Engineering plug-in, TIVAD expander shaft.....	124
Figure 72 TIVAD Inserter technical drawing.....	127
Figure 73 TIVAD Expander technical drawing	128
Figure 74 TIVAD inserter & expander workflow	133

Table of Tables

Table 1 Overview of T-scores (Department of Health et al., 2018)	23
Table 2 TIVAD surgical procedure: non-essential (yellow) & essential (green)	29
Table 3 Harris profile (van Boeijen et al., 2014)	40
Table 4 VCF Device dimensions	43
Table 5 Insertion torque summary of PCF5 / 20 / 30 specimens.....	46
Table 6 Insertion torque table SBS vs. CVB.....	48
Table 7 QIA BMD Results & Insertional torque results Stage 2A.....	49
Table 8 TIVAD Expansion torque results.....	52
Table 9 Hand dimensions test subjects	54
Table 10 Risk analysis – Usability.....	61
Table 11 TIVAD Inserter & Expander shaft material overview	62
Table 12 TIVAD Inserter & Expander handle material overview	64
Table 13 Cost price overview – TIVAD inserter & expander	70
Table 14 List of Requirements	95
Table 15 TIVAD Surgical procedure steps.....	107
Table 16 Torque sensor calibration	111
Table 17 Sawbone SBS density properties.....	113
Table 18 HA Phantom properties	116
Table 19 BMD-Greyscale calibration table of CVB T10/T11/T12	117
Table 20 Datasheet Synthetic Bone Specimens.....	119
Table 21 Risk Analysis - General.....	120
Table 22 Risk Factor Overview	122
Table 23 Risk factor frequency	122
Table 24 Cost price calculation (estimation)	125

Abbreviations

Abbreviation	Meaning
BKP	Balloon Kyphoplasty
BMD	Bone Mineral Density
BME	Biomedical Engineering
CVB	Cadaveric Vertebral Body
EO	Ethylene Oxide
FDM	Fused Deposition Modeling
FEM	Finite Element Modeling
FS	Fluoroscopy
ID	Inner Diameter
IDE	Industrial Design Engineering
IPD	Integrated Product Design
LoR	List of Requirements
LoQ	List of Questions
MD	Medical Device
MIS	Minimally Invasive Surgery
Nm	Newton Meter
OD	Outer Diameter
PCF	Pound per Cubic Foot
PLA	Poly lactide
PMMA	Polymethyl Methacrylate
PMS	Post Market Surveillance
POM	Polyoxymethylene
PS	Pedicle Screw
QIA	Quantitative Image Analysis
ROI	Region of Interest
SBS	Synthetic Bone Specimen
SD	Standard Deviation
SIS	Surgical Instrument Set
TIVAD	Titanium Implantable Vertebral Augmentation Device
VB	Vertebral Body
VBS	Vertebral Body Stenting
VCF	Vertebral Compression Fracture
VP	Vertebroplasty
WHO	World Health Organization
3D	Three-Dimensional
3mE	Mechanical, Maritime and Materials Engineering

Abstract

Purpose

As a result of the worldwide aging population, Vertebral Compression Fractures (VCF) are commonly detected in osteoporotic patients; these can originate from traumatic events or occur spontaneously. The existing VCF devices and their corresponding surgical instruments have their limitations in terms of short- and long-term performance, efficiency, safety, and complications. Amber Implants has developed an innovative new Titanium Implantable Vertebral Augmentation Device (TIVAD) that overcomes the shortcomings of the available state-of-the-art VCF devices. However, the specific surgical instruments required for the insertion and deployment of the TIVAD are yet to be developed.

Methods

A knowledge-driven iterative design process that includes extensive theoretical and empirical research together with spine surgeons, concept development, and experimental verification phases has been executed.

Results

The outcomes of the experiments have shown that the final TIVAD inserter and expander met the predefined requirements regarding efficiency, mechanical properties, and usability. These results lead to a significant contribution to the overall TIVAD procedure.

Conclusions

To summarize, it can be stated that the essential surgical instruments, the TIVAD inserter, and expander, enable the surgeon to insert and deploy the TIVAD to relieve the patient from its pain sensation and to restore the adequate spine curve while reducing the number of surgical steps, the overall surgery time, and thus costs. Additionally, the risk of infection and pulmonary embolisms is decreased significantly due to the TIVAD's non-PMMA minimally invasive surgical procedure.

Preface

In front of you lies my double Master thesis report - the final part of my Double Master of Science in Integrated Product Design (IPD) of the faculty of Industrial Design Engineering (IDE) and Biomedical Engineering (BME) of the faculty of Mechanical, Maritime and Materials Engineering (3mE) at the Delft University of Technology. The thesis focuses on a medical topic in the specialization area of the Medisign and Biomaterials & Tissue Biomechanics. To accomplish the thesis, a collaboration with Amber Implants BV and the Orthopaedic department of the Utrecht University Medical Centre (UMC) Utrecht is granted by both faculties IDE and 3mE of the Delft University of Technology. The thesis describes the research I carried out to explore the possibilities of a new surgical instrument set for a newly developed titanium implantable vertebral augmentation device (TIVAD) to treat vertebral compression fractures (VCF). Dr. J. Zhou, Dr. ir. J. F. M. Molenbroek and Dr. Y. Song of the Delft University of Technology supervised this thesis project.

Throughout the project, I have learned to design with and for healthcare professionals. The topic of the devices and their corresponding surgical instruments to treat vertebral compression fractures (VCF) is around for many years, but there is no optimal solution yet, ultimately, to improve a patient's quality of life. I believe that this combination of a medical and design engineering perspective fits the final chapter of my curriculum at the TU Delft.

I want to express my gratitude to everyone involved in supporting me. Firstly, Johan Molenbroek and Wolf Song for their sincere support, pleasant positive and constructive feedback, and enthusiasm throughout the project. Jie Zhou, for his guidance during the project, for keeping me focused when needed, and for being open-minded from a non-design point of view with an emphasis on the scientific aspects of a master's degree thesis.

Also, I would like to express my gratitude to Banafsheh Sajadi for her always supportive feedback, letting me feel welcome at Amber Implants, and giving me the opportunity to visit Erchinger MedTechnology GmbH. My gratitude goes to Jos van Driel, from the Precision and Microsystems Department (3mE), for assisting me with the sensor & measuring software setup that enabled me to perform the experimental tests. I want to express my gratitude to Sanne Aarts, Rosanna Schipani, and Pim Pellikaan from Amber Implants for their valuable input throughout the project and support during the anatomy lab's cadaver tests UMC Utrecht.

My sincere gratitude goes to Dr. Wilco Peul (LUMC), Dr. Joost Rutges (Erasmus MC), Dr. Robert van der Wal (LUMC), and especially Dr. Paul van Urk (ACIBADEM IMC) for their valuable feedback as being the surgeons who perform the VCF surgeries on daily bases and providing me with their expertise.

Lastly, I would like to express my gratitude to my family and friends for supporting me in their own way during this final project and throughout my whole studies.

*D.C. Sarwin
Delft, June 2021*

1. Introduction

1.1 Context

In 2005, Approximately 1.4 million osteoporotic vertebral compression fractures (VCFs) were reported worldwide, and numbers are expected to rise, according to (Johnell & Kanis, 2006). Osteoporosis is characterized by a loss of mineral bone density and micro-architectural deterioration of bone tissue, which is inherent to decreased bone strength. Osteoporotic fractures can be caused by traumatic events or occur spontaneously. VCFs account for approximately half of all osteoporosis-related fractures and are among the most prevalent types of osteoporotic fractures (Rockville (MD): Office of the Surgeon General (US), 2004). The increasing number of VCFs is mainly related to the fact that osteoporosis is closely associated with age. The world population has been rapidly aging over the past decades, and that trend is continuing. In particular, postmenopausal women are susceptible to these osteoporotic fractures with an annual incidence rate almost twice that of men (Cooper et al., 2009).

When a patient suffers a VCF, one or more vertebral bodies (VBs) are compressed due to a load. As a result, the original height of the VB is reduced by at least 15-20% (Thaler et al., 2013) (Fig. 1), and the original curvature of the spine is altered, leading to pain sensation for the patient (Kunz, 1993). Short-term symptoms of VCFs include pain, incontinence, and numbness. These symptoms can result in severe long-term consequences in daily life, such as chronic pain, physical impairment, and limited activity. Consequently, these complications can lead to depression, isolation, and ultimately decreased quality of life (Ghofrani et al., 2010). Furthermore, a study by Kado et al. (2003) states that VCFs are directly correlated to an increased risk of mortality and morbidity.

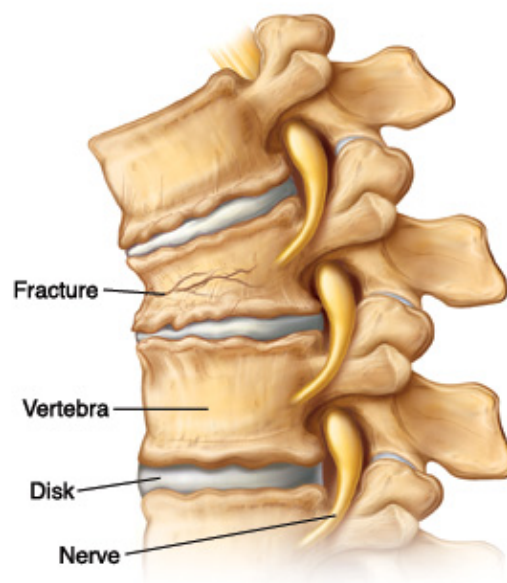


Figure 1 | Vertebral Compression Fracture (AO, 2006)

1.2 Medical relevance

The current state-of-the-art solutions to treat VCFs consist of 2nd and 3rd generation VCF devices, such as balloon kyphoplasty (BKP), vertebral body stenting (VBS), spinejack, and pedicle screw (PS) systems. However, these devices still have their deficiencies in terms of short- and long-term performance, efficiency, and especially risks and complications related to the leakage of Polymethylmethacrylate (PMMA) bone cement. PMMA is commonly used in these 2nd and 3rd generation VCF devices to fixate the fractured VB and the respective implanted device. The associated leakage still has a high incidence of 58.2%. Univariate analysis performed by Zhu et al. (2016) showed that four factors were significantly associated with PMMA bone cement leakage. These factors included the volume of the PMMA bone cement ($P < 0.001$), fracture severity ($P < 0.001$), surgical approach ($P < 0.001$), and gender ($P = 0.016$).

1.3 Problem definition

Based on the aforementioned analysis, Amber Implants has developed a new unique solution that can treat VCFs without PMMA bone cement. The newly designed solution called the Titanium Implantable Vertebral Augmentation Device (TIVAD) spine system will provide a massive advantage over the current state-of-the-art VCF devices. Fig. 3 shows the TIVAD in a closed and expanded configuration, the expansion screw (blue), and finally, the expansion mechanism anteriorly (most left part of the TIVAD implant).

The TIVAD spine system resembles, in principle, a car jack mechanism. The applied mechanism uses the properties of a screw thread to compress the device in one direction (Fig. 2, the distance between A & B) and thereby expanding the device in the other direction. In other words, the rotational motion (Fig. 2, Force T) from the screw is converted into a linear motion (Fig. 2, increase length of \mathbf{y}) that expands the TIVAD implant to restore the uncompressed vertebral body (VB) height.

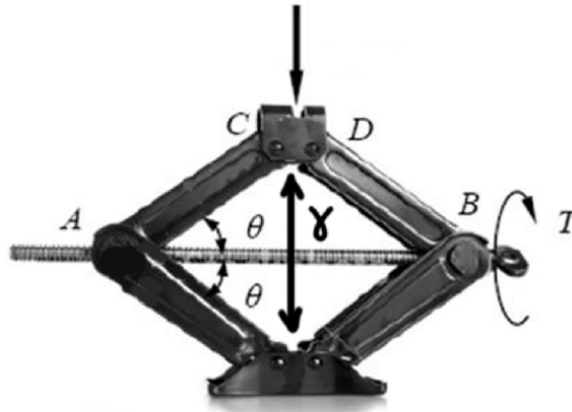


Figure 2 | Car Jack Principle



Figure 3 | TIVAD implant in closed (upper) and open (lower) position

The TIVAD spine system is based on a more natural approach to treat VCFs because it mainly focuses on restoring the anterior VB height as this region is mostly compressed in the case of a VCF. The design has been optimized for excellent mechanical properties, maximum height restoration, optimal Osseo-inductivity, and its wedge-shaped opening for better angle correction. Additionally, it features pedicle anchorage for better fixation and optional posterior fixation to inferior or superior VB levels using rods (Fig. 6).

Moreover, omitting the PMMA bone cement from the TIVAD spine system results in various additional benefits. Such as a reduction in surgical steps, fewer inconvenient surgical instruments, a shorter overall surgery duration which decreases the risk of infection and ultimately reduced costs. According to a study by Cheng et al. (2017), the risk of infection increases by 17% for every additional 30 minutes of surgery time. Along with these benefits, the new TIVAD spine system will provide an immense added value for the patient, the surgeon, and the hospital.

1.4 Goal

Finally, Amber Implants' new solution called the TIVAD spine system includes the TIVAD itself and its corresponding surgical instruments to support the surgeon during the surgery. So far, the development phase of the TIVAD has been finalized.

However, the corresponding surgical instruments required for TIVAD are not available yet. The goal of the thesis is, therefore, to develop, evaluate and verify a set of tailor-made surgical instruments (SI), with an emphasis on the surgical instruments that enable the insertion and deployment of the TIVAD Spine system. The title of the thesis is:

The design of a new surgical instrument set that enables the surgeon to successfully perform the TIVAD surgical procedure and relieve the patient from its complaints.

Appendix 1 displays the framework in which research (TU Delft), industry (Amber Implants,) and the hospital are shown in the development of a medical device such as the new unique TIVAD spine system.

1.5 Scope

The scope of the thesis is, as mentioned above, to develop a well-suited set of surgical instruments which the surgeon can use to introduce the TIVAD into the region in which the VCF has occurred, to restore the VB height and spine curvature.

The region in which the newly designed TIVAD SIS is used is clarified in Fig. 4., from left to right: the entire spine is shown with its five sections: cervical, thoracic, lumbar, sacrum, and coccyx. A focused region is placed on T11-L2 (highlighted in the circle), as the majority of VCFs occur in this region (Thaler et al., 2013). To the right of it, the TIVAD is shown for which the new surgical instruments are required.

Fig. 5 and Fig. 6 depict the location where the TIVAD will be inserted into the corresponding fractured VB. Fig. 5 shows the presence of the expanded TIVAD in its expanded state in a single VB, whereas Fig. 6 demonstrates the posterior fixation with various VB levels. The number of levels and the addition of posterior VB fixation via rods (using the blue (Fig. 5) and yellow (Fig. 6) tulip-shaped parts) depends on the number of fractured VB levels and the severity of the VCF, meaning that multi-VB level fixation with rods is not always required and is up to the surgeon's preference.

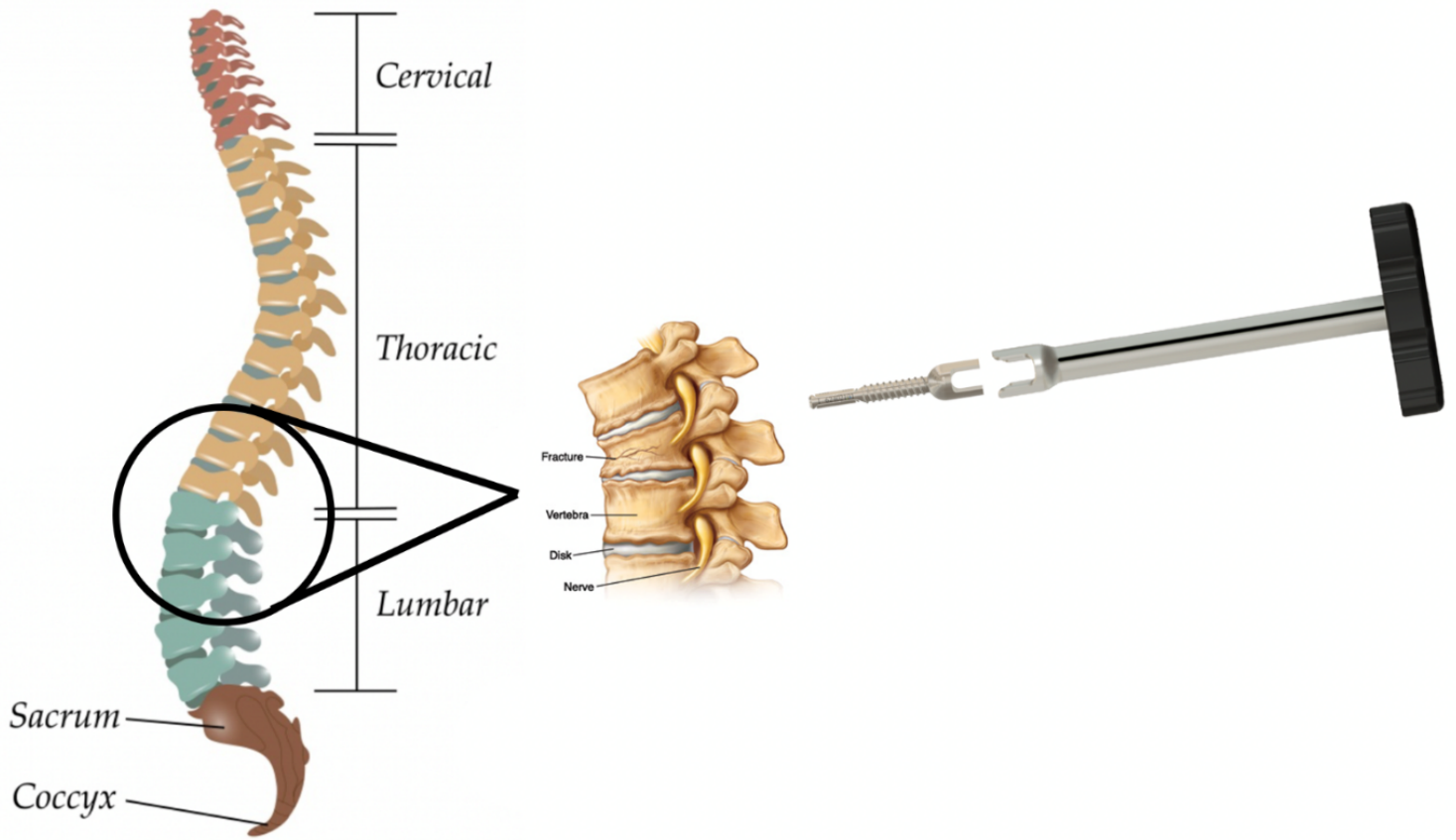


Figure 4 | Thesis scope overview



Figure 5 | In-situ situation of implanted and expanded TIVAD implant

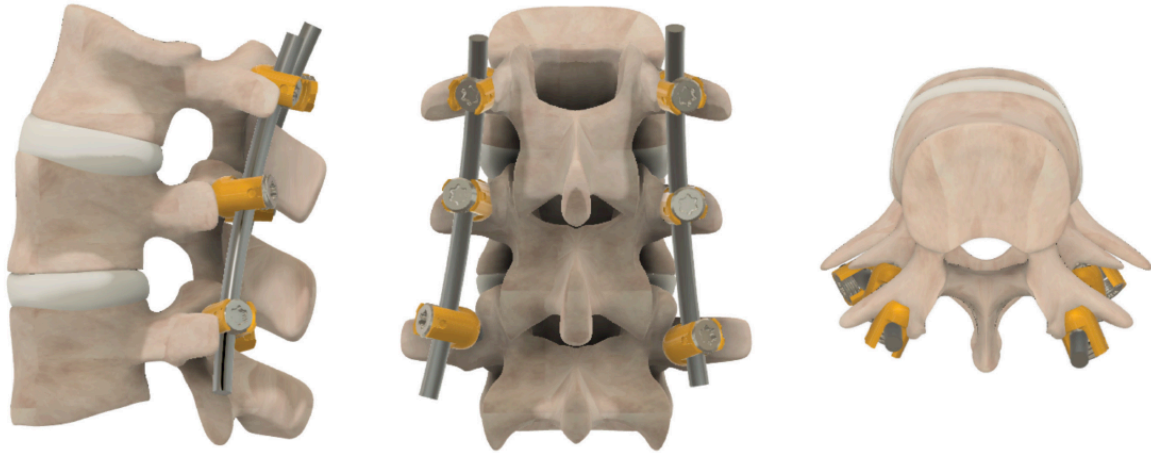


Figure 6 | Post-TIVAD surgery situation. Lateral (left), AP (middle), transverse (right)

1.5 Research questions

The research questions for the thesis goal are the following:

How can the new TIVAD SIS add value to the TIVAD spine system?

What is the added value for the patient, the surgeon, and the hospital of the new TIVAD spine system, composed of the TIVAD implant and TIVAD surgical instruments?

To what extent can 3D printing technology contribute to the modularity and customizability of the new TIVAD SIS?

1.6 The Company

Amber Implants is an innovative med-tech start-up based in the Netherlands, with a focus on design and manufacturing implants for traumatic and osteoporotic spine fractures. The company has extensive knowledge about the mechanical behavior of porous biomaterials created with innovative additive manufacturing techniques. Amber Implants applies this knowledge to develop unique solutions for spinal and other orthopedic pathologies. This is achieved by having close collaborations with the TU Delft, UMC Utrecht, and many other European research institutes.

1.7 Design Process

This thesis project follows the design phases of the Waterfall model (van Boeijen et al., 2020). Fig. 7 shows the reader guide with an overview of the thesis. Additionally, all applied design methods are shown per phase. For an entire explanation of the design methods, see Appendix 2.

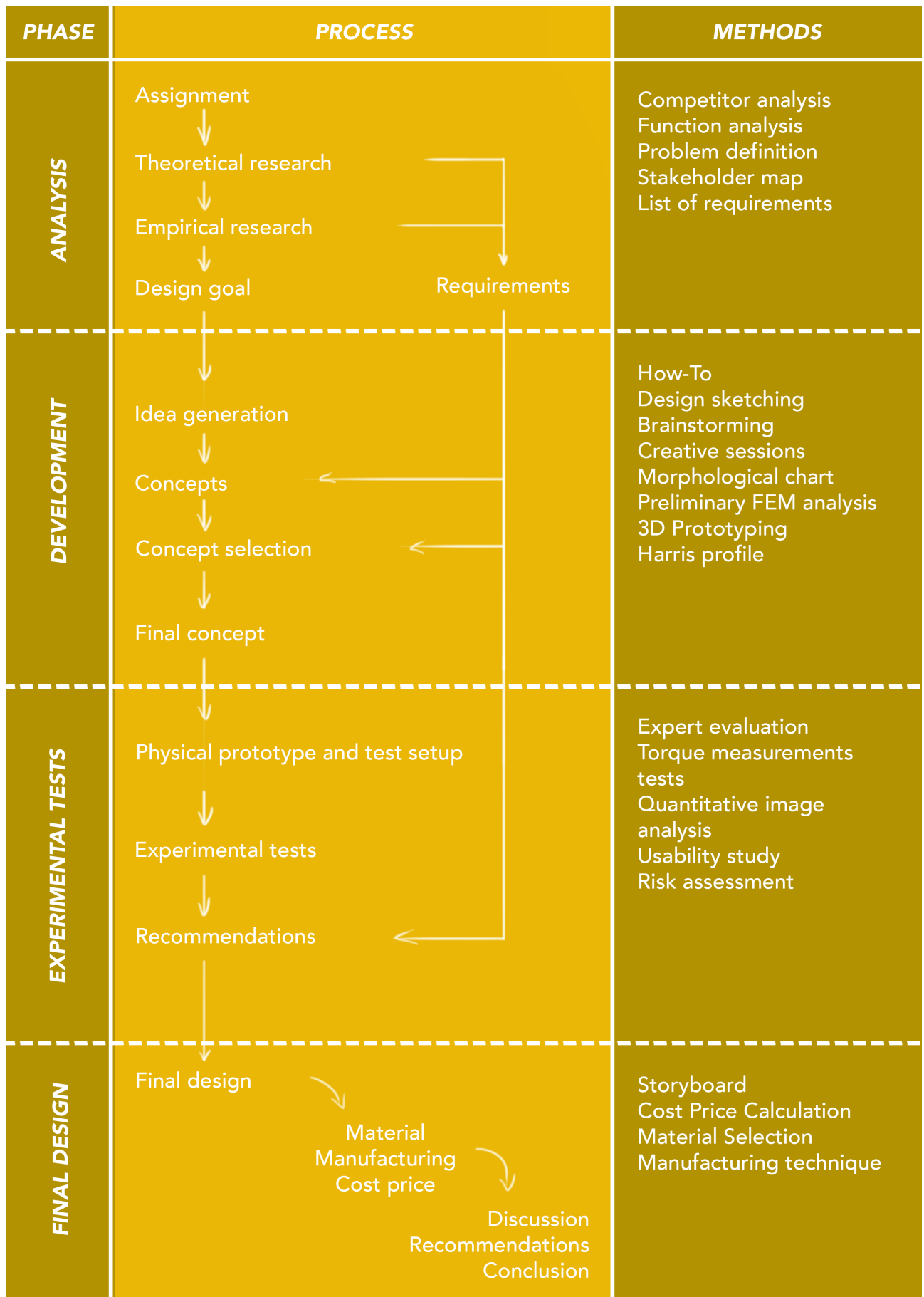


Figure 7 | Reader's guide of design phases, process, and applied design methods

2. Analysis

For the analysis phase, the background information on the physiologic and anatomical relevance is evaluated. Based on this outcome, both theoretical and empirical research approaches are formulated to answer the research questions.

The theoretical research focuses on physiologic and anatomical information related to the human spine, VCFs, state-of-the-art VCF devices, while the empirical research goes through a series of interviews with orthopedic surgeons and observations at VCF-related surgeries.

2.1. Theoretical Research

2.1.1 Spine anatomy

The structure of the segments of the spine

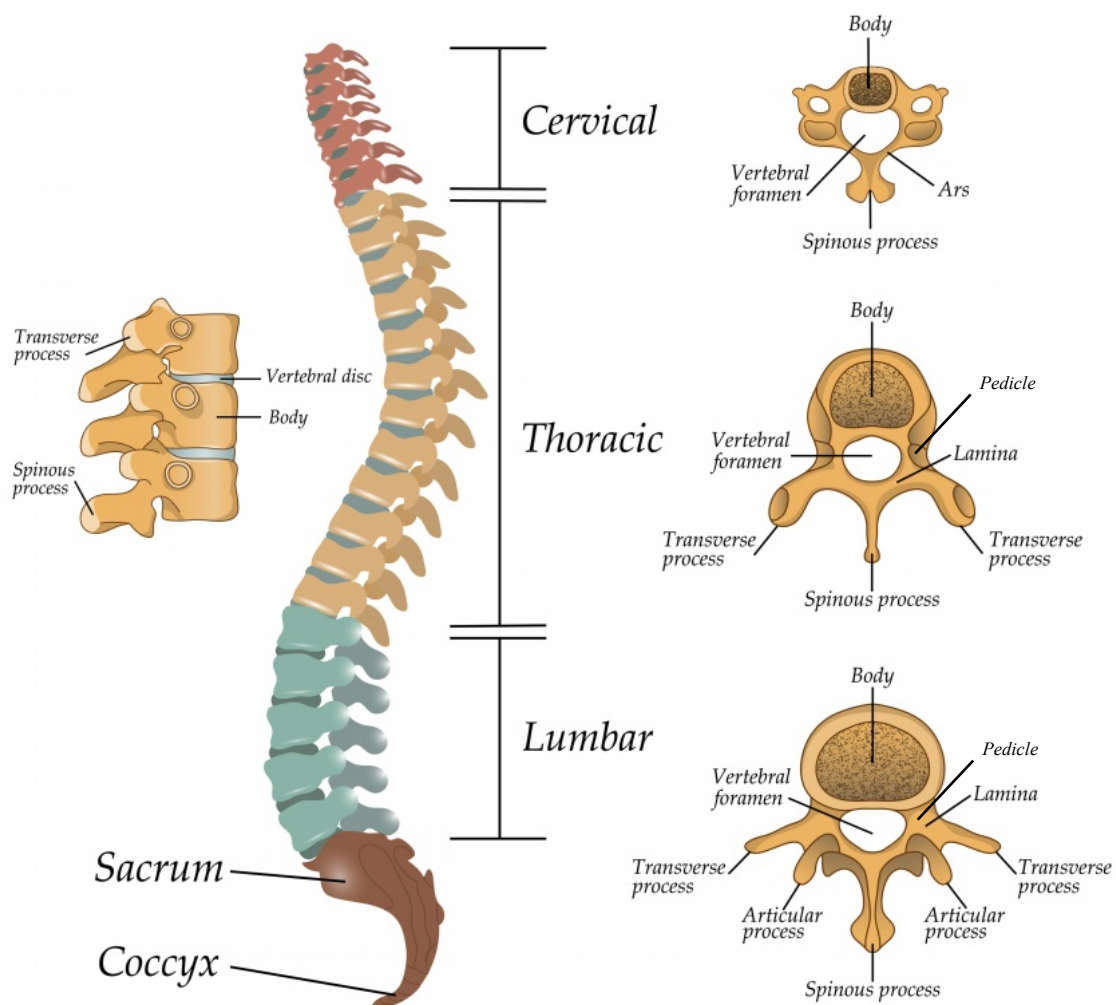


Figure 8 | Spine anatomy overview, spine regions (left), vertebral body shape per region (right) (Frost et al., 2019)

The spine contains of five regions: the cervical (C1-C5), thoracic (T1-T12), lumbar (L1-L5), sacrum, and coccyx and show a natural S-shaped curve in the sagittal plane (Fig. 8). As a result of the S-shaped curve in the spine, both convex and concave regions are present. The convex part can be found in the thoracic and sacral regions and is specified as kyphotic. The concave part is assembled by the cervical and lumbar spine and is named lordotic (Frost et al., 2019). Given this structure, a shock-absorbing system has been created naturally, where each region operates as a spring-like mechanism. Moreover, the curvature is responsible for flexibility and an even load distribution through the spine.

The compressive loads that the spine encounters are predominantly carried by the VBs, as they pass through the center of rotation of each VB. The vectors of these loads are defined as follower loads, which collectively result in the follower path in the spine. Consequently, of the location of the follower loads, the shear forces and bending moments are minimized. Furthermore, the posterior ligaments prevent buckling. As a result, stable and safe load distribution is maintained in the spine (Patwardhan et al., 2016). To conclude, the biomechanical behavior of the VBs is essential in the evaluation of VCFs and surgical procedure.

The VB has many geometrical features such as its body, lamina, transverse process, articular process, spinous process, and vertebral foramen (Fig. 8). Moreover, a VB exists of the inferior and superior cortical shell and its trabecular core (Fig. 9). The inferior and superior cortical endplates both have a thickness of approximately one millimeter. Nonetheless, they have a high resistance against compressive loads. However, most of the VB contains trabecular bone in its center, which is significantly weaker. Therefore, it is not surprising that the majority of VCFs occur in the VB's core (Zhao et al., 2009).

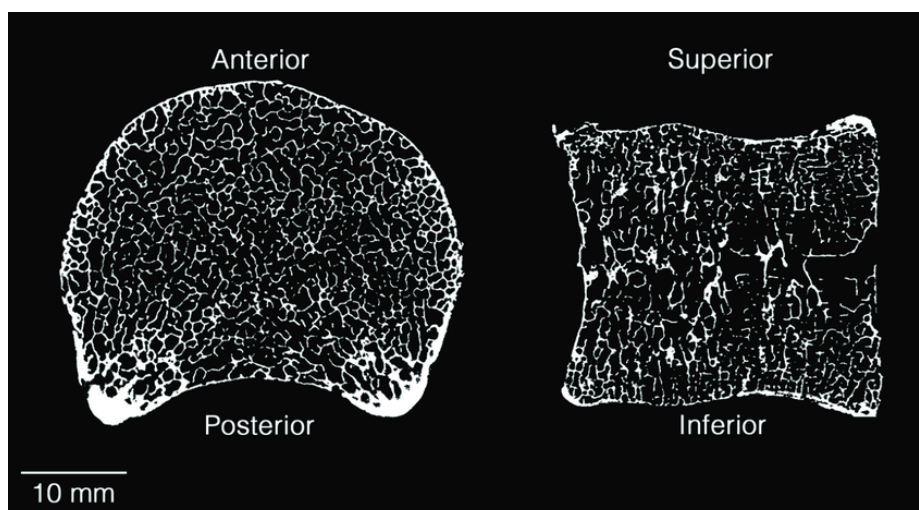


Figure 9 | microCT VB, transverse plane (left), lateral view (right) (Frost et al., 2019; Zhao et al., 2009)

2.1.2 VCF cause, incidence, and consequences

As mentioned in Section 1.5, most VCFs appear in the lower thoracic and lumbar regions. More specifically, these fractures occur at the thoracolumbar junction, where the transition from the kyphotic to lordotic angle in the spine is present (Wilson et al., 2012). As a result, the load distribution is more complex, and the VBs are subjected to higher loads. The reason that the VBs are prone to fracture of adjacent structures is bilateral. The adjacent structures are supported by the rib cage in the upper thoracic region leading to improved spine stability, and powerful ligaments are present in the lower lumbar region, preventing them from rupturing (Frank et al., 2021).

Bone mineral density (BMD), aging, osteoporosis, and the VCF rate are four parameters that are narrowly correlated to each other. Osteoporosis, which is determined by a low, clinically measured BMD and micro-architectural deterioration of bone tissue, is expected to be the single best predictor of VCFs (Johnell & Kanis, 2006). The WHO has developed standardized T-scores to determine osteopenia and osteoporosis, which indicate the levels of BMDs (Table 1).

Table 1 | Overview of T-scores (Department of Health et al., 2018)

Medical condition	T-score
Healthy	$-1 < \text{T-score} < +1$
Osteopenia	$-2.5 < \text{T-score} < -1$
Osteoporosis	-2.5 or lower

Cranney et al. (2007) investigated the relationship between the T-scores and the incidence of VCFs in the lumbar spine. Fig. 10 shows that the VCF rate is influenced by the categories set by the WHO. The numbers of VCF increase significantly for osteopenic and osteoporotic bone. Their results show that 26.2 out of 1000 osteoporotic patients suffer a VCF in the lumbar spine. These results are in line with

the results of studies performed by (Felsenberg et al., 2002; Johnell & Kanis, 2006; Lee et al., 2013)

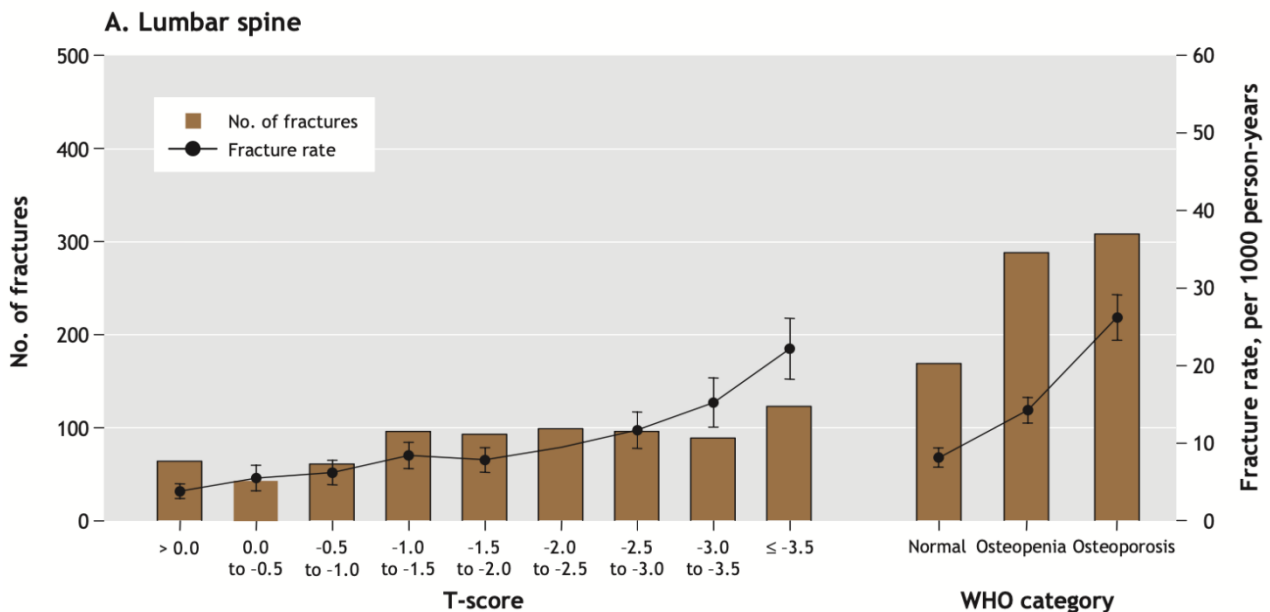


Figure 10 | Relation between T-score and number of VCFs (Cranney et al., 2007)

A symptomatic VCF is most frequently indicated by severe chronic back pain, which will worsen during physical motion. Hence, bed rest is often preferred by patients, which unfortunately can lead to adverse events that affect the whole body, such as muscle fatigue, loss of strength, and ultimately immobility in the long run (Wilkes, 2000). Moreover, various studies have proven that reduced physical activity results in a degradation of emotional and mental health. As a result, isolation and depression are side effects that are appointed repeatedly in patients suffering from a VCF (Paolucci et al., 2018). Therefore, chronic pain is an undesirable consequence of a symptomatic VCF and should be prevented whenever possible.

Furthermore, VCFs can result in hazardous health conditions due to the kyphotic and lordotic deformities of the spine. These deformities result from the reduced VB height after the fracture, which happens most predominantly in the anterior VB. Consequently, a reduction of the thoracic or abdominal cavity can lead to a restricted long volume or protuberant abdomen (Silverman, 1992). Eventually, a remarkable number of patients will have a forward bent posture, which often affects the patient's self-esteem but can also result in an increased risk of falling (Premat et al., 2018).

2.1.3 VCF device competitors

As the non-surgical solutions do not pay off, spine surgery is required for most patients that suffer a symptomatic VCF. Due to the poor quality of the osteoporotic

bone, surgical fixations of various VB levels with regular pedicle screws and rods (Fig. 11) have regularly failed in the past (Cheng et al., 2013).

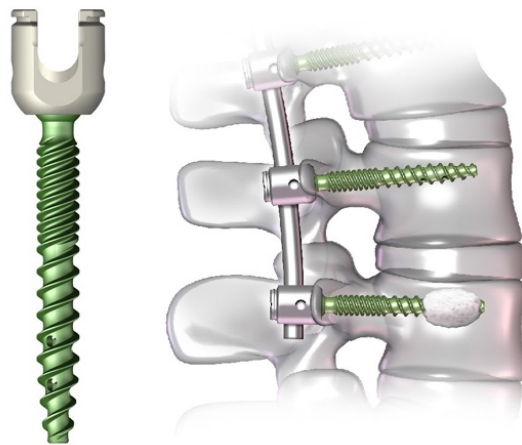


Figure 11 | Pedicle screw system with external rod fixation

Moreover, open surgery approaches increase the risk of complications such as infection, especially in the elderly (Rodriguez, 2019). Therefore, the necessity for a new surgical procedure becomes apparent with fewer risks and an improved surgical outcome. As a result, the current state-of-the-art VCF devices rely on a minimally invasive surgical approach.

In 1987, Galibert et al. (1987) described the 1st generation of minimally invasive surgical procedures for a VCF: VP (Fig. 12). This procedure resulted in the stabilization of the vertebral column and pain relief by injecting PMMA bone cement into the fractured VB. No height restoration of the VB height is achieved with this procedure. The PMMA is often injected via a transpedicular approach (through the pedicles), simultaneous in both pedicles (Han et al., 2005).

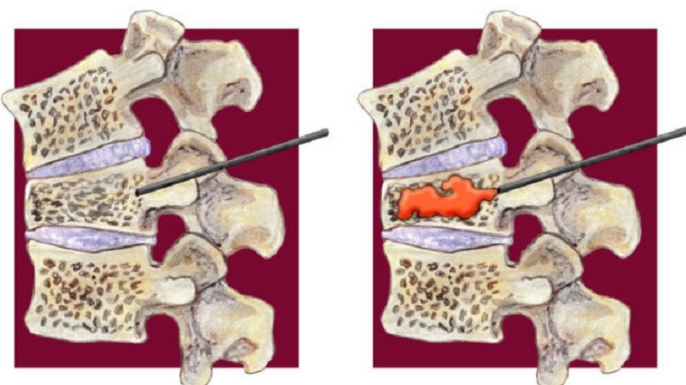


Figure 12 | Vertebroplasty (1st generation) (Jay & Ahn, 2013)

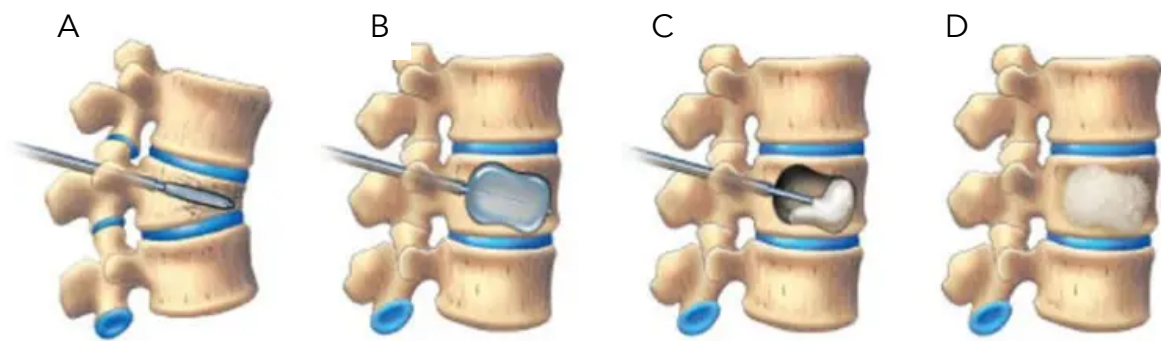


Figure 13 | Balloon kyphoplasty steps (Medical Advisory Secretariat, 2004)

The concept of vertebroplasty has been further developed in the 2nd generation procedure: BKP (Fig. 13). The most significant change, compared to VP, is the addition of an inflatable balloon, which makes it possible to restore the height of the fractured (and thus compressed) VB and correct the spine's angular deformity, which is a result of the fracture. Once the desired height is reached (Fig. 13, B), the balloon is deflated and withdrawn from the fractured VB, and the PMMA bone cement is injected into the remaining cavity (Fig. 13, C). To conclude, the 2nd generation VCF device differs from the 1st generation VCF device by its ability to restore the VB height.

However, studies have concluded that the BKP procedure does not result in the expected optimal outcomes. Regarding the biomechanical consequences, distinct losses for height restoration and angle correction are evaluated. First, the deflation of the balloon before cement injection mainly bore short-term responsibility for this phenomenon (Becker et al., 2011; Levin, 2018). A study by Dohm et al. (2014) depicts an anterior height restoration for BKP of 15.1% at post-OP and 6.3% at the follow-up after 12 months; this clearly indicates a long-term loss of VB height restoration. For the kyphotic or lordotic angle, a correction of 21.9% post-OP and 13.2% during the 12 months follow-up is found, which indicates the loss of angle correction over time. Therefore, it can be concluded that the necessity for a VCF procedure that features better short- and long-term results is highly in need.

Besides proper VB height restoration and angle correction, the main goal of the 3rd generation procedures is to minimize the pitfalls related to the injection of PMMA since this has shown to bring along several safety-related risks and complications. Principally, the PMMA altered the local stiffness of the vertebral bodies as the stiffness of PMMA is much higher than the trabecular bone of the VB core. This leads to an adjustment of the load distribution through the spine leading to adjacent VCFs; this phenomenon results from Wolf's law (Berlemann et al., 2002). Furthermore, it has been observed that the PMMA disables bone healing in the VB due to its non-absorbability, and ultimately it induces the risk of neural or vascular injury due to its

exothermic reaction (Henslee et al., 2012). Additionally, during the injection process of PMMA, a limited quantity often leaks into the VB disc surface depending on the orientation and placement of the PMMA insertion instrument. Eventually, this PMMA leakage could result in a pulmonary embolism or neurological deficits, which might cause a severe risk to the patient's health (Upasani et al., 2010).

The response to the pitfalls of the 2nd generation VCF devices is, logically, the 3rd generation of VCF devices. They distinguish themselves from the 2nd generation VCF devices because the device stays inside the fractured VB after the surgical procedure. A downside still is that these VCF devices need to be fixated with PMMA bone cement. Examples of 3rd generation VCF devices are Vertebral Body Stenting (VBS) and SpineJack.

Fig. 14 shows the principle of VBS (DePuy Synthes, 2016). VBS is comparable to BKP, but the main difference is the addition of an expandable titanium scaffolding structure on the outer surface of the balloon. The primary function of the stent is that it prevents the VB from collapsing during the balloon deflation process. After deflation, the stent remains in place, and its position and geometrical shape is fixated with PMMA.



Figure 14 | Vertebral Body Stenting procedure (DePuy Synthes, 2016)

Another 3rd generation VCF device is SpineJack, see Fig. 15. As the name suggests, the Spinejack (Stryker) procedure includes the insertion of a jack into the VB to ensure that the augmentation is in the correct, inferior, and superior direction (see Fig. 15, picture 4). The expandable jack, composed of a titanium alloy, is mounted on an expander tool. After the bilateral insertion of two implants and after their expansion, the PMMA is injected through the central part of the implant for fixation (Kerschbaumer et al., 2019).

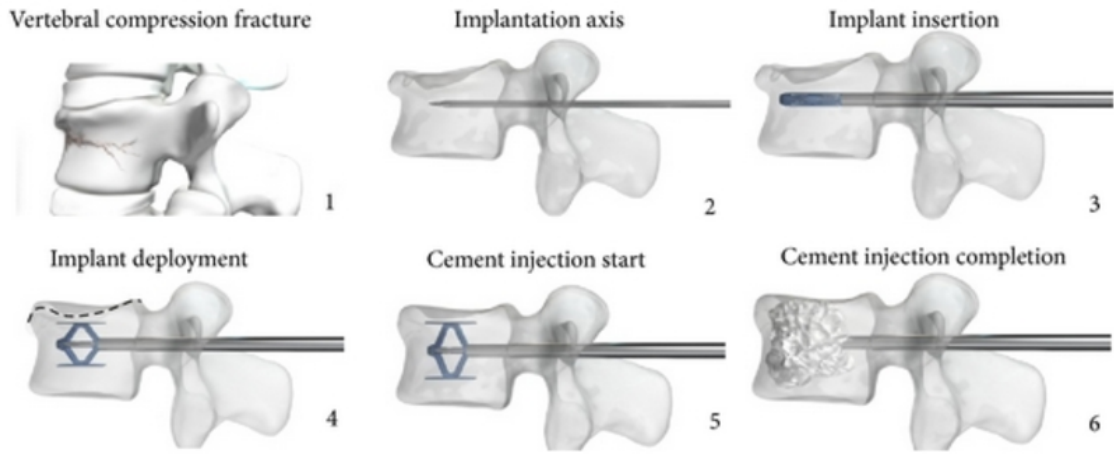


Figure 15 | Spinejack procedure (Premat et al., 2018)

2.1.4 Surgical instruments of VCF device competitors

Based on the outcome of the analysis on the existing VCF devices (Appendix 3) and the required surgical tools, Table 2 is made. Table 2 shows the surgical procedure steps, including each corresponding surgical instrument when the TIVAD spine system is used. Fig. 16 illustrates all these surgical instruments required for the TIVAD procedure.

Table 2 | TIVAD surgical procedure: non-essential (yellow) & essential (green)

Surgical step	Required surgical instrument
Patient positioning	N/A
Implant positioning planning	N/A
Skin incision	Scalpel (Fig. 16, A)
MIS dilator insertion	MIS Dilator (Fig. 16, B)
VB access	Jamshidi needle (Fig. 16, C) Hammer (Fig.16, D)
Implant site preparation	K-wire (Fig. 16, E) Cannulated drill (Fig. 16, F)
Implant insertion	TIVAD Inserter – Thesis assignment (Fig. 16, H)
Implant expansion	TIVAD Expander – Thesis assignment (Fig. 16, G)
Retraction of implant inserter & expander surgical instrument	N/A

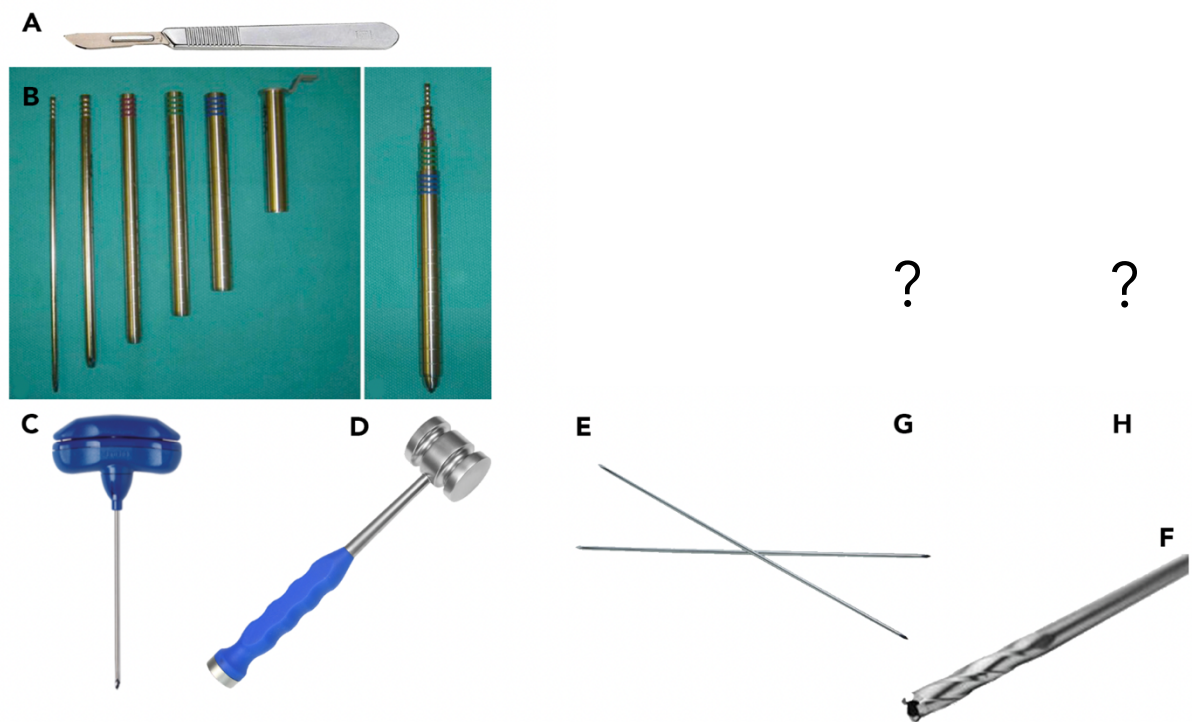


Figure 16 | Non-essential & essential TIVAD surgical instrument overview

2.2. Empirical Research

2.2.1 Interviews

To get a proper understanding of the current situation in the Dutch hospitals, five orthopedic spine surgeons from various academic hospitals in the Netherlands have been interviewed, i.e., the Erasmus Medical Center (EMC), Leiden University of Medical Center (LUMC), and Utrecht University of Medical Center (UMC). The primary goal was to gain information about the daily practices as orthopedic spine surgeons, the preferred VCF devices, the strengths & weaknesses of these VCF devices, what the like/dislike attributes of the complementary surgical instruments are, and the common setup of the surgical team. To capture all attributes, the list of questions (LoQ) is generated. Appendix 4 illustrates the list of questions.

The outcome shows that no matter what preference the surgeon has regarding the VCF device, the preference goes to having the ability to control the VCF device's height expansion accurately. Furthermore, it is noticeable that there is no golden standard with respect to the VCF device that is chosen to treat osteoporotic VCFs as there is considerable diversity between used VCF devices in the different (academic) hospitals and even surgeons within the same (academic) hospital.

It is generally noted by the surgeons that the use of PMMA bone cement brings significant risks, such as pulmonary embolisms, to the patient, which confirms the

literature findings in *Section 2.1.3*. The reason that these VCF devices are still used is that, at the moment of writing, there are no options available that offer a better benefit/risk balance according to the current scientific knowledge.

Furthermore, all surgeons recognize well that correct fitting inside the VB body and pedicles is critical to ensure proper placement and fixation of the VCF device. If a tight fit is not achieved, this potentially could lead to the loosening of the VCF device and ultimately failure and the need for follow-up surgery.

Lastly, with the current VCF devices, there is a constant need to take images with the fluoroscopy (FS) C-arm, which automatically means that the patient and entire surgical team is exposed to an unnecessary amount of ionizing radiation. As a solution, the surgeons asked whether it is possible to implement features to the new TIVAD-SIS system that provide feedback with respect to the insertion and expansion of the TIVAD implant to reduce the number of required FS images and to verify the current situation of the TIVAD implant inside the fractured VB. This would add significant value to the new TIVAD-SIS system for both the patient and the surgical team.

2.2.2 Surgery analysis

To gain a deep understanding of the surgical procedure and to observe how the spine surgeon interacts with its surgical team, a surgery session has been attended, in which a patient is treated who suffered a double osteoporotic VCF, in T12 and L2, which has been caused by lifting a cupboard. The chosen solution is a BKP set by Safe Orthopaedics. Despite the extensive research that has been completed concerning BKP, a lot of new insights were gained with respect to how the surgeon, assistant, nurses, and anesthetist, interact with each other, their responsibilities in- and outside of the sterile area in the operating room, and usability related issues such as workspace, visibility, and operational noise.

The vast number of FS images taken during the surgery is remarkable, which count to at least 90-100 images. As a result, the patient and surgical team are exposed to a relatively extensive amount of ionizing radiation of the FS machine as described in *Section 2.2.1*, with regards to overall surgery time and total ionizing radiation exposure.

Additionally, the C-arm (= FS machine) needs to be changed from the AP position to the lateral view position numerous times (+/- 20 times) during the surgery. During these transitions, utmost attention is required as the instruments that stick out of the patient's back should not be touched and moved by accidental contact between them and the C-arm. Furthermore, the distance between the patient's back and the c-arm is relatively small, approximately 25-30 centimeters (see Fig. 17, red arrow). Accordingly, there is not much space for the surgeon to work within. This also implies

that during the design of the new TIVAD surgical instruments, sufficient length must be taken into consideration to avoid any collisions with the C-arm during use.



Figure 17 | C-arm during spine surgery

Furthermore, the steps of balloon inflation, cement preparation, and insertion processes are followed accurately using FS imaging. The total time for these steps is approximately 30 minutes. By removing these steps, the number of FS images and overall surgery time can be reduced immensely. This is a massive benefit for the new TIVAD spine system compared to the existing VCF devices.

A reduced surgery time also has a positive effect on the comfort of the surgical team, as wearing lead vests and skirts can be minimized to protect against ionizing radiation. The commonly used lead vests and skirts weigh approximately 7kg, which contributes to discomfort during a surgery that can take up to several hours.

Lastly, a reduced number of surgical steps also has another positive impact on the ergonomic working environment of the surgeon. The current practice requests that the surgeon must look up and look away from the surgery spot (during this specific (attended) surgery) every time an FS image is inspected on the monitors. Bearing in mind that they are wearing the lead vest and they need to look up and stay away from the surgery spot for approximately 100 times throughout the entire surgery, extensive stress and discomfort on the surgeon's neck muscles are widely common experiences noticed by the surgeons.

2.2.3 List of requirements

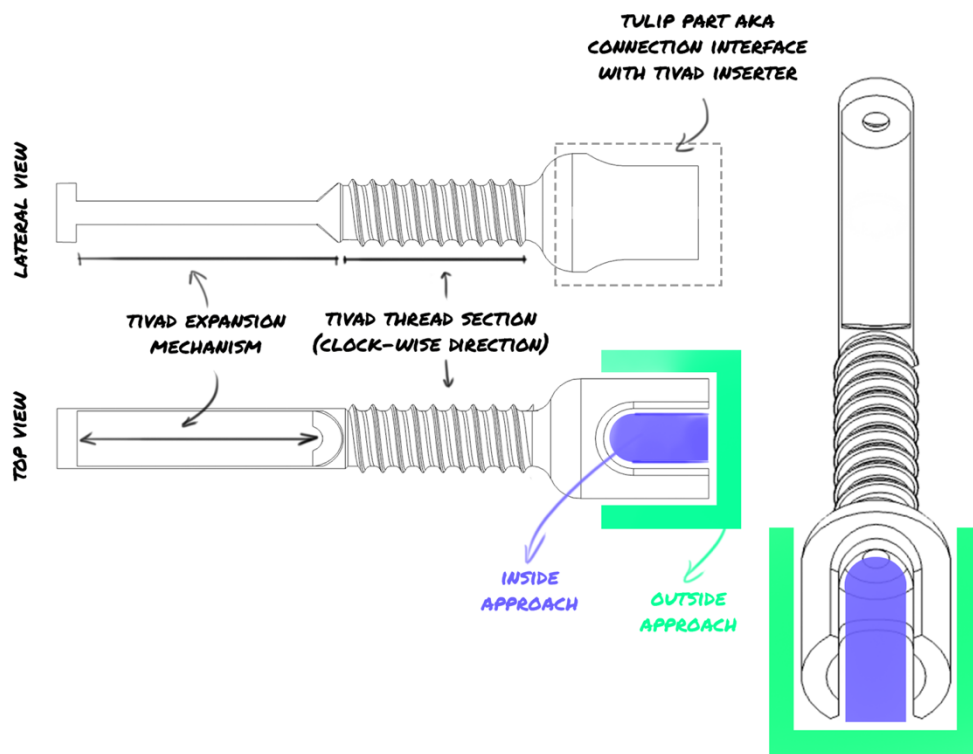
Following the collected knowledge at the phase of the theoretical and empirical research, several key requirements for the TIVAD SI are identified and serve as the foundation for the sequel of the thesis. Appendix 5 shows the entire list of requirements (LoR) for the new TIVAD-SIS (Table 14).

3. Development of concepts

3.1 Development process introduction

The development of concepts is initiated by applying various design methods to generate ideas. The development phase was started with the application of the 'how-to' method. With this method, the functional properties that are defined in the LoR are translated into functions that the generated concepts should have. Each of the sub-problem solutions is then taken into the next phase, where the idea sketching (Fig. 53, Fig. 54, Fig. 55) & brainstorming methods are applied (van Boeijen et al., 2020). Moreover, to get a better understanding of geometrical shapes and dimensions, a preliminary FEM analysis is performed on very early connection design ideas that are created using the morphological chart model by (Roozenburg & Eekels, 2003) (Appendix 6).

Accordingly, three relevant Concepts (1, 2, and 3) for the TIVAD inserter, one for the TIVAD expander, and several TIVAD handle designs are identified and discussed in the following sections. For further information about the methods that are used for the concept generation process, see Appendix 2. See Appendix 7 for the concept sketches. As addressed in section 1.4, the geometrical shape and dimensions of the TIVAD are frozen. As these parameters influence the shape and dimensions of the SI for the insertion and expansion of the TIVAD immensely, they were analyzed extensively (Fig. 18).



3.2 Overview of concepts

3.2.1 TIVAD Inserter – Concept 1

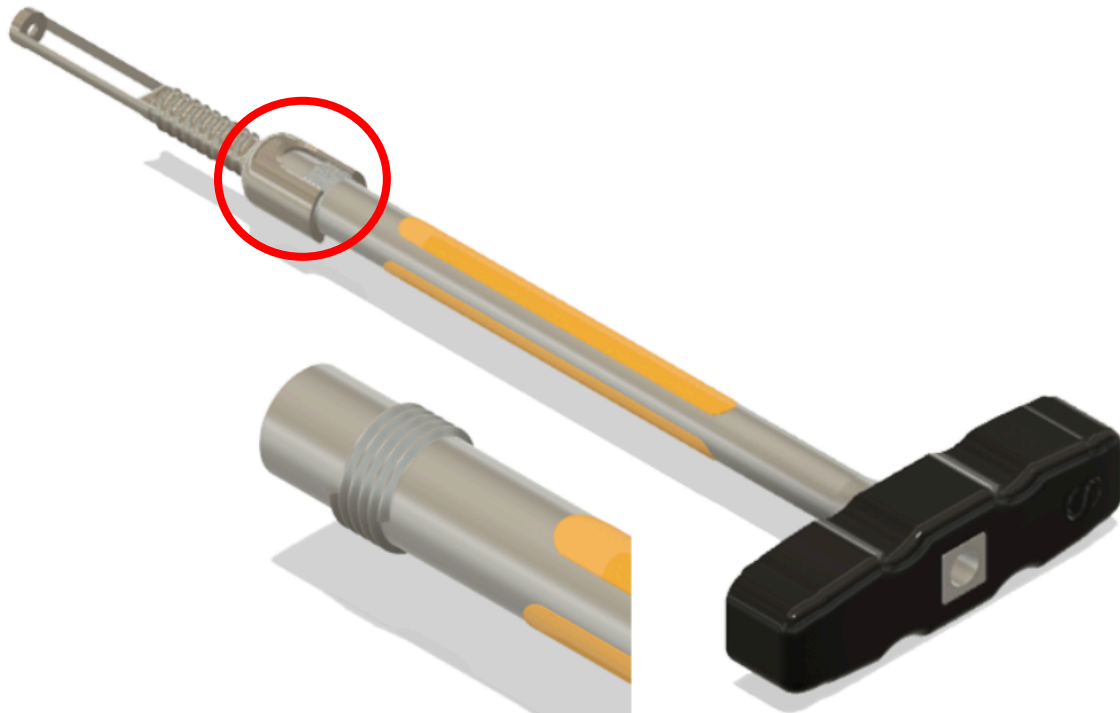


Figure 18 | TIVAD Connection interface

Concept 1 (Fig. 19) is based on a screw thread design to connect the TIVAD inserter to the TIVAD implant's tulip (Fig. 19, indicated with circle). Once the thread is fully seated, the insertion process can start, which is done by applying a clockwise rotation. The handle features a use-cue to show the user how the implant is positioned inside the fractured VB, as the correct positioning of the TIVAD implant is crucial for optimal expansion performance in the short- and long term. The advantage of this connection mechanism compared to the ones from Concept 2 and Concept 3 is that the implant is completely fixed to the TIVAD inserter.

Nevertheless, one downside of this design is that it requires 10+ rotations before the thread is fully wound into the tulip of the TIVAD implant. As a result, the surgeon needs more time to attach Concept 1 successfully to the TIVAD implant tulip. Another disadvantage of Concept 1 is related to its inside tulip approach, meaning that the instrument is prone to failure under a load of 2Nm if it features a hollow cavity for the TIVAD expander. This finding is based on the results of preliminary FEM analyzes performed in Fusion 360; for further information on measurement data, see Appendix 6.

In addition, still being able to approach the TIVAD tulip from inside the referred shaft must be solid. As a result, Concept 1 does not have enough space to make a cavity channel at the core to allow the TIVAD expander to pass through and enable a two-in-one TIVAD insertion and expansion approach. This implies that the TIVAD inserter's hollow cavity cannot act as a guide for TIVAD expander guidance. Ultimately, this makes it harder to get the connection between the TIVAD expander screw and TIVAD expander correct in one go.

3.2.2 TIVAD Inserter - Concept 2

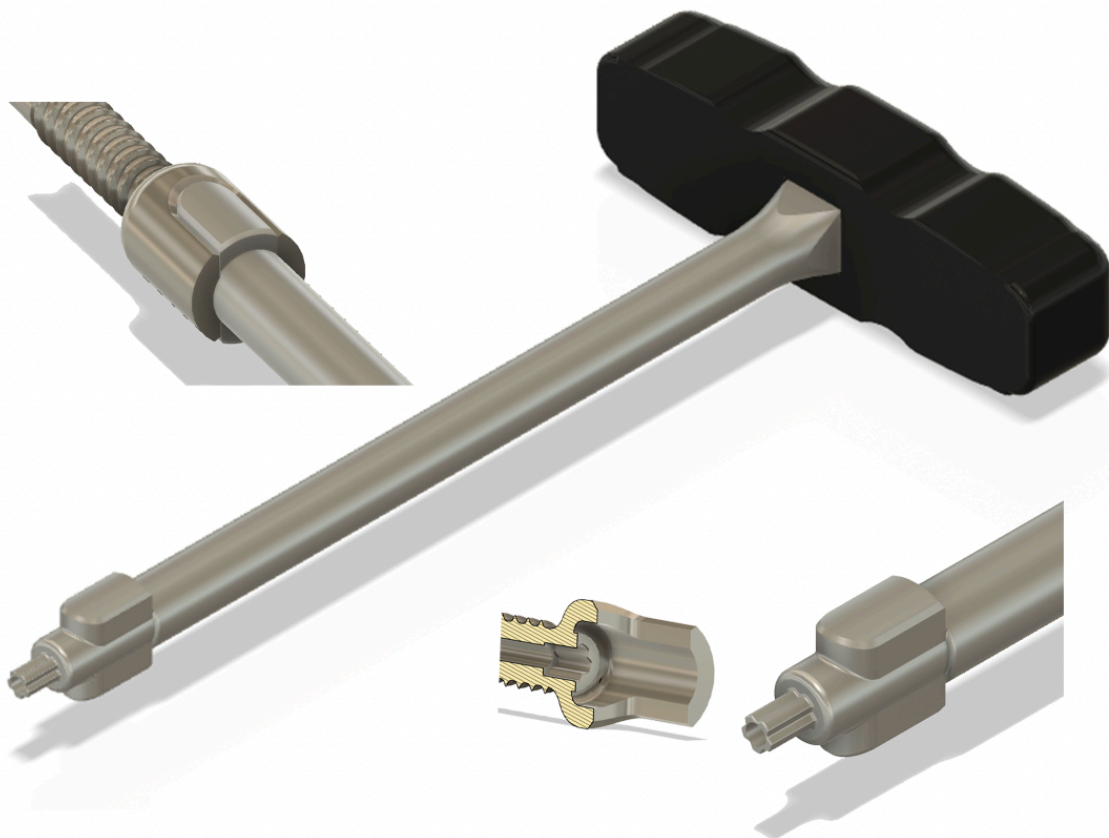


Figure 20 | TIVAD Inserter Concept 2

Concept 2 (Fig. 20) approaches the TIVAD implant from inside of the tulip, which is a similar approach to Concept 1. Removing the external thread, and thereby removing the need to perform 10+ rotations for attachment, from Concept 1 and replacing it with a matching counterpart of the tulip design and a Torx tip, saves time and simplifies the surgical procedure considerably. The main features of this connection design are the Torx tip and the tulip fitted shape (Fig. 20). The idea behind these two contact surfaces is that they would reduce the peak stresses on the edges of the connection due to the fact that the force is evenly spread over a bigger surface. However, the tight tolerances at the Torx connection might be prone to difficult engagement during surgery as there may be some debris that makes flawless

engagement difficult. Just as with Concept 1, Concept 2 also relies on an inside tulip approach, meaning there is not enough material to carry the torque (2Nm) during use when it features a hollow cavity for the TIVAD expander. Furthermore, due to the inside tulip approach, Concept 2 does not have the space to make a cavity channel at the core to allow the TIVAD expander to pass through and enable a two-in-one TIVAD insertion & expansion approach.

3.2.3 TIVAD Inserter - Concept 3

The third concept, Concept 3, distinguishes itself from Concept 1 and 2 in such a manner that the inserter connects to the outside of the TIVAD tulip and fits, basically, like a glove around the TIVAD tulip (Fig. 21). As a result, unwanted de-attachment is hardly possible. Moreover, due to the nature of the outside approach, it enables the design to feature thicker walls (greater wall thickness), which improves mechanical performance against the torque from the surgeon. As a result, concept 3 can feature a hollow circular cavity that allows room for the TIVAD expander to pass through (Fig. 23).

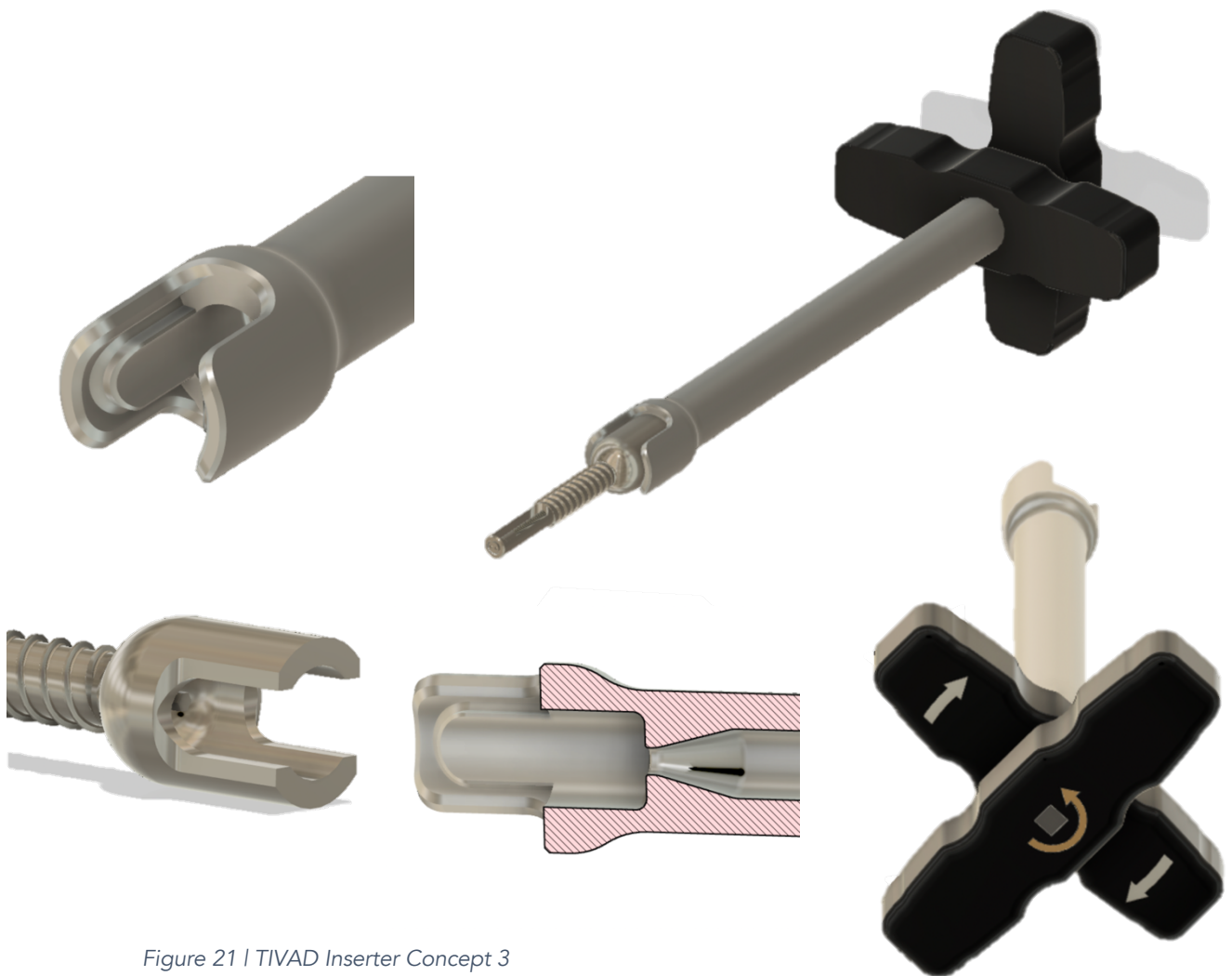


Figure 21 | TIVAD Inserter Concept 3

3.2.4 TIVAD Expander

Fig. 22 illustrates the final TIVAD expander concept. The main function is to expand the TIVAD implant once it has been inserted and positioned into the desired orientation and depth inside the fractured VB. The TIVAD implant can be expanded by applying a rotational motion onto the expansion screw (Fig. 3, blue part). From a closed position to a fully expanded TIVAD requires 15-17 full rotations, depending on the implant size (small – extra-large).

The key design feature of the TIVAD expander is the hexagonal connection that attaches to the expansion screw of the TIVAD implant (Fig. 3, blue part). Secondly, it is designed to fit the circular cavity of the TIVAD inserter. As a result, through this two-in-one approach, the expander is easily guided by the inserter's cavity into the desired direction and depth. Fig. 22 (right bottom corner) and Fig. 23 show how this 2-in-1 approach looks like when they are assembled.

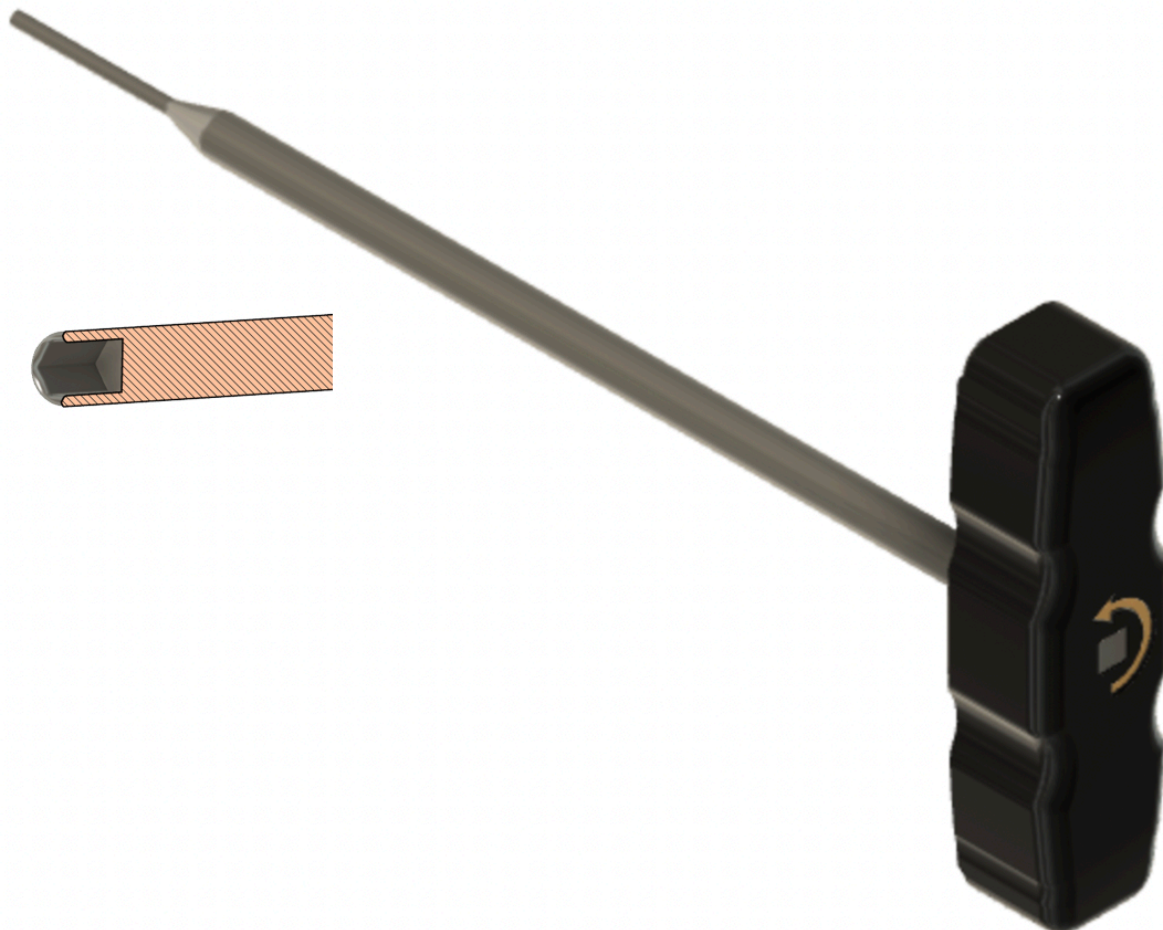


Figure 22 | TIVAD Expander Concept

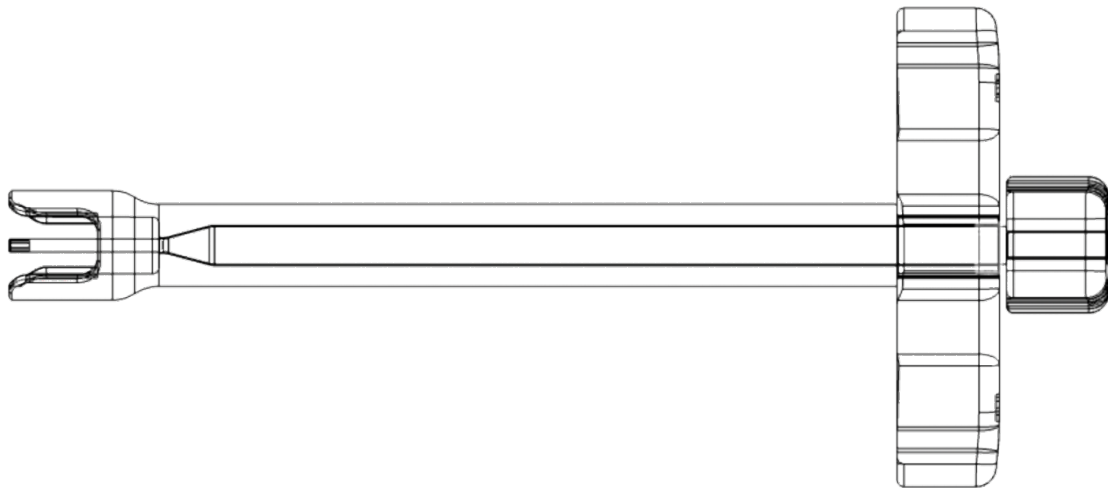


Figure 23 | Transparent view TIVAD Expander Concept: 2-in-1 approach

3.2.5 Handle concepts

Convenience for the surgeon during the TIVAD procedure is of utmost importance. Therefore, the design process of the handles is paramount since the handle is in direct contact with the surgeon's hand and plays an incredibly important role in assuring comfort and transferring the applied force during use.



Figure 24 | TIVAD inserter handle (left), TIVAD expander handle (right)

Accordingly, various handle design shapes are proposed (Appendix 7, Fig. 56). Through thorough analysis of competitor handles and handles of ordinary tools, the most promising options are selected and manufactured using FDM 3D printers. These are evaluated during the experimental tests as so-called add-ons to the torque sensor setup, which made it easy to switch handles and measure torque output at the same time across different handle designs.

Both the inserter and expander handle (Fig. 24) feature a squared cavity that allows room for assembly with the TIVAD inserter and expander's shafts and carry arrows to indicate the correct rotation direction for each of the instruments, as the TIVAD

insertion is clockwise, and the expansion is achieved via a counterclockwise rotation. The TIVAD inserter handle carries the white arrows towards the distal ends of the handle as the center is covered by the TIVAD expander's handle.

3.3 Selection of best concept

3.3.1 Harris profile – TIVAD Inserter

For the selection of the best TIVAD inserter concept, the Harris profile method is applied. The Harris profile (Table 3) is a graphic representation of the strengths and weaknesses of the final concepts with respect to the predefined design requirements, which are included in the list of requirements (LoR), see Appendix 5 (van Boeijen et al., 2020).

The first column contains the key criteria for the assessment. The following columns include the identified three concepts with the scores for each of the individual criteria. Table 3 shows that Concept 3 scores the best on the criteria, and specifically on the following points: connection speed, connection success rate, visibility on the medical imaging, and its ability to conquer the force that is applied during the TIVAD insertion process. The next section elaborates why concept three scores so high on these criteria compared to Concept 1 and Concept 2.

Table 3 | Harris profile (van Boeijen et al., 2014)

Criteria	Concept 1				Concept 2				Concept 3			
	--	-	+	++	--	-	+	++	--	-	+	++
1. Fulfills function during the insertion process												
2. Locking feature, TIVAD does not get loose												
3. TIVAD inserter visible on FS												
4. Ergonomic handle												
5. No interference with TIVAD expander												
6. Strong enough for 4Nm of torque												
7. TIVAD connection speed												
8. TIVAD connection success rate												
9. Price												

3.3.2 Fulfills function

All three concepts score the maximum points as they all perform as intended and enable the surgeon to successfully insert the TIVAD.

3.3.3 Locking feature

Concept 2 scores worst on this criterium since it does not feature any locking design features. Concepts 1 and 3 score both the maximum points as they ensure a proper fix with the TIVAD. Concept 1 does it with the thread design, and Concept 3 does it with a very snug fit. Please note, very low tolerances are required to achieve this.

3.3.4 Visibility

Concept 3 is scored best on visibility, as this concept is the only one with an outside TIVAD tulip approach. Concept 1 and Concept 2 approach the TIVAD tulip from the inside. This means that during FS, the tulip 'blocks' a fraction of the radiation resulting that the TIVAD inserter's tip is less likely to be visible on the FS images. This is essential, as this gives an indication of how far the TIVAD implant is introduced into the targeted fractured VB.

3.3.5 Ergonomic handle

All three TIVAD inserters carry the same handle; therefore, they have the same score for this criterium.

3.3.6 No interference

Concept 1 and Concept 2 do not feature the cylindrical cavity that allows the TIVAD expander to pass through; therefore, they have the lowest score for this criterium. Concept 3 allows for effortless passage, providing easier TIVAD expander insertion due to the guidance during the insertion process.

3.3.7 Mechanical performance

All three concepts did not fail during the preliminary FEM analysis. However, Concept 1 and Concept 2 feature a solid shaft due to their inside TIVAD approach. Whereas Concept 3 approaches the TIVAD tulip from the outside is allows for a bigger diameter and thus a hollow shaft design. Therefore, it scores better than the other two concepts.

3.3.8 Connection speed

Concept 3 has better scores on connection speed than Concept 1 and Concept 2 because only a linear movement is required. Whereas Concept 1 must be rotated until the entire thread is seated into the thread of the TIVAD tulip takes more time. And Concept 2, the double connection feature is prone to tight tolerances that might

result in a difficult connection, which is in line with the next point: connection success rate.

3.3.9 Connection success rate

Both the thread design (Concept 1) and the double connection design (Concept 2) are prone to an error within the environment in which the instrument will be used. As the connection design relies on tight tolerances, it could happen that debris (blood, fat, and/or soft tissues) interfere with between the TIVAD tulip and the tip of the TIVAD inserter (Concept 1 and Concept 2).

3.3.10 Price

Concept 2 has the most complex shape at its tip, which results in the highest manufacturing price compared to Concept 1 and Concept 3. The difference in price between Concept 1 and Concept 3 is that with Concept 1, the TIVAD tulip needs to be adjusted to the thread. In other words, the thread needs to be made into the inside of the TIVAD tulip. With concept 3, no additional manufacturing steps are required for the TIVAD tulip.

Based on the Harris profile in Table 3, Concept 3 is the best concept and will be further developed for the experimental tests.

4. Experimental evaluation

4.1 Experimental tests

To evaluate the final TIVAD inserter and expander concept together with the non-essential surgical instruments, physical prototypes are made and tested during experimental tests to validate various properties, such as the required maximum insertional torque, usability factors, and mechanical performance of the concepts when the required torque is applied to insert and expand the TIVAD prototype into different specimens. Furthermore, a risk analysis is performed with the final TIVAD inserter and expander to identify any possible risks, pre, during, or after use, and subsequently find ways to mitigate these potential risks.

4.1.1 Performance test: insertion & expansion torque

According to Carmouche et al. (2005); Daftari et al. (1994); Zdeblick et al. (1993) the maximum measured torque for the insertion of an almost identical VCF device, with respect to dimensions and geometry, is 2Nm. Table 4 shows a dimension overview of the device that is used in literature and during the experimental tests, and Fig. 25 depicts the TIVAD, and the pedicle screw used as well, where the red line indicates the area that is almost identical between the two devices. The TIVAD prototype has almost identical dimensions compared to the PS, a minimal difference in the ID of 0.4 mm is observed, but the OD and length are identical. Carmouche et al. (2005) performed the tests on thoracic and lumbar VB, with a WHO T-score of $-1 < \text{T-score} < +1$. With this information at our disposal, these insertional torque results are used as a reference for the experimental tests for this thesis.

Moreover, DINED depicts that with two hands, a mean torque of 7Nm (SD: 2) can be applied by a person between 20-30 years old. As an indication, the maximum mean value of 9 Nm is used as a worst-case scenario value, divided by two gives 4.5 Nm (Molenbroek, 1980) (Appendix 8).

Table 4 | VCF Device dimensions

Device	Outside diameter [mm]	Minor core diameter [mm]	Length [mm]
PS (Carmouche et al., 2005; Daftari et al., 1994; Zdeblick et al., 1993)	6.2	4.8	40
TIVAD-implant prototype	6.2	5.2	40



Figure 25 | TIVAD (left), Pedicle screw (right)

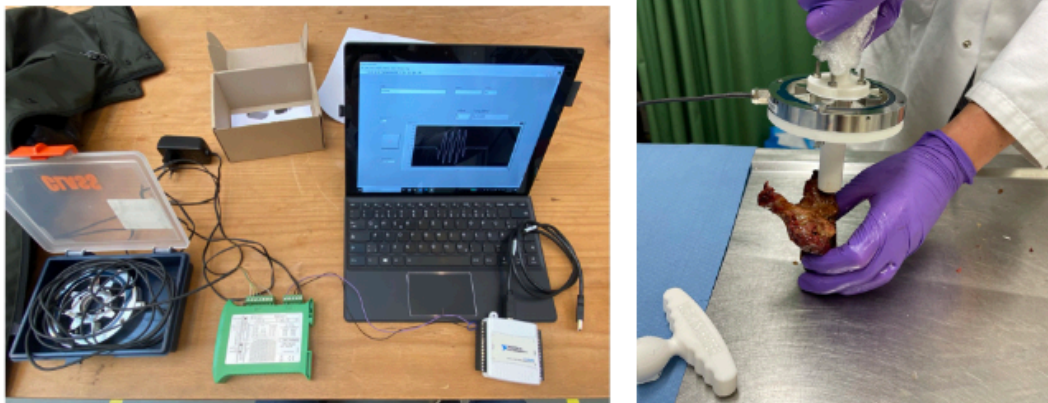


Figure 26 | Torque sensor setup: laptop, signal amplifier & DAQ unit (left). TIVAD adapter, torque sensor & Handle concept (right)

4.1.2 Test setup

To measure the required torque for the insertion and expansion of the TIVAD prototype, a custom-made torque sensor setup has been designed (Fig. 26 and Fig. 27). This experimental setup consists of the following equipment: a torque sensor, a signal amplifier, a data acquisition module (DAQ), and a laptop that is running the LabVIEW software.

During the stage 1 test, the TIVAD insertion torque is measured for synthetic bone specimens (SBS). During stage 2A, which focuses on the insertion of the TIVAD prototype into cadaveric vertebral bodies (CVB), the required torque for TIVAD expansion is determined. The torque for TIVAD expansion is only measured in CVBs as the fracture can't be mimicked in the SBS. Additionally, three cadavers are used for the stage 2A & 2B tests.

Sensor handle Torque sensor 3D printed sensor adapter VCFix inserter

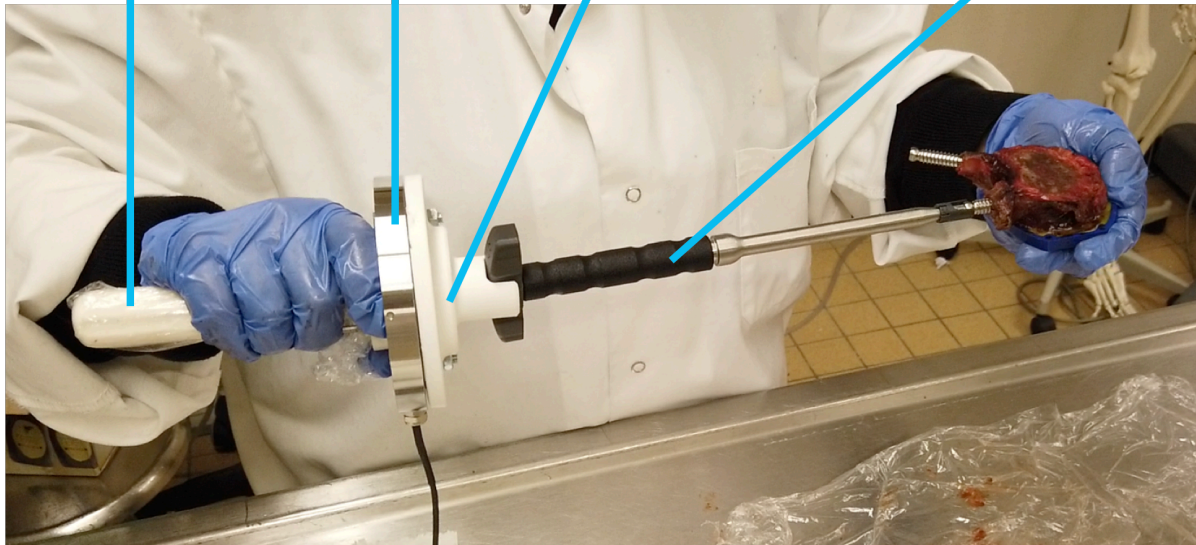


Figure 27 | TIVAD Inserter during stage 2A experimental test

4.1.3 Specimen BMD

The BMDs of the SBS are known, as they are provided by the manufacturer (see Appendix 9 for further details). However, there is no information available regarding the BMDs of the CVBs. To be able to compare the TIVAD insertion torque results, the BMD values of the CVBs are required. For that reason, a Quantitative Image Analysis (QIA) is added to these experimental tests. The main reason why the BMD is needed is that the BMD values have a major influence on the required insertional torque. A study performed by (Buhler et al., 1998) even found a linear correlation between the insertion torque and bone mineral density.

For the methods and materials, please see Appendix 9.

Hypothesis 1 (Stage 1 & 2A)

The insertional torque will increase the deeper the TIVAD implant is inserted.

Hypothesis 2 (Stage 2B)

The required torque for expansion will increase the further the TIVAD implant is expanded inside the fractured (collapsed) VB.

4.1.4 Stage 1 – TIVAD Insertion Torque Results (SBS)

This section shows the results of the insertional torque test that has been performed with the TIVAD prototype on SBS with PCF 5, 20, and 30 BMD values.

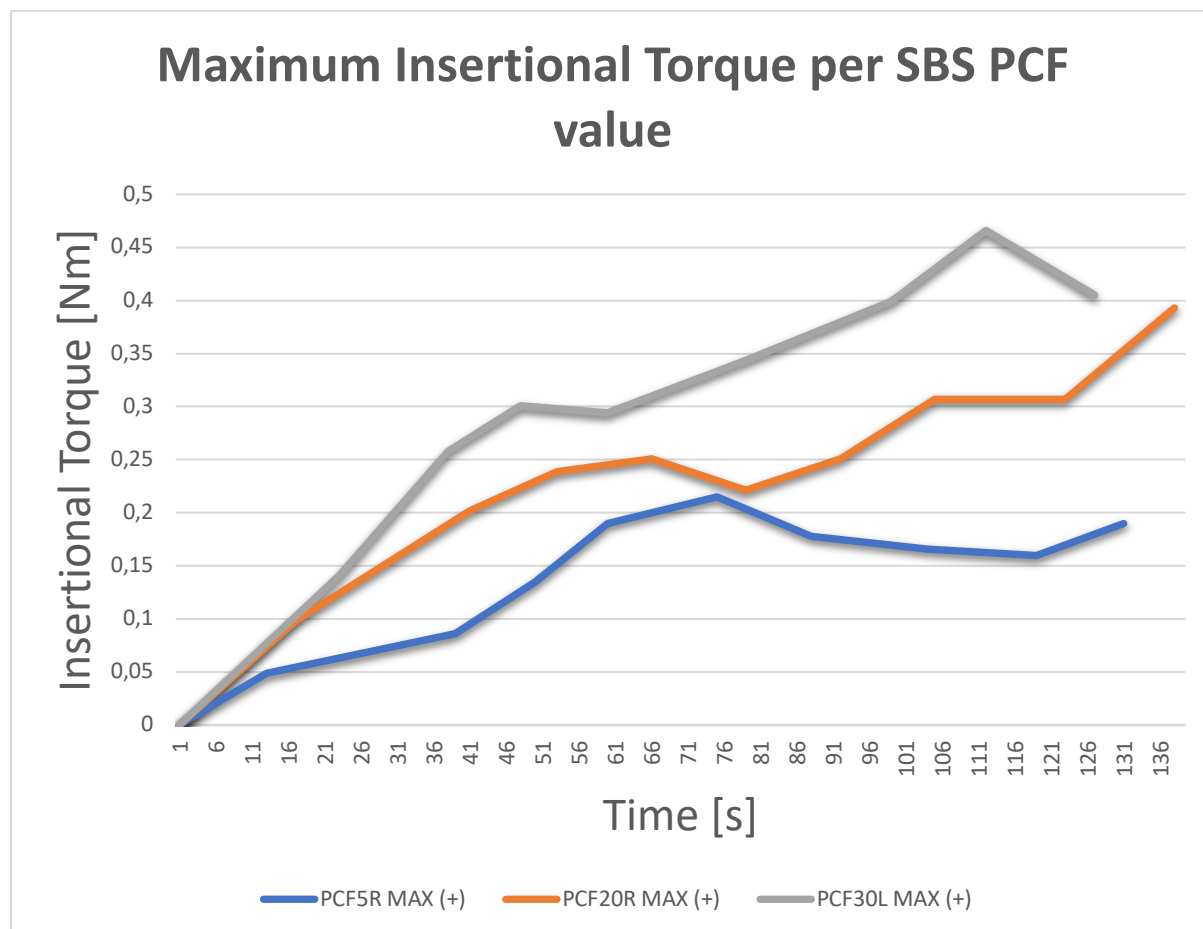


Figure 28 | Insertional torque in SBS

Table 5 | Insertion torque summary of PCF5 / 20 / 30 specimens

Specimen	Mass density <i>BMD</i> [g/cm ³]	Insertional Torque		
		Mean torque [Nm]	SD	Maximum torque [Nm]
PCF 5	0.08	0.157	0.035	0.245
PCF 20	0.35	0.218	0.071	0.393
PCF 30	0.47	0.254	0.095	0.473

Fig. 28 demonstrates how insertional torque behaves over time. It is apparent that for all three SBS density values, the required insertional torque increases over time. This indicates that the deeper the TIVAD is inserted, the higher the required torque is. Furthermore, it is evident that the insertional torque for the denser SBS densities is higher, which is plausible, as these higher densities pose a greater resistance.

Table 5 summarizes the mean torque, SD, and maximum measured torque values for the insertion of the TIVAD into the various SBSs. For each PCF value, ten insertion tests were performed. In addition, Table 5 shows that the mean torque for the PCF5, PCF20, and PCF30 SBS densities is 0.157Nm, 0.218Nm, and 0.254Nm, respectively. The maximum insertion torque was measured in the PCF30 SBS with a value of 0.473Nm. Compared to the results found by Carmouche et al. (2005), the maximum insertional torque results are 4 – 8 times smaller. No mechanical related failures or usability-related issues of the TIVAD inserter were reported.

4.1.5 Stage 2A – TIVAD Insertion Torque Results (CVB) & QIA Results

This section shows the results of the insertional torque test performed with the TIVAD inserter prototype on the CVBs from two cadavers (#1 & #6). The results are divided into separate graphs for the thoracic and lumbar spine for cadaver one and lumbar spine for cadaver 6 to improve the readability of the figures.

Fig. 29 shows the insertional torque over time of the TIVAD into the thoracic VB of cadaver 1. All six tests show that the insertional torque increases over time, meaning that the deeper the TIVAD is inserted, the higher the required torque. This is in line with the results found during the stage 1 test. However, there is a significant difference in the magnitude of the torque and the way the torque develops over time/insertion between the inferior thoracic VBs (T7, T8, T9) and the superior thoracic VBs (T10, T11, T12). An exponential increase of the measured insertion torque is observed for T10, T11, and T12 (Fig. 29: yellow, light blue, and green line, respectively) after approximately 85 seconds of insertion, which is equivalent to 5-7 rotations of the TIVAD prototype. In the case of T7, T8, T9 (Fig. 29: dark blue, orange, and grey line, respectively), a more gradual increase of torque is visible, with maximum measured torques of 0.400Nm, 0.454Nm, and 0.326Nm, respectively (Table 6). This significant difference between the measured insertional torque between the inferior and superior thoracic VBs can be justified by the fact that cadaver 1 was suffering from ankylosing spondylitis (AS). Research has shown that AS can result in unexpected low bone mineral densities (BMD) across the thoracic and lumbar region (Hinze & Louie, 2016). This means that it can affect a few VBs and not the entire spine. As a result, the low VB BMD value offers less resistance against the TIVAD while it is being inserted. Therefore, the insertional torque values are lower.

The torque measurement results of the lumbar region of cadaver 1 are displayed in Fig. 30. It was observed that L3 and L4 require a max torque that is almost twice as high compared to the max torque results of L1 and L2 (Table 6). The cadaver's AS condition may have affected these two VBs (L1 & L2) as well, just as it did with T7, T8, T9. As depicted in Table 6, the maximum insertional torque values for L3-L5 are closer to the maximum insertional torque results found in the studies by (Carmouche et al., 2005). The same applies to the insertional torque measurements in the lumbar VB of cadaver 6, which are shown in Fig. 31 and included in Table 6. Especially for L4, as

the maximum measured torque in this CVB is exactly in line with what is published by Carmouche et al. (2005). To end with, the great variance in maximum insertional torque values among the tested CVBs indicates that the BMD of the VBs (Cadaver 1 & 6) have a significant disparity in trabecular bone structure & density. As depicted in Table 6, four insertional torque ranges are identified to be able to categorize each sample (both SBS and CVB). The SDs of T10/T11/T12/L3/L4/L5 (cadaver 1) and L1 (cadaver 6) are relatively high ($SD > 0.100$) compared to the other VBs. This indicates that the range of applied insertional torque is bigger than the VBs with smaller SDs. The reason for this greater range can be explained by the fact that during the insertion process, rotations of roughly 180 degrees were applied, followed by an overgrip to reposition the wrist, and grab again onto the grip. During this overgrip process, a 0 Nm torque measurement is read by the torque sensor. As these specific VBs produced the highest maximum torques, it resulted in higher SD values.

Based on the results of the stage 1 & 2A tests, it can be concluded that hypothesis 1 is confirmed. Furthermore, during the stage 2A test, no mechanical performance-related failures are reported. However, stage 2A showed various interesting insights with respect to usability; these are discussed in section 4.1.7.

Table 6 | Insertion torque table SBS vs. CVB

		Group 1 (0.0 – 0.4) [Nm]	Group 2 (0.4 – 0.8) [Nm]	Group 3 (0.8 – 1.2) [Nm]	Group 4 (1.2+) [Nm]	Mean torque [Nm]	SD	Max. torque value [Nm]
SBS	PCF5					0.157	0.035	0.245
	PCF20					0.218	0.071	0.393
	PCF30					0.254	0.095	0.473
Cadaver 1	T7					0.160	0.079	0.400
	T8					0.210	0.079	0.454
	T9					0.160	0.052	0.326
	T10					0.220	0.110	0.510
	T11					0.240	0.203	0.829
	T12					0.300	0.163	0.639
	L1					0.230	0.097	0.430
	L2					0.230	0.175	0.694
	L3					0.220	0.221	1.173
	L4					0.510	0.499	2.002
L5					0.350	0.255	0.847	
Cadaver 6	L1					0.460	0.407	1.487
	L2					0.350	0.170	0.768

Table 7 illustrates the QIA BMD results, including SDs, together with the mean and maximum torque that was required to insert the TIVAD implant into these three CVBs. It is surprising that the BMDs are rather high compared to the mean torque that was required to insert the TIVAD into these three CVBs. To be more specific, the mean mass density is calculated using scanIP to be 1.312 g/cm³ (SD: 0.072). As a reference, see Table 6, where a mean torque value of 0.218Nm and 0.254Nm was measured for the PCF20 and PCF30 SBS, with a density of 0.35 – 0.47 g/cm³, respectively.

The difference of factor 2.8 – 3.8 in BMD between the mean BMD of CVBs (T10/T11/T12) and the SBS (PCF20 & PCF30) is remarkable, to say the least since the required mean insertion torque for the CVBs was calculated to be between 0.220Nm - 0.300Nm. And the mean torque for the insertion into the SBS was calculated between 0.218Nm - 254Nm. The difference in mean torque is by no means greater by a factor of 2.8 – 3.8. For more information about this noteworthy finding, see section 6.2.

The maximum measured insertional torque values are higher compared to the ones measured in the SBS. They are ranging from 0.245 – 0.473 Nm in the SBS and 0.510 – 0.829 Nm in the CVB. This difference can be justified by the cortical shell that first need to be penetrated by the threads in the CVB. The SBS did not have such a cortical shell, as they exist foam blocks that only mimic the trabecular bone.

Table 7 | QIA BMD Results & Insertional torque results Stage 2A

Specimen	Mass Density		Insertional Torque		
	BMD [g/cm ³]	SD	Mean torque [Nm]	SD	Maximum torque [Nm]
T10	1.301	0.126	0.220	0.110	0.510
T11	1.246	0.165	0.240	0.203	0.829
T12	1.390	0.213	0.300	0.163	0.639
Mean	1.312				
SD	0.072				

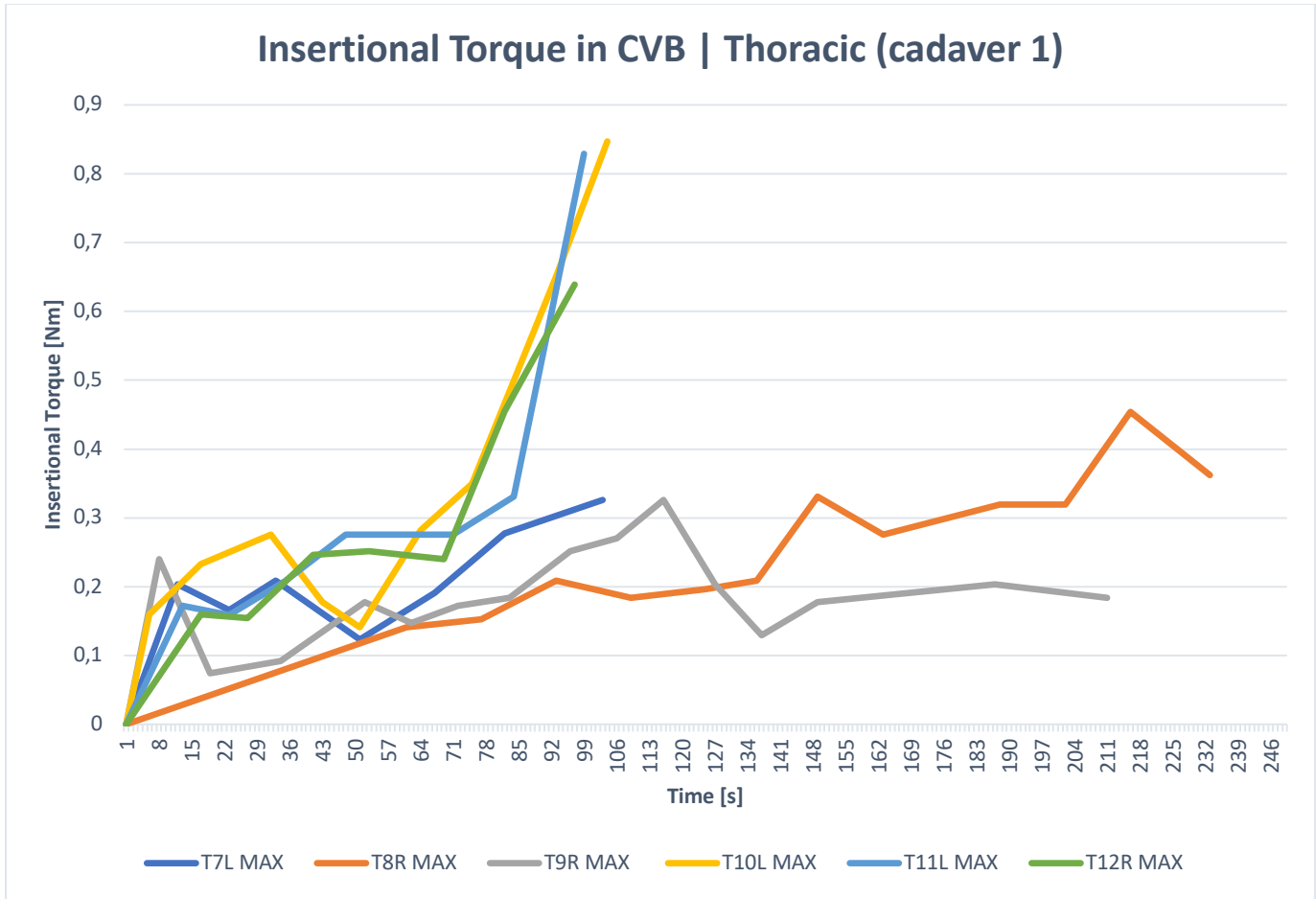


Figure 29 | Insertional Torque in CVB (thoracic region, cadaver 1)

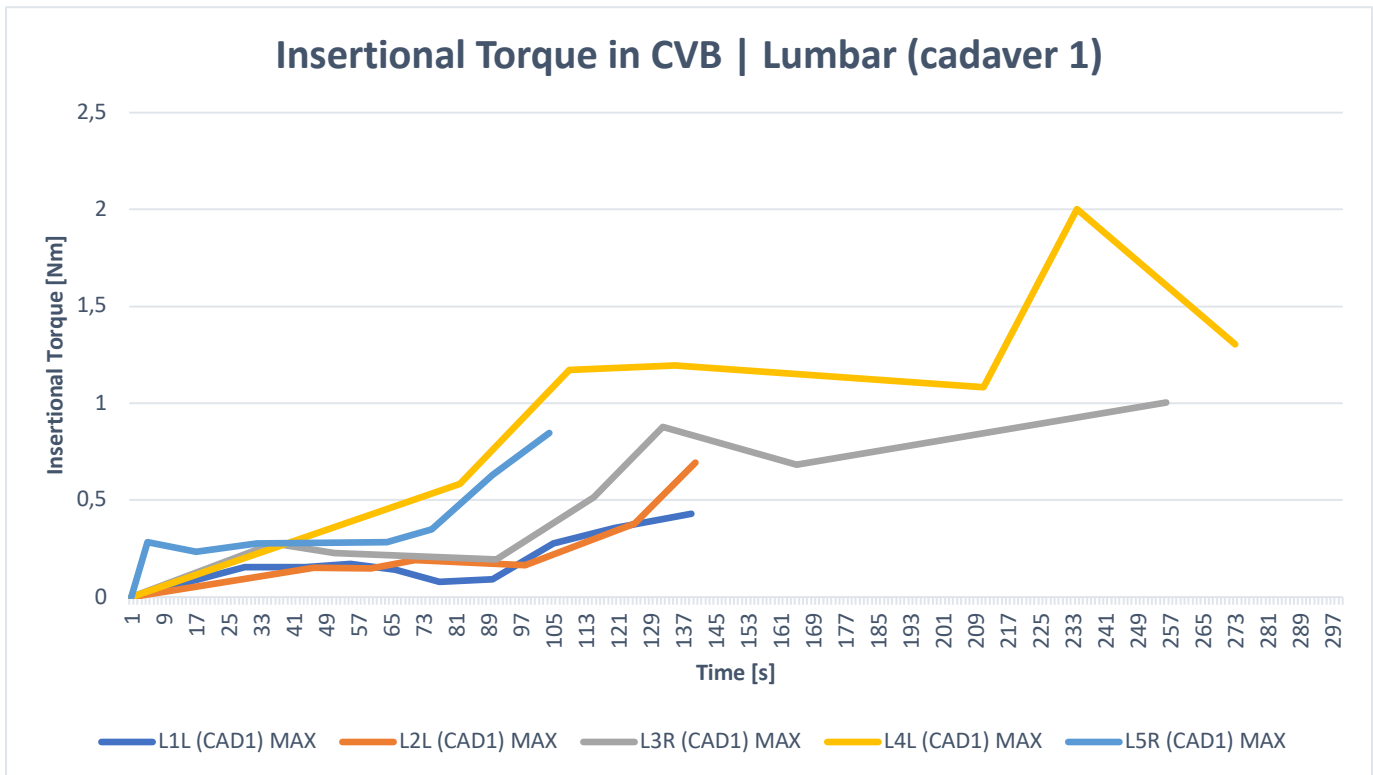


Figure 30 | Insertional Torque in CVB (lumbar region, cadaver 1)

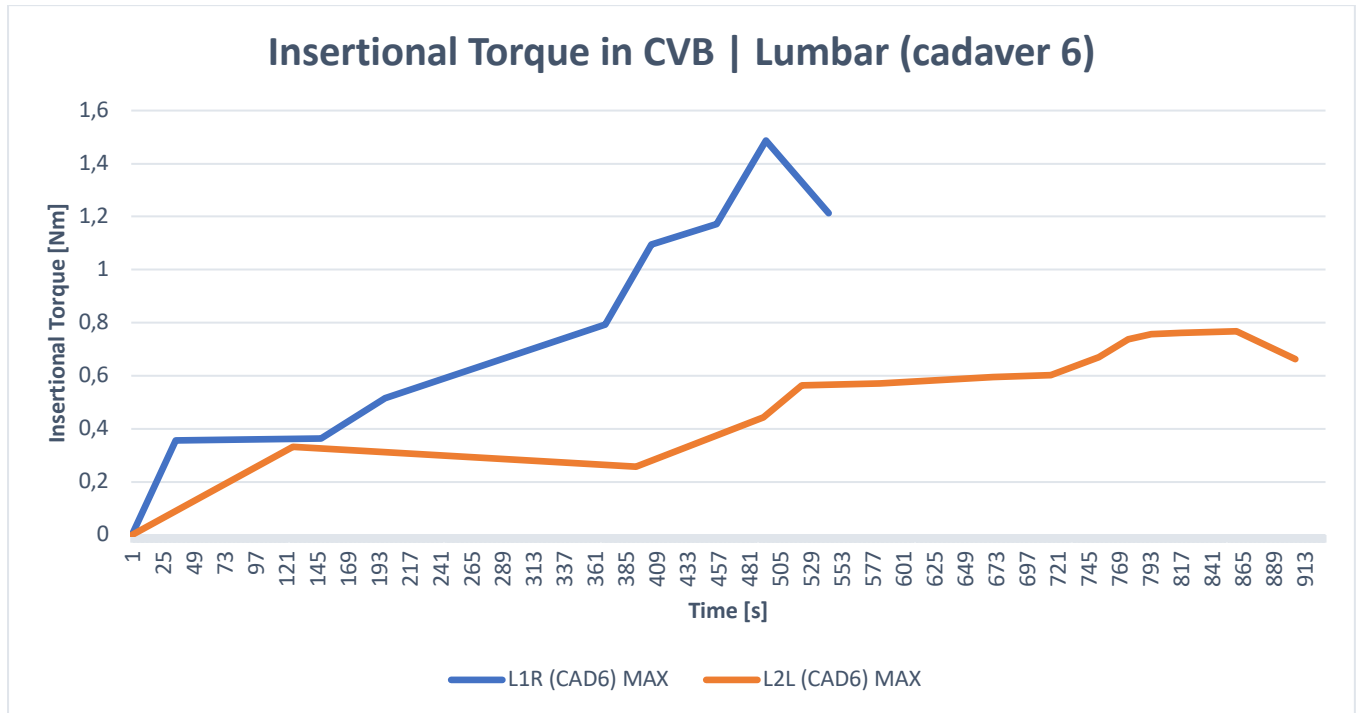


Figure 31 | Insertional Torque in CVB (lumbar, cadaver 6)

4.1.6 Stage 2B – TIVAD Expansion torque results (CVB)

Fig. 32 illustrates the torque results over time (from a closed to fully expanded state) that are required for the expansion of the TIVAD prototype in the CVBs of cadaver 5 & 6. During the expansion of the TIVAD into CVB T7 and T9, the peak torque values of 0.288Nm and 0.411Nm, respectively, were measured. However, these values were reached in the first half of the TIVAD expansion process and not in the second half, which would make more sense, as more resistance should be given by the internal VB trabecular bone structures and cortical shell. The required torque for TIVAD expansion even seems to decrease over time (read: the more the TIVAD is expanded). Moreover, Fig. 32 confirms that the expansion torque measurement results for L1 are contradictory compared to those of T7 and T9 since the expansion torque measurements increase over time and are thus in line with hypothesis 2. However, it is noteworthy to mention that T7 & T9 were from cadaver 5 and L1 from cadaver 6. The cause for the decrease of the torque required for TIVAD expansion in cadaver 5 could be that the CVBs are more osteoporotic compared to cadaver 6.

Table 8 depicts that the mean value for TIVAD expansion was 0.172Nm for T7 and T9 (cadaver 5) with a SD of 0.044 and 0.069, respectively, and 0.256Nm for L1 (cadaver 6) with a SD of 0.096. The maximum measured torque values are 0.288Nm, 0.411Nm, and 0.666Nm, respectively. However, this maximum torque, of 0.666Nm, was measured at a certain moment during the expansion where the expansion screw failed. Further information about this failure can be found in section 6.2.1.2.

Finally, based on the maximum measured torque values and the observations made during these TIVAD expansion tests, it can be concluded that between the range of 0 – 0.666Nm, no problems occurred with respect to usability concerns, such as a difficulty for the surgeon to apply the force and/or a slipping grip or failure of the TIVAD expander.

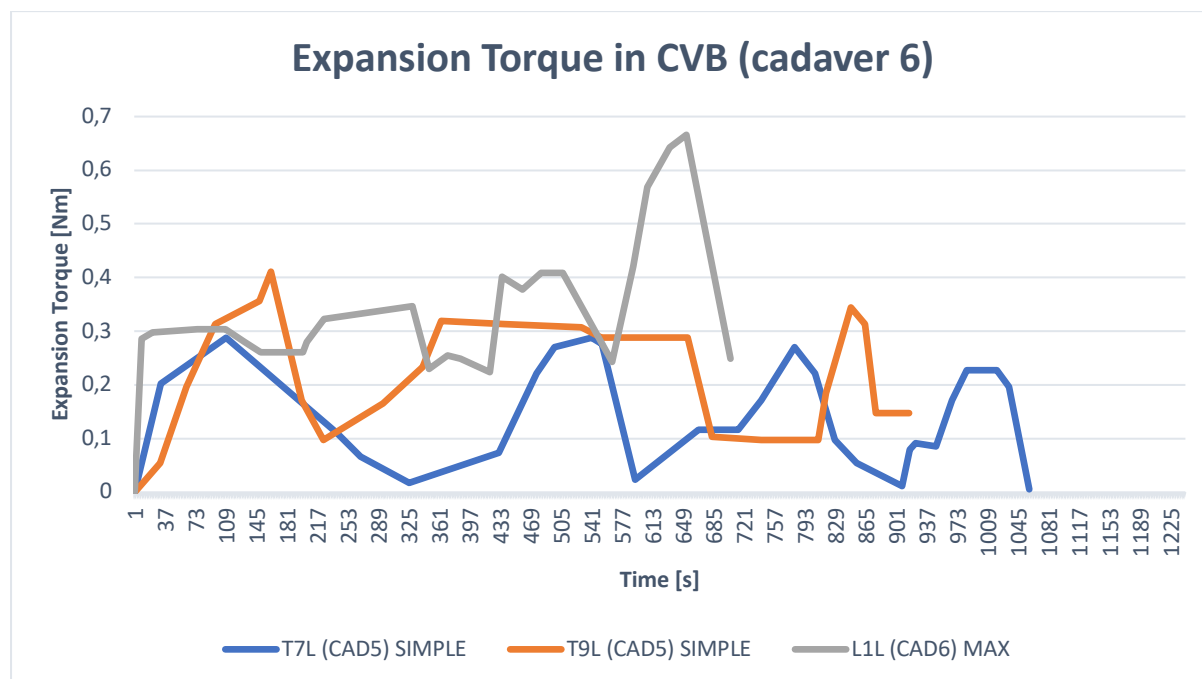


Figure 32 | Expansion Torque in CVB (cadaver 5: T7, T9; cadaver 6: L1)

Table 8 | TIVAD Expansion torque results

		Mean measured expansion torque [Nm]	SD expansion torque	Max. measured expansion torque [Nm]
Cadaver 5	T7	0.172	0.044	0.288
	T9	0.172	0.069	0.411
Cadaver 6	L1	0.256	0.096	0.666

4.1.7 Usability test results

While performing the TIVAD insertion and expansion torque measurement tests, simultaneously, attention was paid to the usability aspects of the TIVAD surgical procedure. This allowed me to observe and evaluate how the non-essential and essential TIVAD instruments interact with each other step-by-step. Nevertheless, the emphasis was put on the interaction between the TIVAD implant and the inserter and

expander instrument, with factors such as connection time, connection success rate, user feedback, and handle ergonomics.

4.1.7.1 Usability test results

Handle ergonomics

It is recognized that handle design impacts usability immensely. This finding is confirmed by various observations during the experimental tests on the CVBs. First, the wrist position is influenced significantly by the shape of the handle and the way the user grasps onto the handle. See Fig. 33, where both a T-shaped and a straight handle are displayed. It is immediately visible that the wrist position with the straight handle design is not comfortable (angled wrist joint indicated by red arrows) and that this problem is easily solved by the usage of a T-shaped handle (see straight wrist joint).



Figure 33 | T-shaped handle (left) vs. straight handle (right)

Furthermore, during the stage 2A test, insertional torque values higher than 1Nm were measured; this resulted in a slipping grip when the straight handle designs were used. This effect could worsen during the TIVAD surgical procedure when the user's hands are covered with blood and body fluids which does not improve the grip. During the tests where T-shaped handles were used, the slipping issue was not observed. Based on these observations, it can be supposed that the T-shaped handles provide more leverage which enables the application of a higher force.

Moreover, the handles have been tested with different test users, as different hand sizes should also be taken into consideration when the most ideal handle design and dimensions are chosen. Table 9 shows the hand dimensions (Appendix 8 shows how

this is measured) of the four test subjects that participated in the usability test, and Fig. 34 shows how different handle designs and sizes impact usability. Moreover, according to the test subjects, a thicker grip provides better control over the force that is applied, especially in cases when micro-adjustments are required. Therefore, the dimensions of the final TIVAD inserter & expander handles will be increased.

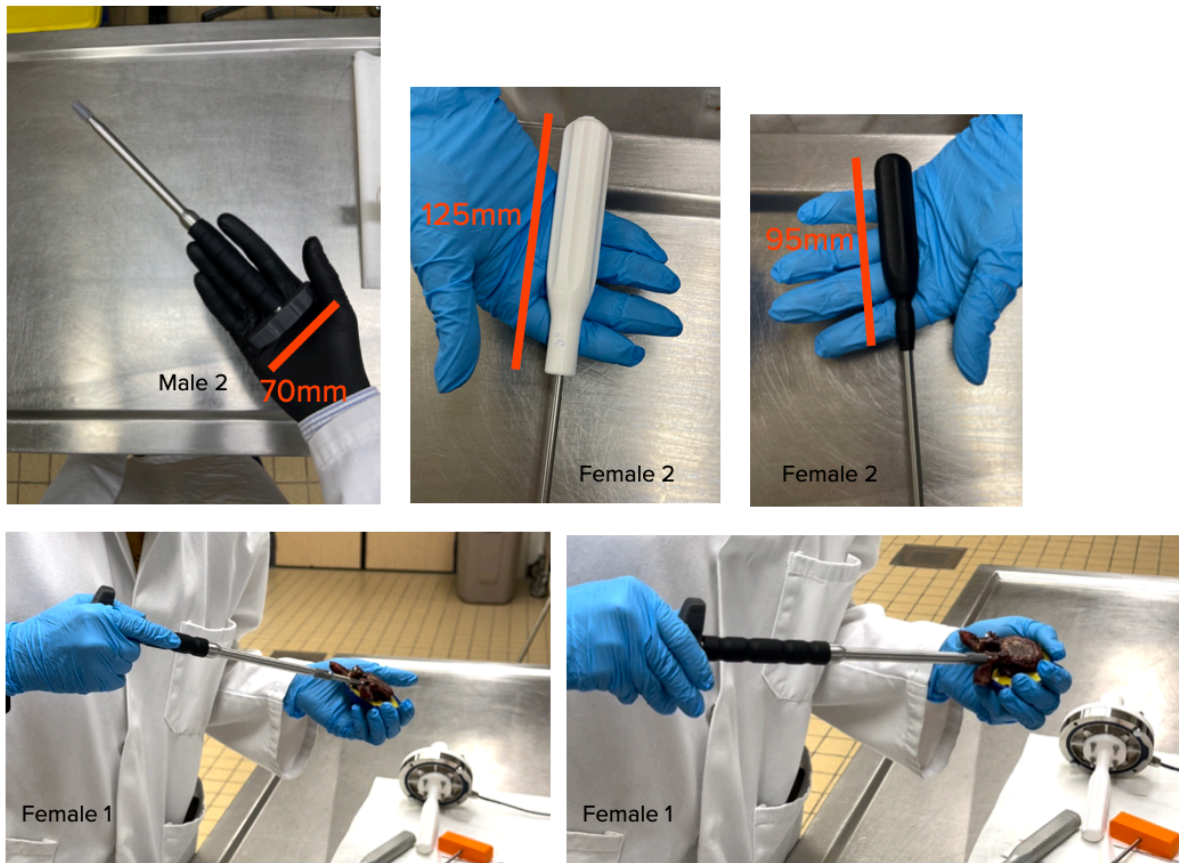


Figure 34 | Handle dimensions tests with different hand size

Table 9 | Hand dimensions test subjects

Test subject	Length [mm]	Circumference [mm]
Male 1	250	220
Male 2	256	223
Female 1	170	195
Female 2	170	190

TIVAD inserter | TIVAD prototype

Fig. 35 shows the TIVAD inserter (Concept 3) in use during the stage 2A experimental test (performed by Dr. van Urk). The usability of the TIVAD inserter is assessed with the help of the requirements in the LoR. With respect to connection speed, connection reliability, and force transfer, the TIVAD inserter performed as intended, and no major issues were observed. Furthermore, the 2-in-1 design showed to be beneficial, as the TIVAD expander's tip was guided perfectly through the circular

cavity in the TIVAD inserter to ensure quick and successful attachment to the TIVAD's expander screw (Fig. 36). Moreover, the attachment onto the TIVAD went quickly without any problems, and both did not come loose unexpectedly.

Lastly, the TIVAD prototype needs to be positioned in a way that the expansion is perfect in a linear way inferiorly and superiorly (100% vertically) since previous cadaver tests have shown that the TIVAD's performance decreases when positioned under an angle. To make sure that the expansion mechanism is placed vertically, the handle features an 'I' (for inferior) and 'S' (for superior). However, this was not immediately clear for the test user. Therefore, it would be beneficial to replace the letters with a visual use-cue that indicates that a specific side is up.



Figure 35 | TIVAD Inserter (Concept 3) during experimental test



Figure 36 | TIVAD Inserter (Concept 3) & Expander (Concept 1, still with straight handle) in action

TIVAD expander

The TIVAD expander that was tested during the stage 2B tests had a straight handle design, which was 3D printed in black PLA. The combination of geometric shape and color made it very hard to keep track of the number of rotations (15-17 full rotations required, depending on TIVAD size). It is important to know the number of successful rotations as this is directly correlated to the TIVAD expansion status.

During the third attempt to expand the TIVAD prototype, a failure of the TIVAD expansion screw was noticed at a torque of 0.666Nm, as mentioned in section 4.1.6. This occurred close to the connection interface between the implant expander and expansion screw, which is a hex connection. Obviously, this is a disaster if it were to happen during a real surgery. Therefore, this issue needs to be solved as soon as possible with the highest priority.



Figure 37 | TIVAD expansion screw (left), inside TIVAD implant (right)

The failure was seen exactly on the line/boundary where the hexagon shape transfers into the thread of the expansion screw (Fig. 37). It is not surprising that the TIVAD expansion screw failed at this specific point. Due to the abrupt change of shape, stress concentrations build up, causing the TIVAD expansion screw to fail. Recommendations on how this issue can be solved are mentioned in sections 6.2 and 6.3.

Thereafter, changes were made regarding the drilled hole size diameter, from an undercut of 1mm to a diameter which is the same as the anterior TIVAD to the exact same diameter as the anterior TIVAD has, and a proper cleaning step of the cavity was added, which ultimately resulted in two successful expansions. During the two following attempts, the TIVAD expander was used as intended (through the cannulated implant inserter, see Fig. 36); accordingly, the tip of the TIVAD expander found the TIVAD expansion screw rather easy, which resulted in successful attachments.

No issues were observed transferring force from the user onto the handle and subsequently from the TIVAD expander onto the TIVAD expansion screw.

In summary, it was no problem to apply the required force with the straight handle. The only issue related to the straight handle was the rotation counting problem. This problem was not observed with tests where a T-shaped handle was attached to the TIVAD expander. This can be explained based on the nature of how a T-shaped handle is used. As a human's wrist freedom of motion is not limitless, the user must overtake his/her grip every ± 180 degrees after a clockwise rotation (Fig. 38). The fact that the user must change his/her grip after every 180 degrees helps significantly in keeping track of how many rotations are performed; this conclusion has been confirmed by the test subjects.

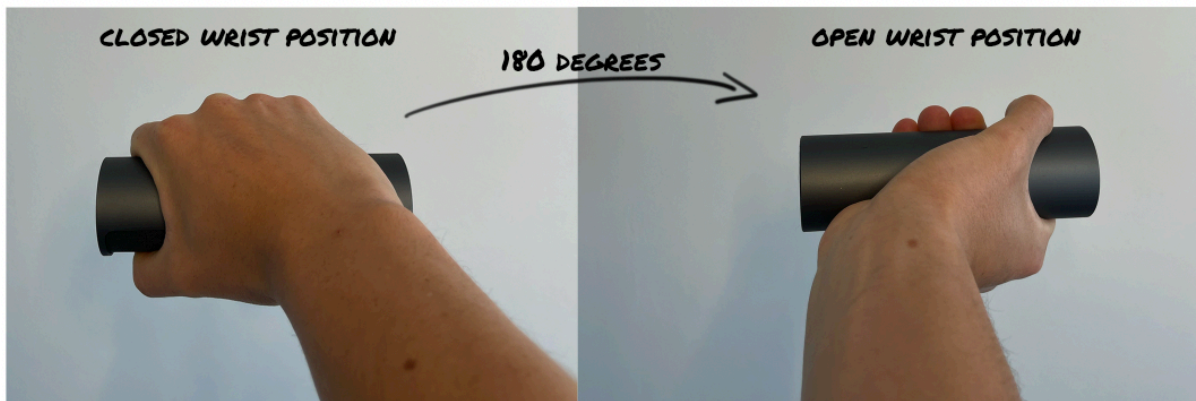


Figure 38 | Wrist position

4.2 Risk assessment

The aim of the risk assessment is to identify any unforeseen risks and try to mitigate these risks as much as possible. From a regulatory perspective, risk management is a requirement to be compliant with the EU MDR 2017/745. The regulation states that the legal manufacturer must establish, document, implement and maintain a system for risk management (European Union, 2017). More information can be found in Annex I Chapter I of the EU MDR 2017/745. Furthermore, the risk assessment procedure for medical devices is described in the ISO 14971:2019¹ and ISO 24971:2020² standards, in Annex C and F, respectively. Generally, the risk assessment is applied to the entire product lifecycle. All the way from the research & development phase to production, during use, and disposal of the medical device. For this thesis, the risk assessment is split up into a general risk (safety hazards) assessment matrix (Appendix 11) and a matrix that focuses on usability (TIVAD surgical procedure) related risks (Table 10). Table 22 in Appendix 11 shows how the risk factor is determined based on the risk severity and the probability.

As a conclusion of the performed risk analysis, it can be stated that from the TIVAD SIS itself, essential and non-essential, acceptable and tolerable risks are expected as summarized in Table 23 (Appendix 11). Major hazards, like the multiple use of single-use SIS and abrasive sterilization methods (off-label use, but this development is seen in hospitals nowadays to reduce costs), should be deemed to minimize the risks. Following the proposed risk mitigation steps of identified hazards, more benefits than risks are identified regarding the TIVAD SIS for the patient and surgical team, resulting in a positive balance.

However, it should be considered that updating and re-evaluating the risk analysis, based on new experiences, and probably changed state-of-the-art technologies, on a regular basis is crucial. Data should be generated during the design & development process, production, and in this case, especially post-market surveillance due to malpractice, according to current literature (Cancel, 2016).

¹ This document specifies the terminology, principles, and a process for the risk management of medical devices, including software as a medical device and in-vitro diagnostic medical devices. The process described in this document intends to serve manufacturers of medical devices to identify the hazards associated with their medical device, to estimate and evaluate the associated risks, to control these risks, and to monitor the effectiveness of the controls.

² This document provides guidance for the development, implementation, and maintenance of a risk management system for medical devices according to ISO 14971:2020.

Surgery phase	Surgical procedure step	Foreseeable event	Hazardous situation	Risk factor	How to mitigate the risk?
Pre-surgery	Unpack TIVAD inserter and expander	Drop the TIVAD inserter and expander onto the ground	Tip of both TIVAD inserter and expander might break	2C	Explicitly mention in IFU that after dropping an instrument, a visual inspection must be performed to assess if any damage is done to the instrument that is dropped onto the ground
		Damage to sterile packaging	The use of unsterile products can lead to infections	2B	Check sterile barrier before opening packaging on any damages
	Nurse handing TIVAD inserter or expander over to the surgeon	Drop the TIVAD inserter and expander onto the ground	Tip of both TIVAD inserter and expander might break -> surgeon might	2C	Explicitly mention in IFU that after dropping an instrument, a visual inspection must be performed to assess if any damage is done to the instrument that is dropped onto the ground
Pedicle preparation	Skin incision	A hole that is too big	Bigger incision --> higher risk of infection	2E	Explicitly mention in the IFU the required incision length
	Dilator insertion	Damage soft tissues with dilator tip	damaged muscles/tendons	2D	Insert dilator in a delicate way
	Jamshidi insertion	Trocar insertion is too converging through the pedicle	Sharp trocar tip can move towards vertebral foramen and damage/penetrate the spinal cord	1B	Jamshidi insertion process is closely monitored using FS from A/P and lateral views
		Trocar insertion is too deep	Sharp trocar tip penetrates anterior VB wall and can damage/penetrate vena cava	1B	Jamshidi insertion process is closely monitored using FS from A/P and lateral views

	Retracting inner Jamshidi needle	by accident, also retract the outer Jamshidi needle	Surgeon loses the point of VB entry, depth, and orientation of sequel surgical instruments	3D	Push down the outer Jamshidi Needle while retracting the inner Jamshidi needle
	Inserting k-wire through outer Jamshidi needle	push too hard while inserting the k-wire	the surgeon can push k-wire through the anterior VB wall	1B	K-wire insertion process is closely monitored using FS from A/P and lateral views
	Retracting outer Jamshidi needle	by accident, also retract k-wire	Surgeon loses the point of VB entry, depth, and orientation of sequel surgical instruments	3D	Push down on the posterior tip of k-wire while retracting outer Jamshidi needle
TIVAD hole preparation	Drilling over the k-wire (with a cannulated drill)	Drill too deep	Anterior VB wall can be damaged	1B	The drilling process is closely monitored using FS from A/P and lateral views
	Retract cannulated drill and k-wire	not linear retraction of cannulated drill and k-wire can damage TIVAD implant cavity	TIVAD implant insertion process might be difficult	1D	retract cannulated drill and k-wire in a linear movement
TIVAD insertion	Insertion of TIVAD implant	The surgeon rotates the TIVAD inserter into the wrong direction	TIVAD implant is not being inserted	3E	Apply arrows for the correct rotation direction on the TIVAD inserter handle & mentioned insertion rotation direction explicitly in IFU
		Inserting the TIVAD implant to incorrect depth	TIVAD expansion might cause problems	2D	Verify correct TIVAD depth using FS from A/P and lateral views
		TIVAD is not positioned perfectly vertical	TIVAD expansion under an angle, which decreases its performance	2D	Arrows on the TIVAD inserter handle indicate what part of the handle has to face up

		By accident retract the TIVAD inserter	TIVAD inserter decouples from TIVAD attachment point (tulip)	2D	Design features have been added that make it difficult to detach the TIVAD inserter accidentally from the TIVAD
TIVAD expansion	Expansion of TIVAD	TIVAD expander does not connect properly to the expansion screw	The surgeon is not able to expand the TIVAD	2D	
		The surgeon rotates the TIVAD expander into the wrong direction	TIVAD is not being expanded	3E	Apply arrows for the correct rotation direction on the TIVAD expander handle & mentioned expansion rotation direction explicitly in IFU

Table 10 | Risk analysis – Usability

5. The embodiment

5.1 Material selection

This section covers the material selection process for the TIVAD inserter & expander's shaft and their handles. Based on the input from material experts (TU Delft) and CES Edupack, the material selection was performed, shown in Tables 11 & 12. The materials covered in the tables are very commonly used materials for surgical instruments.

The mechanical properties can't be neglected. With the CES Edupack engineering solver plug-in, the minimum Shear stress (GPa) and Yield strength (MPa) are calculated, which the material must endure (Appendix 12).

TIVAD Inserter shaft (Applied torque: 2 Nm, safety factor 2):

Min. shear modulus (GPa) = 35.9

Min. yield strength (MPa) = 50.1

TIVAD Expander (Applied torque: 1Nm, safety factor 2):

Min. shear modulus (GPa) = 67.5

Min. yield strength (MPa) = 141

Table 11 | TIVAD Inserter & Expander shaft material overview

Property	304 SS	316 SS	Titanium	Tantalum	Platinum	Palladium
Biocompatible	yes	yes	yes	yes	yes	yes
Ethylene oxide sterilization resistant	yes	yes	yes	yes	yes	yes
Steam autoclave sterilization resistant	excellent	excellent	excellent	excellent	excellent	excellent
Price/kg (€)	2,58	3,31	201,10	259,00	22.400,00	25.900,00
Density (kg/m ³)	7850	7870	4410	16500	21500	12000
Young's modulus (Pa)	1.9*10 ¹¹	1.89*10 ¹¹	1.1*10 ¹¹	1.75*10 ¹¹	1.68*10 ¹¹	1.18*10 ¹¹
Yield strength (Ys) (Pa)	2.05*10 ⁸	2.05*10 ⁸	7.68*10 ⁸	1.35*10 ⁸	7.83*10 ⁶	9.81*10 ⁶

Shear Modulus (GPa)	74	74	40	64	60	42
Max. service temp (Celsius)	750	750	350	1370	340	280
Malleable	high	high	high	high	high	high
Ductility	high	high	high	Very high	high	high
Corrosion resistance	less resistant than 316; no molybdenum	very resistant	100% resistant	highly corrosion resistant	highly corrosion resistant	highly corrosion resistant
Strength (related to Ys)	tough metal	tough metal	superior strength	less strength compared to SS	superior strength	superior strength
Weight (related to density)	N/A	N/A	40% lighter than SS	2 times heavy as SS	3 times as heavy as SS	1.5 times as heavy as SS

5.1.1 TIVAD Inserter

Most of the stainless-steel alloys are biocompatible and are generally resistant against corrosion and sterilization methods, such as ethylene oxide or steam autoclave sterilization. Furthermore, to be able to create a long cylindrical shape with a relatively small radius, as spine-related surgical instruments often have such a shape, a material needs to be highly malleable and ductile.

According to the calculated minimum Shear modulus and Yield strength, titanium seems a risky choice as its shear modulus is rather close to the 35.9GPa. Furthermore, due to the extremely high price/kg of tantalum, platinum, and palladium, they are not a plausible option. This leaves us with 304 & 316 stainless steel (SS), which are two very similar stainless-steel variants. The only difference is that 316 SS is more resistant to corrosion due to the presence of molybdenum, an alloy that drastically improves corrosion resistance, especially within saline or chloride-exposed environment, which is, for instance, the case in autoclaves (Granta Design Limited, 2020). As a result, the price/kg is slightly higher, but in this case, it is worth choosing 316 SS. Especially with the trend of re-use of single-use devices in mind as addressed in the risk assessment section.

5.1.2 TIVAD Expander

With the minimum Shear modulus requirement of 67.5 GPa, titanium, tantalum, platinum, and palladium are no options for the TIVAD expander's shaft. As a result, the choice is between the same materials as for the TIVAD inserter's shaft. To ensure the corrosion resistance characteristics, 316 SS is also the material of choice for the TIVAD expander's shaft.

5.1.3 TIVAD Inserter & Expander handle

There are two routes to take for the material choice for the handle. If the goal is to mitigate the risk of the re-use of single-use devices, the material of choice is nylon (see Table 12) as this polymer FDM filament has the best resistance, of the listed polymers, against steam autoclave sterilization which is commonly used in hospitals. All other FDM polymer filaments score poor or mediocre on this prerequisite. One downside is that Nylon's price is +/- 5 times as high as the other commonly used FDM polymer filaments.

If the re-use of single-use devices risk is not mitigated, the most suitable choice is POM since it ticks all the boxes regarding biocompatibility, EO sterilization, Young's modulus, and Yield strength. For reference purposes, the prototypes for the experimental test were printed with PLA and have shown no signs whatsoever of failure during the load application. However, POM scores better in all aspects.

Table 12 | TIVAD Inserter & Expander handle material overview

Property	PLA	Nylon	ABS	PC	ULTEM	POM
Biocompatible	excellent	excellent	poor	Poor (release bisphenol A at room temp.)	excellent	excellent
Ethylene oxide sterilization resistant	excellent	good	good	excellent	excellent	excellent
Steam autoclave sterilization resistant	poor	moderate	poor	marginal	marginal	marginal
Price/kg (€)	2,56	1,60	1,75	2,06	8,77	1,41
Density (kg/m ³)	1110	980	1010	1140	1200	1390

Young's modulus (GPa)	2.3	1.26	1.1	2.21	1.93	2.6
Yield strength (Ys) (MPa)	34	45.4	18.5	59	65	57.2
Shear Modulus (Pa)*10 ⁸	8.33	4.89	3.66	7.89	7	9.33
Max. service temp (Celsius)	45	197	63	128	?	83

5.2 Manufacturing technique

This section presents the chosen manufacturing process for each part of the TIVAD inserter and expander. The manufacturing technique decisions are based on interviews with surgical instrument manufacturing experts. With the final TIVAD inserter and expander designs as a starting point, various manufacturing techniques were evaluated. Based on the geometrical shape and features, suitable manufacturing techniques are chosen within the mind of what is practically possible and to find a balance between what shapes are required and how to manufacture these parts for an attractive price.



Figure 39 | TIVAD Inserter (front) & Expander (back) Exploded view

As shown in Fig. 39, both the TIVAD inserter and expander exist of two parts: a shaft and the handle. For both instruments, the same handle shape is used even though these handles have slight differences with respect to the use-cues they carry (rotation direction arrows). The handles are bonded to the shafts with an adhesive: Loctite 401. Because Loctite 401 is designed to assemble difficult-to-bond materials which require uniform stress distribution, strong tension, and/or shear strength, and more

importantly, the adhesive is biocompatible. Therefore, it is a widely used adhesive for bonding parts in medical devices. Furthermore, it provides rapid bonding of a wide range of materials, including metals and plastics, which is the case for the TIVAD inserter and expander and is resistant against ethylene oxide sterilization (Henkel, 2012).

The technical drawings are shown in Appendix 14 (Fig. 72 and Fig. 73).

5.2.1 TIVAD inserter & expander shaft



Figure 40 | Turning machine (left), Broaching machine (middle), 3-axis CNC (right)

For the manufacturing of the TIVAD inserter and expander shafts, three machines are required: a turning machine, broaching machine, and 3-axis CNC (see Fig. 40).

5.2.1.1 Manufacturing steps TIVAD inserter

Step 1 – Turning: reduce OD from 304L start cylinder to OD from TIVAD inserter tip (Fig. 41).

Step 2 – Turning: reduce OD from remaining shaft (Fig. 41)

Step 3 – Drilling: circular cavity for TIVAD expander pass through (Fig. 41)

Step 4 – CNC: create details of the shaft that connect with the TIVAD implant (tulip) (Fig. 41)

Step 5 – Broaching: create a posterior squared feature for handle attachment (Fig. 41)

Step 6 – Clean up

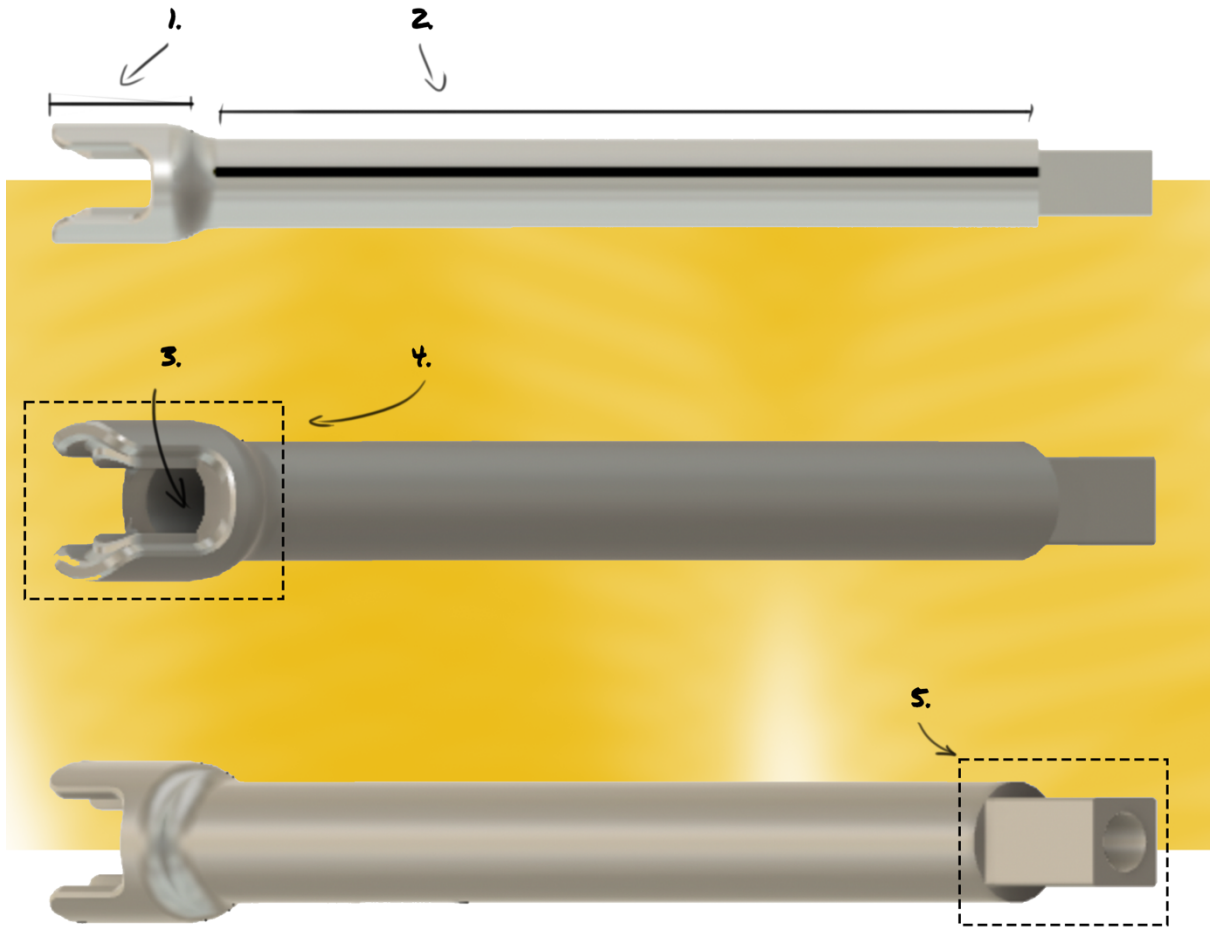


Figure 41 | TIVAD Inserter shaft

5.2.1.2 Manufacturing steps TIVAD expander

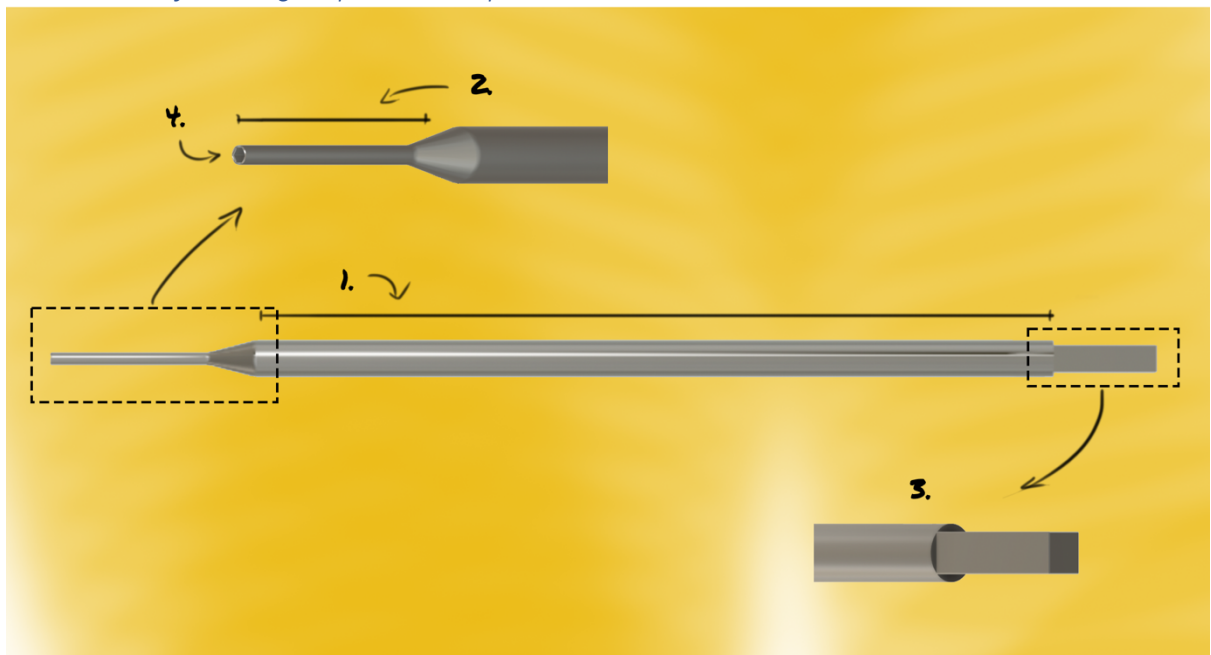


Figure 42 | TIVAD Expander shaft

Step 1 – Turning: reduce OD from 304L start cylinder to OD from TIVAD expander (Fig. 42)

Step 2 – Turning: reduce OD TIVAD expander front tip with chamfer detail (Fig. 42)

Step 3 – Broaching: create a posterior squared feature for handle attachment (Fig. 42)

Step 4 – Broaching: create a female hexagon indent (Fig. 42) for the TIVAD expansion screw connection

5.2.2 TIVAD handle

The Fused Deposition Modelling (FDM) 3D printing technique has been chosen to manufacture the handles of the TIVAD inserter and expander. This decision is based on the fact that Amber Implants wants to offer the ability to the user to customize their TIVAD inserter & expander handles.

With the FDM 3D printing method, many layers of material are fused together to create a new part. The fact that FDM has a low cost-to-size ratio and a variety of thermoplastic materials can be printed make it an attractive 3D printing technique.

The downside of FDM 3D printing is the build quality, which is a result of its character that the material is extruded in layers. These layers have a certain thickness that is predefined by the nozzle. To achieve a clean look, post-processing is needed.

5.2.2.1 Manufacturing steps TIVAD inserter & expander handle

Step 1 – Design part in CAD software (Fusion 360)

Step 2 – export as .STL file

Step 3 – import into slicing software and export .gcode

Step 4 – import .gcode file into 3D printer

Step 5 – start 3D print

Step 6 – post-processing / clean up

5.3 Cost price

The cost price for the TIVAD inserter and expander is composed of the machine costs, labor costs, material costs, and profit. See Table 13 for an overview of the costs. See Appendix 13 for a more detailed price calculation.

NOTE: for the cost price calculation, assumptions are made regarding the machine, labor, and material costs. These can highly variate dependent on the manufacturer and/or supplier.

Table 13 | Cost price overview – TIVAD inserter & expander

Part	Machine costs/ part	Labour costs/ part	Material costs/ part	Profit for Amber Implants	Total cost price per part
TIVAD inserter shaft	€ 8,00	€ 7,00	€ 0,78	20%	€ 18,94
TIVAD expander shaft	€ 8,00	€ 7,00	€ 0,16	20%	€ 18,19
TIVAD inserter handle	€ 3,64	€ 3,00	€ 0,66	20%	€ 9,00
TIVAD expander handle	€ 3,64	€ 3,00	€ 0,66	20%	€ 9,00

6. Final design

6.1 Description

As shown in Section 4, experimental evaluation, the final design of the TIVAD inserter and expander successfully contribute to the overall TIVAD surgical procedure in a way that they allow the surgeon to insert and expand the TIVAD implant and thereby restoring both the reduced VB height and alternated VB angle. This leads to pain relief and a better quality of life for the patient.

The final designs of these two essential TIVAD surgical instruments are the end product of an extensive design process (Fig. 43), including analysis, conceptualization, and experimental test phase, which distinguishes itself with its iterative approach.

The core features of the TIVAD inserter include an outside TIVAD implant tulip connection that enables a 2-in-1 approach with the TIVAD expander (Fig 44). This configuration allows space for a cavity that provides accurate guidance to the TIVAD expander and a successful connection rate onto the TIVAD expander screw. The elimination of PMMA bone cement results in the removal of PMMA bone cement-specific instruments and the additional surgical steps, such as PMMA bone cement preparation and injection. Given the possibilities to eliminate PMMA bone cement, the application of the 2-in1 approach surgical instrument set designed specifically for TIVAD ultimately allows fewer surgical steps, shorter and thus lower-cost surgeries, and fewer risks of infection. The TIVAD surgical technique is shown in Appendix 15 (Fig. 74).

The extensively tested custom T-shaped handle design ensures that the surgeon can accurately apply the required torque, improves the ability to count the number of rotations, and indicates the correct insertion direction with its use-cues that mitigate the risks of incorrect rotation direction for both insertion and expansion of the TIVAD implant.

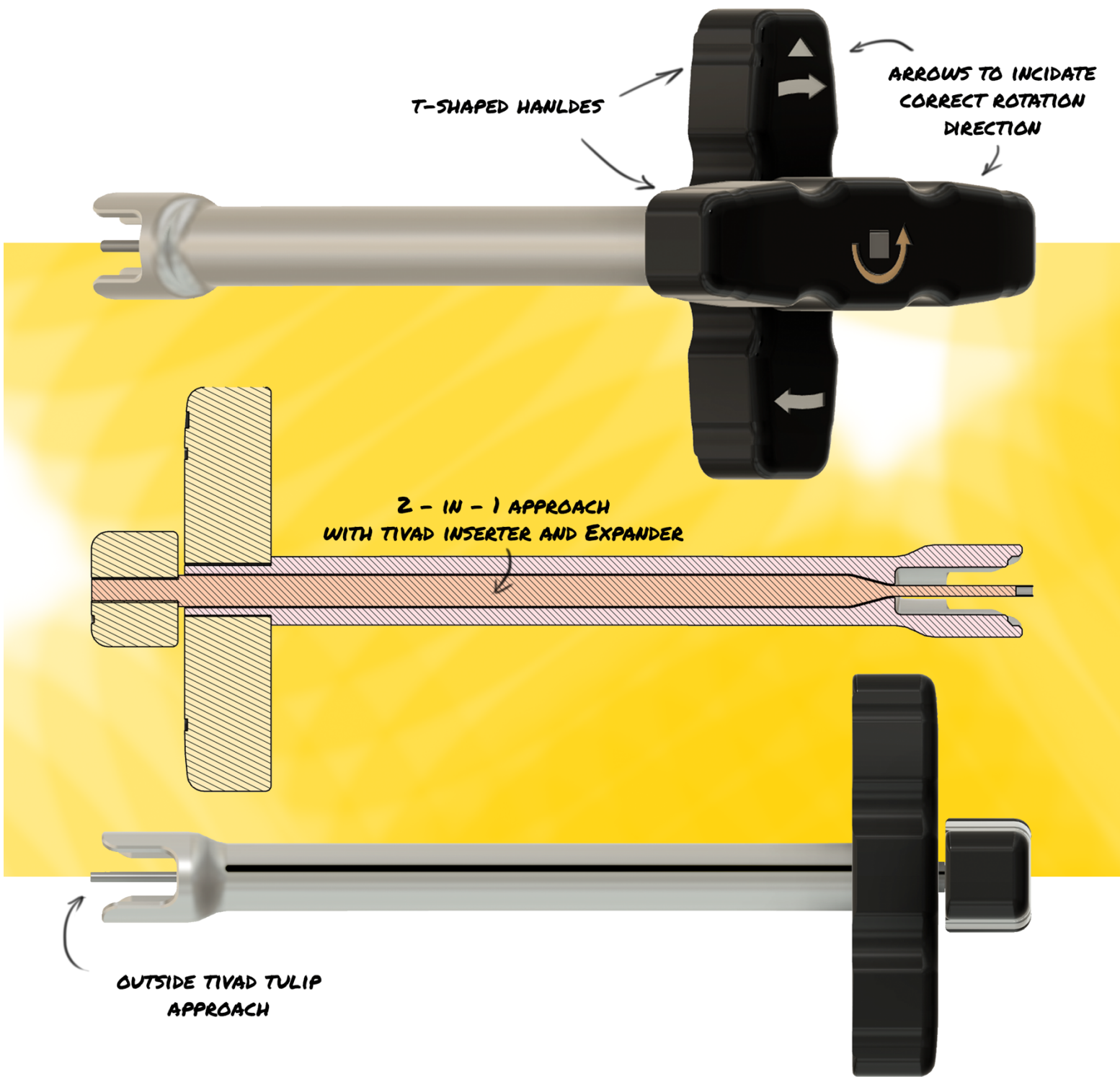


Figure 43 | Final TIVAD Inserter & Expander design

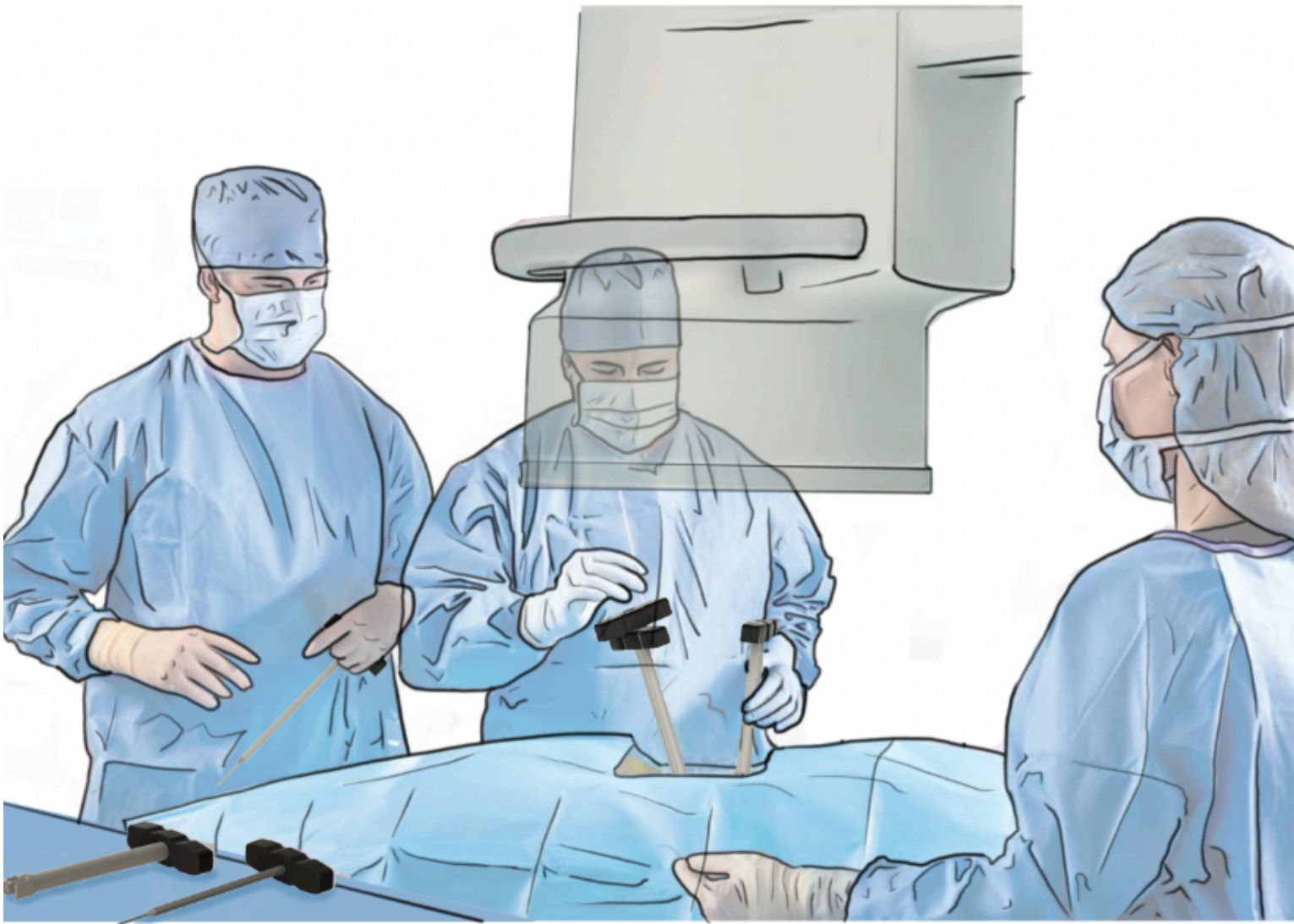


Figure 44 | TIVAD inserter and expander in use

By providing the surgeon with these abilities, the patient can be treated, and ultimately the pain and spine angle disturbance is solved or reduced significantly.

Fig. 44 illustrates the TIVAD inserter and expander when used in the real TIVAD surgical procedure, while Fig. 45 (left) provides a lateral view of the TIVAD inserter in action when the TIVAD is fully inserted. The latter depicts how deep (15-20mm) the tip of the inserter enters the patient's body.

Fig. 45 (middle) illustrates the addition of the TIVAD expander with the TIVAD fully expanded. Once the desired expansion height is reached, both instruments can be de-attached from the TIVAD and are ready for removal, Fig. 45 (right) shows that only the TIVAD will stay behind in the restored fractured VB.

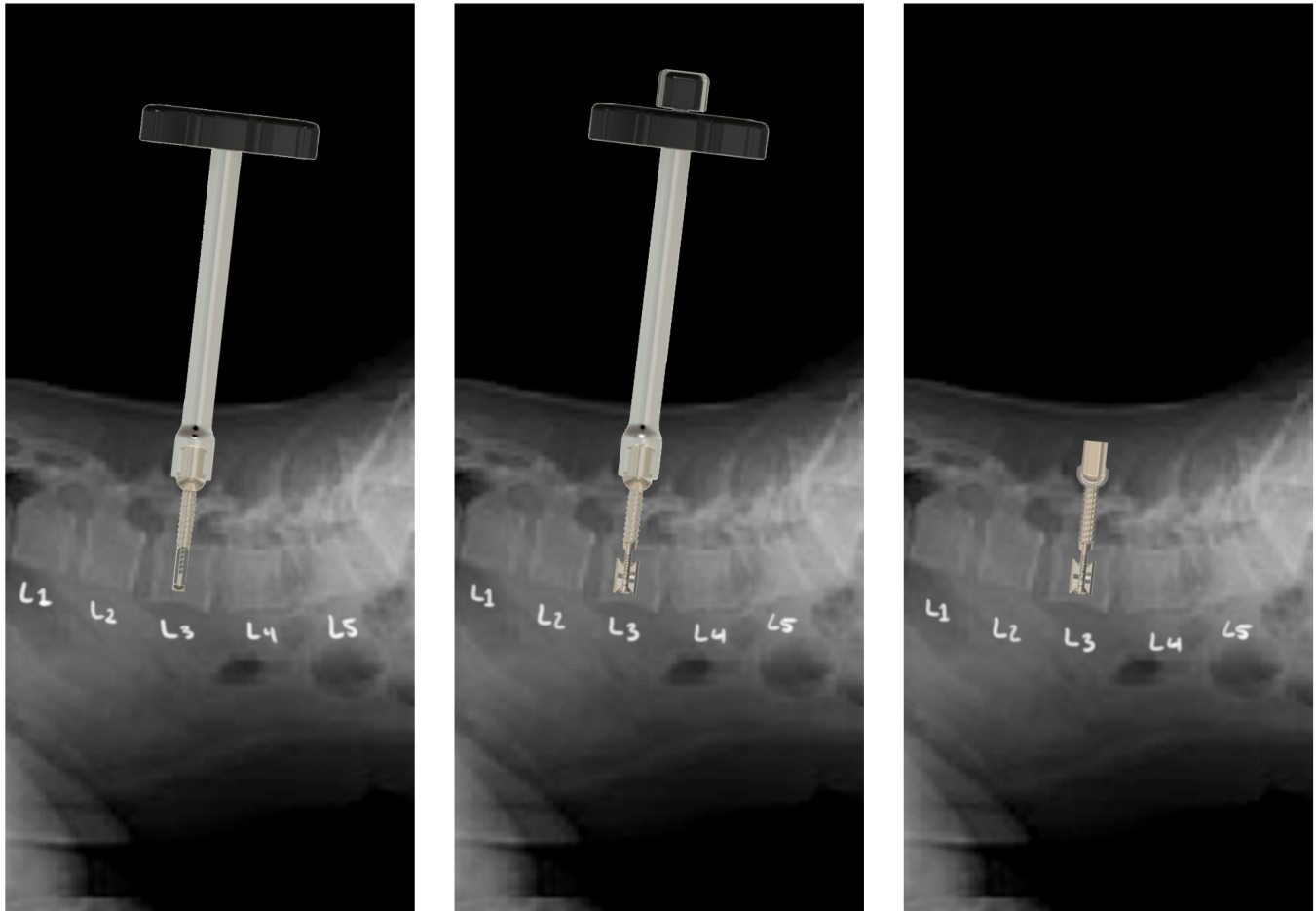


Figure 45 | TIVAD Inserter (left) & Expander (middle) in context (lumbar spine: L1-L5), patient in a prone position (lateral view), the dilator is not shown in this figure. TIVAD will stay behind in restored fractured VB (right)

Lastly, the ability that the FDM 3D printing technology adds to be able to change the design - of both the TIVAD inserter and expander handles upon user's preference – short lead times and low batch numbers sets the TIVAD inserter and expander apart from what is currently available on the market in terms of customization of surgical instruments for VCF related devices.

6.2 Discussion

6.2.1 Stage 1, 2A & 2B

6.2.1.1 TIVAD insertion into CVB – stage 2A

It is evident that the insertion torque values for T7-L1 are lower than those published by (Carmouche et al., 2005). This observation can be justified by the fact that the patient was suffering from the AS condition.

6.2.1.2 TIVAD expansion screw failure – stage 2B

Upon the evaluation phase, the failure of the TIVAD expansion screw is observed at 0.666Nm. After deep investigation, this failure is caused by the diameter that is drilled inside the pedicle of the VB. The size of this diameter was too small. Upon testing, it became clear that for the TIVAD implant to expand, the hole diameter should have at least the same as the diameter of the anterior part of the TIVAD and not a smaller diameter as was done before. Moreover, proper cleaning (pushing all loose bone particles, during drilling, to the cavity walls) of the hole before insertion proved also to be beneficial. This can be done with an additional surgical instrument called a template; for future testing, it is therefore recommended to add this SI to the TIVAD procedure.

6.2.1.3 Test environment

All experimental tests were performed on individual CVBs ex-vivo. This implies that the VBs were not attached to the inferior and superior CVBs. Besides that, the orientation is different, and their presence makes sure that forces act of the fractured VB from inferior and superior directions, which may affect the torque required for TIVAD expansion. Furthermore, because the VBs were not fixed during the performed experimental tests, it makes it hard to hold them during the insertion and expansion tests. As a result, the TIVAD inserter and expander are held horizontally instead of vertically (see Fig. 46). Therefore, it is highly recommended to perform additional tests in complete cadavers rather than on single CVBs in future experimental tests.



Figure 46 | Experimental test with TIVAD Inserter and CVB in a horizontal position

6.2.1.4 TIVAD Expansion results

Another observation raised the question: *Why did the torque not increase during TIVAD expansion in T7 & T9?*

The fact that the torque for TIVAD expansion did not increase over time with the TIVAD expansion attempts in cadaver 5 could be a result of the fact that the CVBs from cadaver 5 were very osteoporotic and especially the trabecular bone that is compressed by the TIVAD expansion plates during expansion.

6.2.1.5 Quantitative Image Analysis

How is a very similar mean insertional torque achieved with a BMD difference of factor 3,2?

The cause might be the presence of deviations in the QIA process. The first deviation might be that only three CVBs (T10/T11/T12) were scanned with the microCT machine. To reduce the rather big variance in the BMD measurements between CVB and SBS, it would be better if all samples, both SBS and CVB are scanned in the same microCT machine together with the same phantom attached in each scan.

Second, the density calculation is based on the initially set threshold in the scanIP workflow, as mentioned in Appendix 10. The selection of the threshold is rather subjective on visual perception and experience. Subtle differences in the threshold can significantly alter the results of the BMD measurement. Obviously, it has been done as good as possible, but there is always human error involved in the process.

Third, during this thesis, it was the first time that I've performed a QIA with the scanIP software, which may result in human error-like deviations. However, an extensive training workshop (via Zoom) from a technical support specialist from scanIP has been attended to be able to understand and work with the scanIP software.

Lastly, the difference in BMD composition between the two types of specimens obviously plays a huge role. The SBS have a homogeneously distributed density. Whereas the BMD of the CVBs is not homogeneously distributed due to the nature of real bone and bone diseases such as osteoporosis.

6.2.1.6 Additional features

During the interviews and surgery observation design features like feedback mechanisms or surgery navigation technology such as Brainlab were discussed. After consultation with experts, it turned out that the addition of these design features would not be profitable for a single-use SI. Therefore, they are not included during the development process.

6.3 Recommendations

The final design of the TIVAD inserter and expander have been tested in ex-vivo on single VBs in the anatomy lab (UMC Utrecht). The next step would be to test them in a cadaver that is intact, just like during the real TIVAD surgical procedure with patients. The fact that the region of interest (ROI) is significantly different in these 'in-vivo' tests, regarding visibility, surrounding tissues & organs, will most probably result in very interesting new insights that can improve the overall quality of the TIVAD-SIS and ultimately the entire TIVAD spine system. Based on these new insights, the risk analysis should be updated accordingly.

The selection of the manufacturing method for the TIVAD inserter and expander's shaft is based on manufacturing expert feedback. The manufacturing processes and techniques of the TIVAD inserter and expander and their delicate design features will have to be validated during further research, and testing needs to be performed.

The cost price indication is based on the basic assumptions related to manufacturing techniques, materials, operation and business, and input from manufacturing experts. To calculate the exact cost price of the TIVAD inserter and expander, further detailed research needs to be conducted.

Based on the studies performed by Mastrangelo et al. (2005) and Zadeh et al. (1997), which show that radiation-exposed orthopedic (spine) surgeons have a 5x higher chance on tumors, it is clear that there is a need to address the radiation exposure problem in the near future. This could be achieved by implementing input feedback design features or surgical navigation technologies, such as Brainlab or robotic surgery. The first technology reduces the number of FS images drastically as the surgical tools, fractured VB, and other important anatomical subjects carry tags that are visible in a digital environment which are visible to the surgeon on the monitors or even via augmented reality. The evolution of robotic surgery is even more promising since physical attendance is not required anymore during these procedures.

To ensure compliance with the EU MDR 2017:745, it is advisable for Amber Implants to perform a more extensive risk assessment that covers the entire lifecycle of the TIVAD SIS. Furthermore, to keep track of any adverse events while the MD is on the EU market and to be compliant with another requirement, namely: Post Market Surveillance (PMS) activities.

The EU MDR 2017:745 defines PMS as:

“All activities carried out by manufacturers in cooperation with other economic operators to institute and maintain a systematic procedure to proactively collect and review experience gained from devices they place on the market, make available on the market, or put into service for the purpose of identifying any need to immediately apply any necessary corrective or preventive actions” (European Union, 2017).

6.4 Conclusion

It is apparent that a safe and practical surgical technique to treat Vertebral Compression Fracture (VCF) is required more than ever. The existing VCF devices and their corresponding surgical tools have its limitation in terms of short- and long-term performance, efficiency, safety, and complications. This thesis has demonstrated that the newly developed TIVAD spine system can be used to overcome these limitations significantly by applying the specially designed TIVAD inserter & expander.

Through a knowledge-driven design process including a theoretical, empirical, and experimental evaluation phase, the TIVAD SIS is the end-product, which is supported by the non-essential and, especially, the essential surgical TIVAD instruments. The latter enables a two-in-one approach to insert and expand the TIVAD implant and thereby increases the ease of use and eliminates additional surgical tools.

But more importantly, while maintaining the benefits, it reduces the risk of unintended de-attachments during use significantly, which could be catastrophic or even lethal.

Moreover, it is noticeable that this TIVAD procedure outperforms the existing VCF solutions by omitting the use of PMMA bone cement. Consequently, the TIVAD procedure shows to be beneficial with fewer surgical steps and shorter surgical time. For patients, surgeons, hospital, and healthcare insurance, it means:

1. No need for specialized surgical instruments required for PMMA bone cement preparation and insertion (cheaper for hospital)
2. Less surgical steps → shorter overall surgery times (increased focus and comfort for the surgical team and especially the surgeon) → cheaper surgeries and lower risk of infection (patient, hospital & insurance)
3. No risks related to PMMA bone cement (patient)

What is the added value for the patient, the surgeon, and the hospital of the new TIVAD spine system?

The main goal of the TIVAD spine system is to relieve the pain and improve the patient's quality of life by using a time-efficient, safe, cost-saving, and comfortable surgical procedure. This is accomplished through the effortless collaboration between the TIVAD SIS and the TIVAD implant by restoring the reduced VB height and spine angle without the need for PMMA bone cement. This results in a huge added value with respect to the safety of the patient and the prevention of serious adverse events. This concern has been expressed explicitly by the surgeons during the interviews as a major critical weakness of the current VCF treatment.

How can the new TIVAD SIS add value to the overall TIVAD spine system?

The development of the new TIVAD SIS complements the TIVAD spine system, since the TIVAD SIS enables the surgeon to implant and deploy the TIVAD inside the fractured VB. This is achieved through its innovative two-in-one approach, unique connection design, cementless procedure, and custom-made handle possibilities.

To what extent can 3D printing technology contribute to the modularity and customizability of the new TIVAD SIS?

The ability to manufacture custom 3D-printed handles makes the TIVAD SIS appealing to surgeons who prioritize ergonomically designed surgical instruments to be able to work in a comfortable and efficient manner. The fact that such options are not available yet for SIS of competitors gives Amber Implants a strong competitive position in the VCF solution market.

References

- Becker, S., Dabirrahmani, D., Hogg, M., Appleyard, R., Baroud, G., & Gillies M. (2011). Disadvantages of Balloon Kyphoplasty with PMMA - a Clinical and Biomechanical Statement. *Journal Fur Mineralstoffwechsel & Muskuloskelettale Erkrankungen*, 18(1), 9–12.
- Berlemann, U., Ferguson, S. J., Nolte, L.-P., & Heini, P. F. (2002). Adjacent vertebral failure after vertebroplasty. *The Journal of Bone and Joint Surgery*, 84(5). <https://doi.org/10.1302/0301-620X.84B5.11841>
- Bidgood, W. D., Horii, S. C., Prior, F. W., & van Syckle, D. E. (1997). Understanding and Using DICOM, the Data Interchange Standard for Biomedical Imaging. *Journal of the American Medical Informatics Association*, 4(3). <https://doi.org/10.1136/jamia.1997.0040199>
- Buhler, D. W., Berlemann, U., Oxland, T. R., & Nolte, L.-P. (1998). Moments and Forces During Pedicle Screw Insertion. *Spine*, 23(11), 1220–1227. <https://doi.org/10.1097/00007632-199806010-00009>
- Cancel, M. (2016, September). *Insider study: single-use instruments facts everyone should know*. Sklar Research. <https://research.sklarcorp.com/single-use-instrument-facts-everyone-should-know>
- Carmouche, J. J., Molinari, R. W., Gerlinger, T., Devine, J., & Patience, T. (2005). Effects of pilot hole preparation technique on pedicle screw fixation in different regions of the osteoporotic thoracic and lumbar spine. *Journal of Neurosurgery*, 3(5), 364–370. <https://doi.org/10.3171/spi.2005.3.5.0364>.
- Cheng, L. M., Wang, J. J., Zeng, Z. L., Zhu, R., Yu, Y., Li, C., & Wu, Z. R. (2013). Pedicle screw fixation for traumatic fractures of the thoracic and lumbar spine. In *Cochrane Database of Systematic Reviews* (Vol. 2013, Issue 5). John Wiley and Sons Ltd. <https://doi.org/10.1002/14651858.CD009073.pub2>
- Cooper, C., Atkinson, E. J., Michael O'Fallon, W., & Melton, J. L. (2009). Incidence of clinically diagnosed vertebral fractures: A population-based study in rochester, minnesota, 1985-1989. *Journal of Bone and Mineral Research*, 7(2). <https://doi.org/10.1002/jbmr.5650070214>
- Cranney, A., Jamal, S. A., Tsang, J. F., Josse, R. G., & Leslie, W. D. (2007). Low bone mineral density and fracture burden in postmenopausal women. *CMAJ*, 177(6), 575–580. <https://doi.org/10.1503/cmaj.070234>
- Daftari, T. K., Horton, W. C., & Hutton, W. C. (1994). Correlations Between Screw Hole Preparation, Torque of Insertion, and Pullout Strength for Spinal Screws. *Journal of Spinal Disorders*, 7(2), 139–145. <https://doi.org/10.1097/00002517-199407020-00007>
- DePuy Synthes. (2016). *Vertebral Body Stenting - SURGICAL TECHNIQUE*. <http://emea.depuysynthes.com/hcp/reprocessing-care-maintenance>
- Dohm, M., Black, C. M., Dacre, A., Tillman, J. B., & Fueredi, G. (2014). A Randomized Trial Comparing Balloon Kyphoplasty and Vertebroplasty for Vertebral Compression Fractures due to Osteoporosis. *American Journal of Neuroradiology*, 35(12). <https://doi.org/10.3174/ajnr.A4127>

- European Union. (2017). (EU) MDR 2017/ 745. *Official Journal of the European Union*.
- Felsenberg, D., Silman, A., Lunt, M., Armbrecht, G., & Ismail, A. (2002). Incidence of Vertebral Fracture in Europe: Results From the European Prospective Osteoporosis Study (EPOS). *Journal of Bone and Mineral Research*, 17(4), 716–724. <https://doi.org/10.1359/jbmr.2002.17.4.716>
- Frank, R. M., Bradsell, H., & Thompson, S. R. (2021). What's New in Sports Medicine. *Journal of Bone and Joint Surgery*, 103(8), 653–659. <https://doi.org/10.2106/jbjs.21.00152>
- Frost, B. A., Camarero-Espinosa, S., & Johan Foster, E. (2019). Materials for the spine: Anatomy, problems, and solutions. *Materials*, 12(2), 253–259. <https://doi.org/10.3390/ma12020253>
- Galibert, P., Deramond, H., Rosat, P., & le Gars, D. (1987). Preliminary note on the treatment of vertebral angioma by percutaneous acrylic vertebroplasty. *Neurochirurgie*, 33(2), 166–168.
- Ghofrani, H., Nunn, T., Robertson, C., Mahar, A., Lee, Y., & Garmin, S. (2010). An Evaluation of Fracture Stabilization Comparing Kyphoplasty and Titanium Mesh Repair Techniques for Vertebral Compression Fractures. *Spine*, 35(16), 768–773.
- Giai, C., Rincón-Ortiz, M., Kappes, M. A., Senko, J., & Iannuzzi, M. (2016). Efficacy of Sterilization Methods and Their Influence on the Electrochemical Behavior of Plain Carbon Steel. *Journal of The Electrochemical Society*, 163(10), 456–461. <https://doi.org/10.1149/2.0271610jes>
- Granta Design Limited. (2020). *CES Edupack 2020 (20.1.1)*. Granta Design Limited.
- Han, K. -R., Kim, C., Eun, J. -S., & Chung, Y. -S. (2005). Extrapedicular approach of percutaneous vertebroplasty in the treatment of upper and mid-thoracic vertebral compression fracture. *Acta Radiologica*, 46(3), 280–287. <https://doi.org/10.1080/02841850510021058>
- Henkel. (2012). *LOCTITE® 401™ Technical Data Sheet*. www.henkel.com/industrial
- Henslee, A. M., Gwak, D. H., Mikos, A. G., & Kasper, F. K. (2012). Development of a biodegradable bone cement for craniofacial applications. *Journal of Biomedical Materials Research - Part A*, 100 A(9), 2252–2259. <https://doi.org/10.1002/jbm.a.34157>
- Hinze, A. M., & Louie, G. H. (2016). Osteoporosis Management in Ankylosing Spondylitis. *Current Treatment Options in Rheumatology*, 2(4), 271–282. <https://doi.org/10.1007/s40674-016-0055-6>
- Jay, B., & Ahn, S. (2013). Vertebroplasty. *Seminars in Interventional Radiology*, 30(03), 297–306. <https://doi.org/10.1055/s-0033-1353483>
- Johnell, O., & Kanis, J. A. (2006). An estimate of the worldwide prevalence and disability associated with osteoporotic fractures. *Osteoporosis International*, 17(12), 1726–1733. <https://doi.org/10.1007/s00198-006-0172-4>
- Kado, D. M., Duong, T., Stone, K. L., Ensrud, K. E., Nevitt, M. C., Greendale, G. A., & Cummings, S. R. (2003). Incident vertebral fractures and mortality in older

- women: A prospective study. *Osteoporosis International*, 14(7), 589–594. <https://doi.org/10.1007/s00198-003-1412-5>
- Kerschbaumer, G., Gaulin, B., Ruatti, S., Tonetti, J., & Boudissa, M. (2019). Clinical and radiological outcomes in thoracolumbar fractures using the SpineJack device. A prospective study of seventy-four patients with a two point three year mean of follow-up. *International Orthopaedics*, 43(12), 2773–2779. <https://doi.org/10.1007/s00264-019-04391-1>
- Kumar, V. (2012). *101 Design Methods: A Structured Approach for Driving Innovation in Your Organization*. Wiley.
- Lee, J., Lee, S., Jang, S., & Ryu, O. H. (2013). Age-Related Changes in the Prevalence of Osteoporosis according to Gender and Skeletal Site: The Korea National Health and Nutrition Examination Survey 2008-2010. *Endocrinology and Metabolism*, 28(3), 180–191. <https://doi.org/10.3803/enm.2013.28.3.180>
- Lerouge, S., & Simmons, A. (2012). *Sterilisation of Biomaterials and Medical Devices*. Woodhead Publishing.
- Levin, R. (2018). *Kyphoplasty Risks and Potential Complications*. Spine-Health. <https://www.spine-health.com/treatment/back-surgery/kyphoplasty-risks-and-potential-complications>
- Mastrangelo, G., Fedeli, U., Fadda, E., Giovanazzi, A., Scozzato, L., & Saia, B. (2005). Increased cancer risk among surgeons in an orthopaedic hospital. *Occupational Medicine*, 55(6), 498–500. <https://doi.org/10.1093/occmed/kqi048>
- Medical Advisory Secretariat. (2004). Balloon Kyphoplasty An Evidence-Based Analysis Medical Advisory Secretariat Ministry of Health and Long-Term Care. *Ontario Health Technology Assessment Series*, 4. http://www.health.gov.on.ca/english/providers/program/ohtac/public_engage_overview.html
- Molenbroek, J. F. M. (1980). *DINED Antropometric database*. Applied Ergonomics and Design Section of the Human-Centered Design Department. <https://dined.io.tudelft.nl/en/database/tool>
- Paolucci, E. M., Loukov, D., Bowdish, D. M. E., & Heisz, J. J. (2018). Exercise reduces depression and inflammation but intensity matters. *Biological Psychology*, 133(2), 79–84. <https://doi.org/10.1016/j.biopsycho.2018.01.015>
- Patwardhan, A., Meade, K., & Gavin, T. (2016). *Biomechanics of the spine*. <https://musculoskeletalkey.com/biomechanics-of-the-spine/>
- Premat, K., vande Perre, S., Cormier, É., Shotar, E., Degos, V., Morardet, L., Fargeot, C., Clarençon, F., & Chiras, J. (2018). Vertebral augmentation with the SpineJack® in chronic vertebral compression fractures with major kyphosis. *European Radiology*, 28(12), 4985–4991. <https://doi.org/10.1007/s00330-018-5544-6>
- Rezaei, F., Yarmohammadian, M., Ferdosi, M., & Haghshenas, A. (2015). Principles of risk management in surgery departments. *Archives of Clinical and Experimental Surgery (ACES)*, 4(3), 21–30. <https://doi.org/10.5455/aces.20140925015830>

- Rockville (MD): Office of the Surgeon General (US). (2004). *Bone Health and Osteoporosis: A Report of the Surgeon General*.
- Rodriguez, M. (2019). *Laminectomy and Spinal Stenosis: Risks and Complications*. Spine Health. <https://www.spine-health.com/treatment/back-surgery/laminectomy-and-spinal-stenosis-risks-and-complications>
- Roozenburg, N. F. M., & Eekels, J. (2003). *Productontwerpen, structuur en methoden* (2nd ed.). Boom Lemma Uitgevers. <https://doi.org/9789051897067>
- Silverman, S. L. (1992). The Clinical Consequences of Vertebral Compression Fracture. *Bone*, 13(2), 27–31. [https://doi.org/10.1016/8756-3282\(92\)90193-z](https://doi.org/10.1016/8756-3282(92)90193-z)
- Speer, J. (2015, August 6). UNDERSTANDING ISO 14971 MEDICAL DEVICE RISK MANAGEMENT. UNDERSTANDING ISO 14971 MEDICAL DEVICE RISK MANAGEMENT
- Tassoul, M. (2009). *Creative Facilitation* (3rd ed.). VSSD.
- Thaler, M., Lechner, R., Nogler, M., Gstöttner, M., & Bach, C. (2013). Surgical procedure and initial radiographic results of a new augmentation technique for vertebral compression fractures. *European Spine Journal*, 22(7), 1608–1616. <https://doi.org/10.1007/s00586-012-2603-6>
- Upasani, V. v., Robertson, C., Lee, D., Tomlinson, T., & Mahar, A. T. (2010). Biomechanical Comparison of Kyphoplasty Versus a Titanium Mesh Implant With Cement for Stabilization of Vertebral Compression Fractures. *Spine*, 35(19), 1783–1788. <https://doi.org/10.1097/BRS.0b013e3181b7cc5d>
- van Boeijen, A., Daalhuizen, J., & Zijlstra, J. (2020). *Delft Design Guide* (Vol. 2). BIS Publishers.
- Weprin, M. (2016). *Design Thinking: Stakeholder Maps*. <https://uxdict.io/design-thinking-stakeholder-maps-6a68b0577064>
- Wilkes, M. S. (2000). Chronic back pain: does bed rest help? *Western Journal of Medicine*, 172(2), 121–127. <https://doi.org/10.1136/ewjm.172.2.121>
- Wilson, D. C., Connolly, R. J., Zhu, Q., Emery, J. L., Kingwell, S. P., Kitchel, S., Cripton, P. A., & Wilson, D. R. (2012). An ex vivo biomechanical comparison of a novel vertebral compression fracture treatment system to kyphoplasty. *Clinical Biomechanics*, 27(4), 346–353. <https://doi.org/10.1016/j.clinbiomech.2011.11.001>
- Zadeh, F., Briggs, T. W. R., & Fracs, M. (1997). Ionising radiation: are orthopaedic surgeons' offspring at risk? Specialist Registrar Grade in Orthopaedics. *Ann R Coll Surg Engl*, 79(3), 214–220.
- Zdeblick, T. A., Kunz, D. N., Cooke, M. E., & McCabe, R. (1993). Pedicle Screw Pullout Strength Correlation with Insertional Torque. *Spine*, 18(12), 1673–1676. <https://doi.org/10.1097/00007632-199309000-00016>
- Zhao, F.-D., Pollintine, P., Hole, B. D., Adams, M. A., & Dolan, P. (2009). Vertebral fractures usually affect the cranial endplate because it is thinner and supported by less-dense trabecular bone. *Bone*, 44(2), 372–379. <https://doi.org/10.1016/j.bone.2008.10.048>

Zhu, S. Y., Zhong, Z. M., Wu, Q., & Chen, J. T. (2016). Risk factors for bone cement leakage in percutaneous vertebroplasty: a retrospective study of four hundred and eighty five patients. *International Orthopaedics*, 40(6), 1205–1210. <https://doi.org/10.1007/s00264-015-3102-2>

Appendix 1 – Stakeholders

The development of the TIVAD Spine system, and more specifically, the TIVAD SIS, depends on the involvement of three parties. These parties are research, the hospital, and the industry (Fig. 47).

Research notices that available VCF solutions still have their weaknesses in terms of short- and long-term performance, efficiency, and safety. There is a need for a new unique VCF solution (implant & SIS) that solves these weaknesses and has a beneficial impact on public health. The industry (Amber Implants) notices the weaknesses of existing VCF solutions in the scientific publications, market evaluations and wants to solve the findings available in the literature. Furthermore, it wants to increase its profits. The hospital wants to improve VCF surgery outcomes, increase patient satisfaction, reduce costs, reduce the incidence rate of infections, and ultimately, perform more surgeries to earn more money.

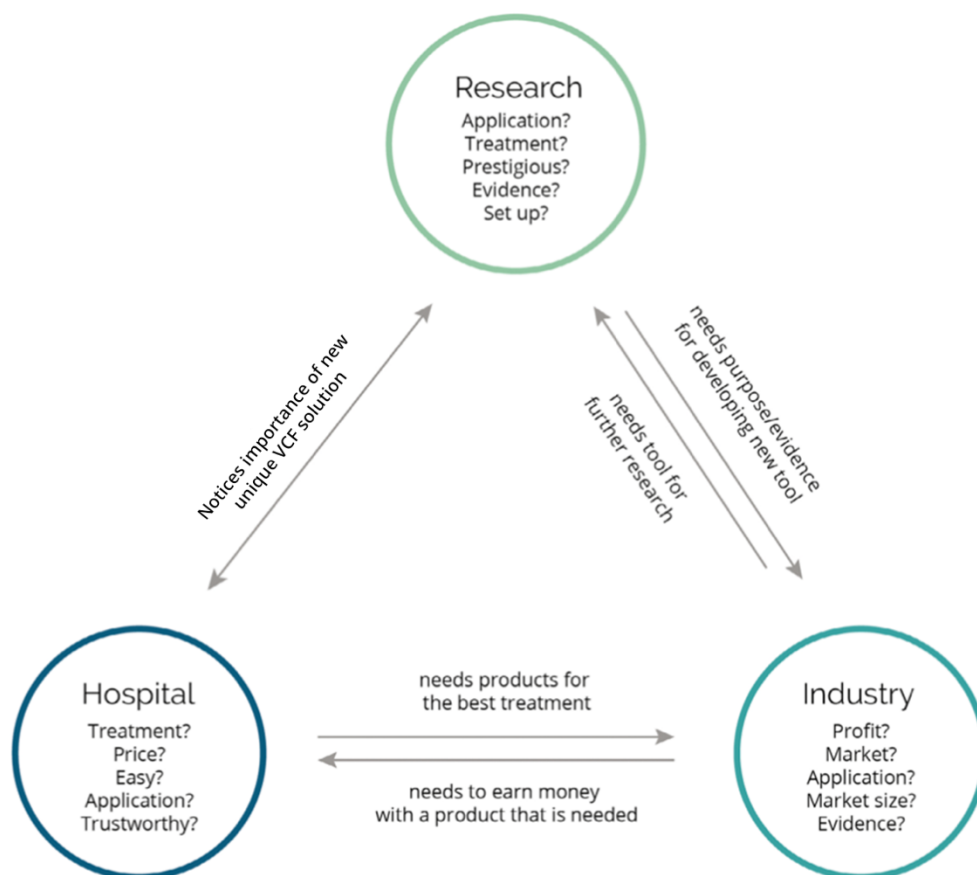


Figure 47 | Stakeholder overview

Appendix 2 – Design methods

During the graduation project, different design methods are applied. The methods are placed in alphabetical order.

Brainwriting and Brain Drawing: Brainwriting and Brain Drawing are alternatives to brainstorming. Participants write or draw their ideas on paper and build upon each other's ideas (van Boeijen et al., 2020).

Competitor Analysis: In the Competitor Analysis, the competitors with similar kinds of products are analyzed on their capabilities, the price of their product, and what the expert's opinion is about their product(s) (van Boeijen et al., 2020).

Expert Evaluation: In an Expert Evaluation, the design of a product or service is evaluated by an expert in the field (Roozenburg & Eekels, 2003)

Feasibility Study: A Feasibility Study is a study based on a test. A test has been executed to evaluate the functionality (van Boeijen et al., 2020)

Function Analysis: Function Analysis is a method for understanding the functional structure of a new concept or an existing product (Roozenburg & Eekels, 2003).

Harris Profile: A Harris Profile is a graphical representation of an assessment of several concepts based on preferences (Van Boeijen et al., 2013).

How-To: How-To questions are used to support idea generation in a creative session (Tassoul, 2009)

Morphological Chart: A Morphological Chart combines partial ideas into principal solutions based on the functional analysis (Van Boeijen et al., 2013).

Naturalistic User Observation: In a Naturalistic User Observation, users are observed in a real-life situation to create a realistic understanding of the user in its context (Interaction Design Foundation, 2017).

Problem Definition: A Problem Definition is set up at the end of the analysis phase to grasp a kind of dissatisfaction in a specific situation (Roozenburg & Eekels, 1995).

List of Requirements: A Programme of Requirements lists all the essential characteristics a product should fulfill to succeed (Van Boeijen et al., 2013).

Risk Analysis: In the Risk Analysis, the potential hazards are analyzed. The risks are evaluated and mitigated to make sure the device is as safe as possible to use

(Speer, 2015).

Stakeholder Map: In a Stakeholder Map are the key stakeholders mapped to show their relationships (Weprin, 2016).

Storyboard: A storyboard is a visual representation of a story about the design in the context of use over time (Van Boeijen et al., 2013).

Three-Dimensional Modelling: Three-Dimensional modeling is a physical form of a product idea to test and evaluate the concept (Van Boeijen et al., 2013).

Appendix 3 – Surgical instruments of existing VCF devices

3.1 Balloon Kyphoplasty (BKP) SIS (2nd generation)

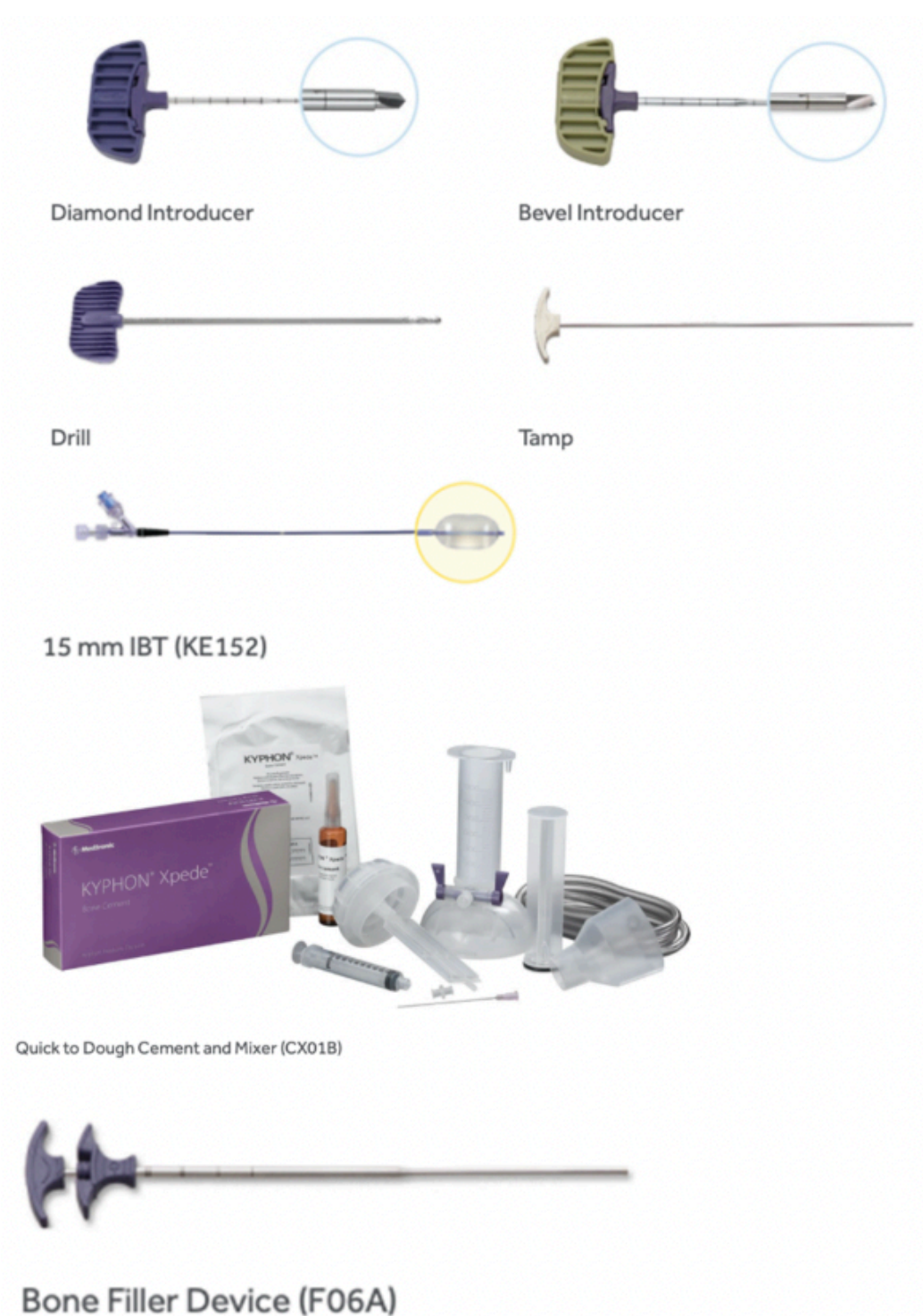


Figure 48 | BKP SIS

Fig. 48 shows that the BKP surgical procedure requires an assembled inner and outer introducer (= Jamshidi needle) for the initial VB access. Thereafter, the inner introducer is retracted, and the drill is inserted into the cavity of the outer introducer, and a hole is created with the desired depth. Once the desired depth is reached, the drill is retracted, and the balloon is inserted and inflated. When the correct height restoration is reached, the balloon is inflated, and the PMMA bone cement is prepared and inserted with the bone filler device.

Fig. 49 illustrates the surgical instruments that are required for the VBS procedure. Compared to the BKP SIS, the only difference is that the VBS set offers a biopsy kit to take a biopsy of the targeted fractured VB.

Fig. 50 depicts the SIS for the Spine Jack surgical procedure. The general surgical instruments such as the JamShidi needle, k-wire, and drills are the same as the BKP and VBS procedures. The difference is apparent with the surgical instrument that is required to insert and deploy the SpineJack device inside the fractured VB.

3.2 Vertebral body stenting (VBS) SIS (3rd generation)

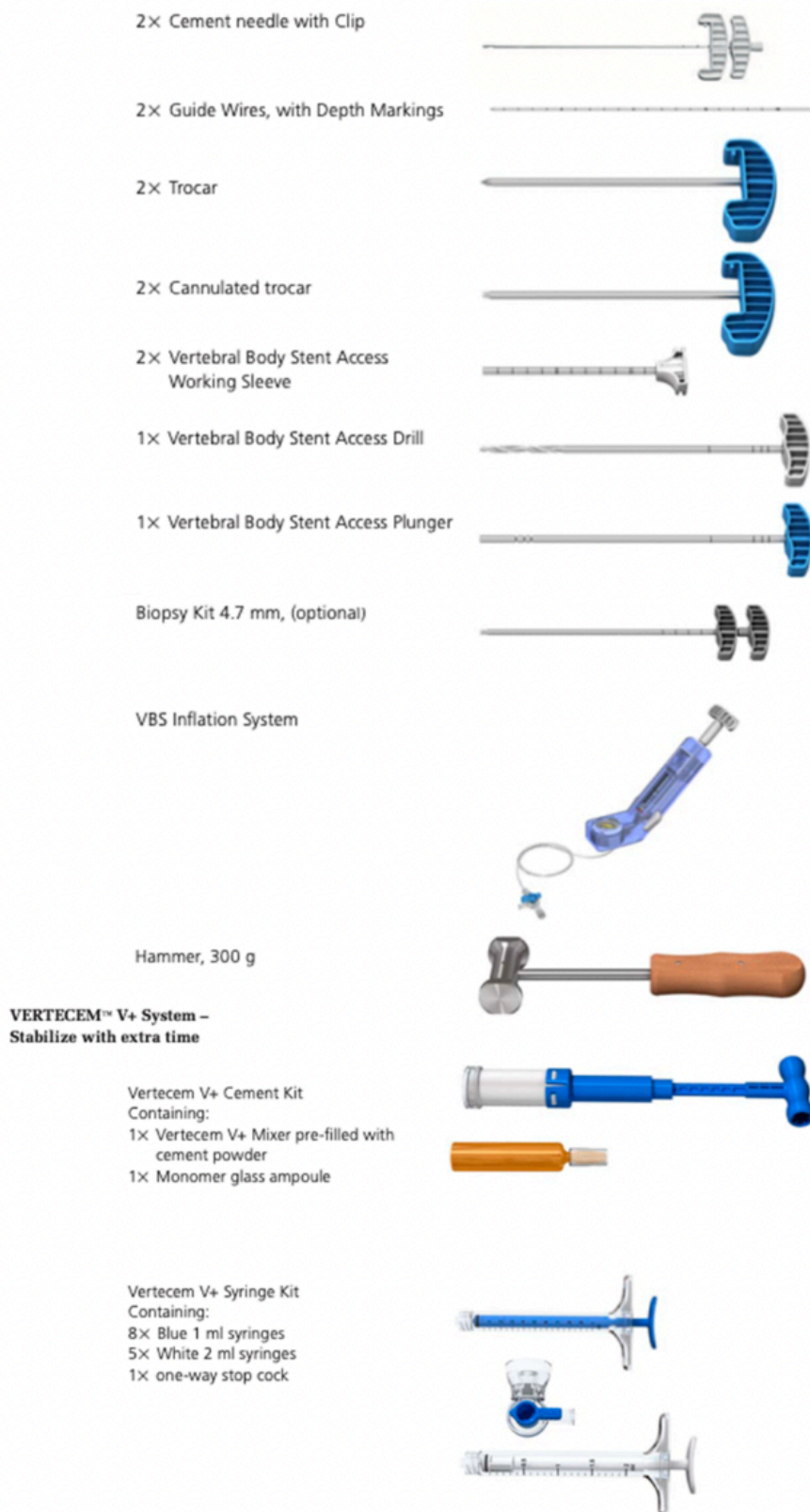


Figure 49 | VBS SIS

3.3 Spine Jack SIS (3rd generation)

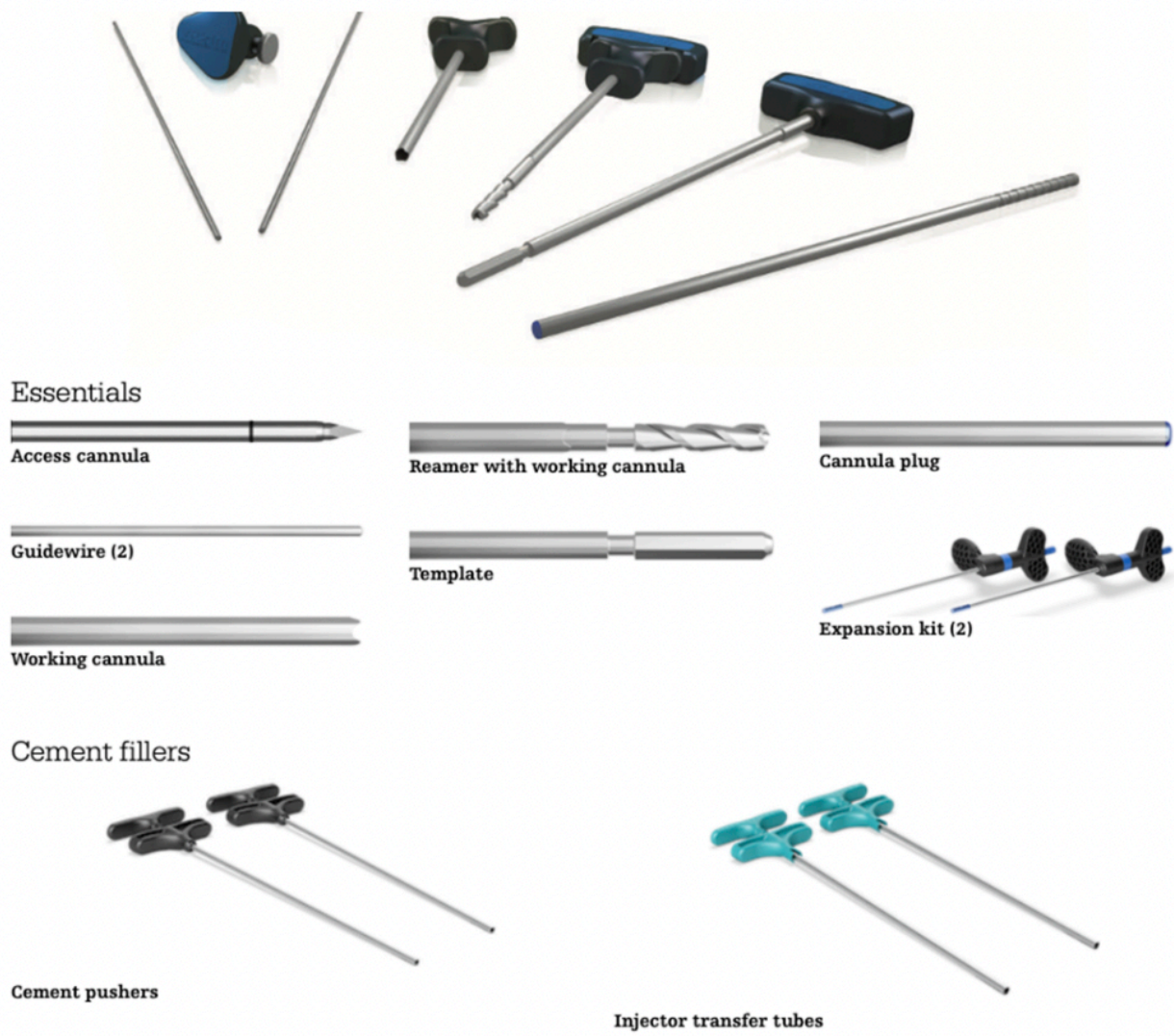


Figure 50 | Spine Jack SIS

Appendix 4 – Interviews

Below, an overview of questions is shown that led the conversations with the various surgeons.

What kind of spine-related surgeries are they performing?

If they perform surgeries to treat vertebral compression fractures, what devices do they use? Do they use 1st, 2nd, 3rd generation VCF devices or something entirely different to solve this issue?

What do they experience as strengths and weaknesses of their 'weapon of choice' (implant of choice), the surgical procedure (required steps to successfully execute procedure), and the required surgical instruments?

What other tools/equipment is used during the surgery besides the surgical instruments in order to execute the surgery successfully?

How does the surgical team composition look like, and what are their responsibilities?

NOTE: all surgeons have given consent to use the content that has been discussed during the interviews with them.

Appendix 5 – List of requirements TIVAD SI

Table 14 | List of Requirements

Instrument	Functional requirement	Mechanical requirement	Shape/size
Dilator	[M] Has to provide protection to soft tissues that lie between the skin and the fractured VB. It acts as an access channel/tunnel for all the surgical instruments that are necessary for the subsequent surgical steps.		[M] Has to have a cylindrical shape as all tools that pass through also have cylindrical shapes. The ID must be at least 12mm, as the biggest tool (TIVAD inserter) that passes through has an OD of 10mm.
JamShidi needle	[M] The two-part trocar needle is used to make a controlled initial insertion into VB via the pedicle, to ensure proper placement of the TIVAD implant.	Similar dimensions as other jamshidi needles to ensure proper mechanical performance. This is a commonly known and used surgical instrument — evaluation based on substantial equivalence with existing products.	<p>[M] The analysis results demonstrate that the outer diameter (OD) of the JamShidi can be a maximum 6mm considering the dimensions of the pedicle as the JamShidi needle passes through the pedicle. After retracting the inner JamShidi part, it needs to have enough room for the next step; insertion of the k-wire. As the OD of the k-wire is 2.5mm, the ID of the outer JamShidi needle needs to be 2.6mm to have enough clearance.</p> <p>[M] To facilitate room for the inner part of the two-part needle, the outer part needs to be hollow, and the inner part can be solid.</p>

			[M] The inner part of the two-part trocar needle is designed to be retracted to make room for the next step, the insertion of the guide pin.
K-wire	[M] The guide pin enables a controlled usage (insertion/placement) of tools that are used in subsequent surgical steps, such as the drill (not for implant inserter and implant expander).	Similar dimensions as other k-wires to ensure proper mechanical performance. This is a commonly known and used surgical instrument — evaluation based on substantial equivalence with existing products.	[M] has to be cylindrical to fit cannulated drills.
Cannulated drill	[M] The drill enables the creation of a hole/cavity for the porous implant (assembly: pedicle screw & expansion mechanism). [M] The drill must slide over the guide pin to ensure proper drilling orientation and depth. [M] The drill must have markers for depth reference purposes.	[M] Torque during drilling is not available. However, the insertional torque of pedicle screws can be used as a measurement → max—torque of 4.5 Nm.	[M] needs to have cylindrical cavity to ensure it can glide over the k-wire.
TIVAD Inserter	[M] The TIVAD inserter enables a controlled implant-tool engagement/fit to enable the user to successfully transfer the input force 'onto' the implant	[M] Has to conquer the maximum measured insertional torque of 4.5 Nm.	[M] has to fit to TIVAD tulip connection interface

	<p><i>Specification: connection must transfer at least 2Nm -> with a safety factor of two the max. torque = 4Nm</i></p> <p>[M] The TIVAD inserter needs a locking feature to ensure that the implant does not get loose of the implant inserter during the insertion process. It is essential that the fixation also can be unlocked once the implant has reached the desired depth</p> <p><i>Specification: locking and unlocking possibility is key</i></p> <p>[M] TIVAD inserter will be single use</p>		
<p>TIVAD Expander</p>	<p>[M] The TIVAD expander must enable a controlled expansion of the TIVAD implant.</p> <p><i>Specification: The expansion of the implant is achieved by rotating the integrated implant screw.</i></p> <p>[M] The TIVAD expander must engage flawlessly with the TIVAD's expansion screw to enable a controlled expansion of the TIVAD.</p> <p><i>Specification: Without engagement, the</i></p>	<p>[M] TIVAD expander has to endure the applied torque during TIVAD expansion.</p> <p><i>Specification: experimental tests shows that the maximum observed torque was 0.7Nm. With a safety factor of 2, the maximum requirement is 1.4Nm of torque.</i></p>	<p>[M] has to fit TIVAD expansion screw connection interface</p>

	<p><i>rotation of the implant screw is not possible.</i></p> <p>[M] The required rotation direction must be clearly indicated.</p> <p>[S] The TIVAD expander's handle should enable the user to comfortably apply the required force for successful TIVAD expansion. <i>Specification: Collaboration between the use of these two handles enables the user to insert and expand the implant successfully.</i></p> <p>[S] The TIVAD expander's handle should not interfere with the TIVAD inserter's handle.</p> <p>[M] TIVAD expander will be single use.</p>		
--	---	--	--

Appendix 6 – FEM Analysis concepts

6.1 FEM analysis – TIVAD connection design

In the early stages of the TIVAD inserter design process, an explorative FEM analysis, with the emphasis on the connection design with the TIVAD, is performed in Fusion360. Several design iterations, varying in OD, hollow or solid, length, and TIVAD approach method were included in this preliminary FEM analysis. The aim of this preliminary FEM analysis was to discover what parameters determined whether a design would withstand the forces that were applied to it during the TIVAD insertion process. For this FEM analysis, the same results were used as during the experimental test, meaning that a torque of 2Nm was applied.

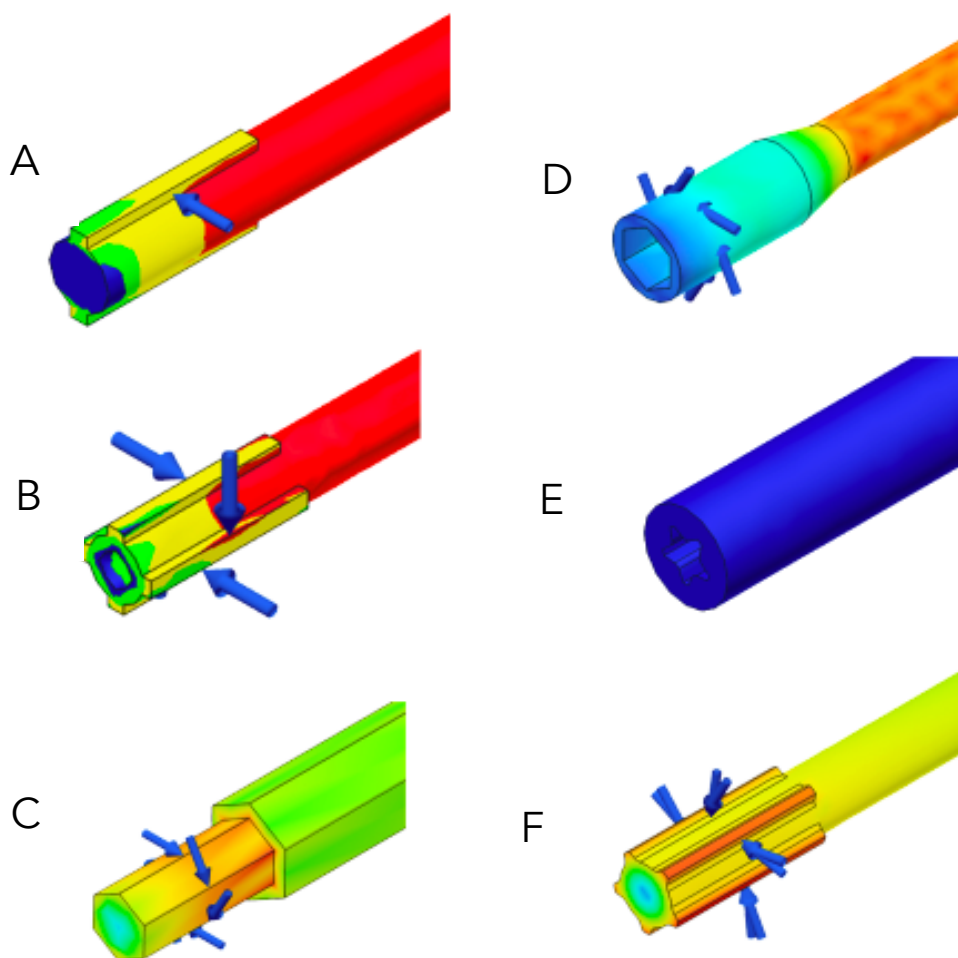


Figure 51 | Preliminary FEM analysis results

Fig. 51 shows some results of connection design iterations that were tested during this preliminary FEM analysis. The main take-aways from this analysis was that the inside approach resulted in a very small OD (less than 10mm) and ultimately, these designs failed (Fig. 51, A & B). Another observation was that the bigger the surface area is that is in contact with the implant, the more evenly distributed the force is and

the lower the peak forces are on the designs; this is depicted by Fig. 51, C & F. Lastly, in Fig. 51, D & E, an outside TIVAD approach is simulated, and it is clearly visible that the peak forces are the lowest in these designs compared to the inside TIVAD approach designs. Another advantage of this approach is that the OD is bigger, which facilitates enough room for a cavity that enables the TIVAD expander to pass through.

Fig. 52 shows the parameters that have been changed during the test and the max. Stress results. Where the connection designs, marked in green, were strong enough to overcome the torque of 2Nm.

6.2 Methods

6.2.1 FEM Analysis settings

Safety factor: 2

Load: 2Nm distributed over the contact surface

Material: 316L Stainless steel

Mesh settings: default

Design	ID [mm]	OD [mm]	Length [mm]	Length connection feature [mm]	Feature height [mm]	Feature width [mm]	Wall-thickness [mm]	Inside/Outside PS	Solid/Hollow	Features	Material	Total Force [N]	Number of edges/faces	Force per edge/face [N]	Min. safety factor	Max. safety factor	Max. stress [Mpa]	Max. deformation [mm]
PS Inserter 2.0	0	6,78	167	5	3,498	NA	6,78	inside	solid	Fillet at T-coupling	316L	800	7	114,28571			54,95	0,4707
PS Inserter 2.1	2,15	6,78	167	5	3,498	NA	4,63	inside	hollow	Fillet at T-coupling	316L	800	7	114,28571	1,887	15	90,1	0,6938
Hex XII	0	6	150	10	4,5	NA		inside	solid	hex all the way with scale up	316L	800	6	133,33333	1,282	15	132,6	0,1117
Hex XIII		6,5	150	10	4,5	NA		inside	solid	hex all the way with scale up	316L	800	4	200	1,275	15	133,3	0,08778
Hex XV	0	6	150	10	4	NA	6	inside	solid	hex all the way with scale up	316L	800	4	200	1,1	15	154,5	0,09921
Hex XIV	0	6	150	10	3,5	NA	6	inside	solid	hex all the way with scale up	316L	800	4	200	0,8328	15	204,1	0,0868
Hex XVI	0	6	150	10	4	NA	6	inside	solid	hex all the way with scale up + handle	316L	800	4	200	0,7429	15	228,8	0,102
Hex I	0	4,5	150	10	4,5	NA	4,5	inside	solid		316L	800	6	133,33333	0,7121	15	238,7	0,1921
Torx I	0	3,5	150	10	4,5		3,5	inside	solid		316L	800	5	160			242,6	
Hex XI	0	5,5	150	150	5,5	NA	NA	inside	solid	hex all the way	316L	800	6	133,33333	0,7002	15	242,8	0,142
Hex II	2,15	4,5	150	10	4,5	NA	2,35	inside	hollow	= Hex I with fillets (5mm) at connection	316L	800	6	133,33333	0,6542	15	259,9	0,2031
Hex VI	0	5,5	150	10	4,5	NA	5,5	inside	solid	= Hex I with fillets (10mm) at connection	316L	800	6	133,33333	0,6409	15	265,2	0,1939
Hex VII	0	5,5	150	10	4,5	NA	5,5	inside	solid		316L	800	6	133,33333	0,6254	15	271,8	0,1943

101 Figure 52 | Results preliminary FEM analysis

Appendix 7 – Concept generation process

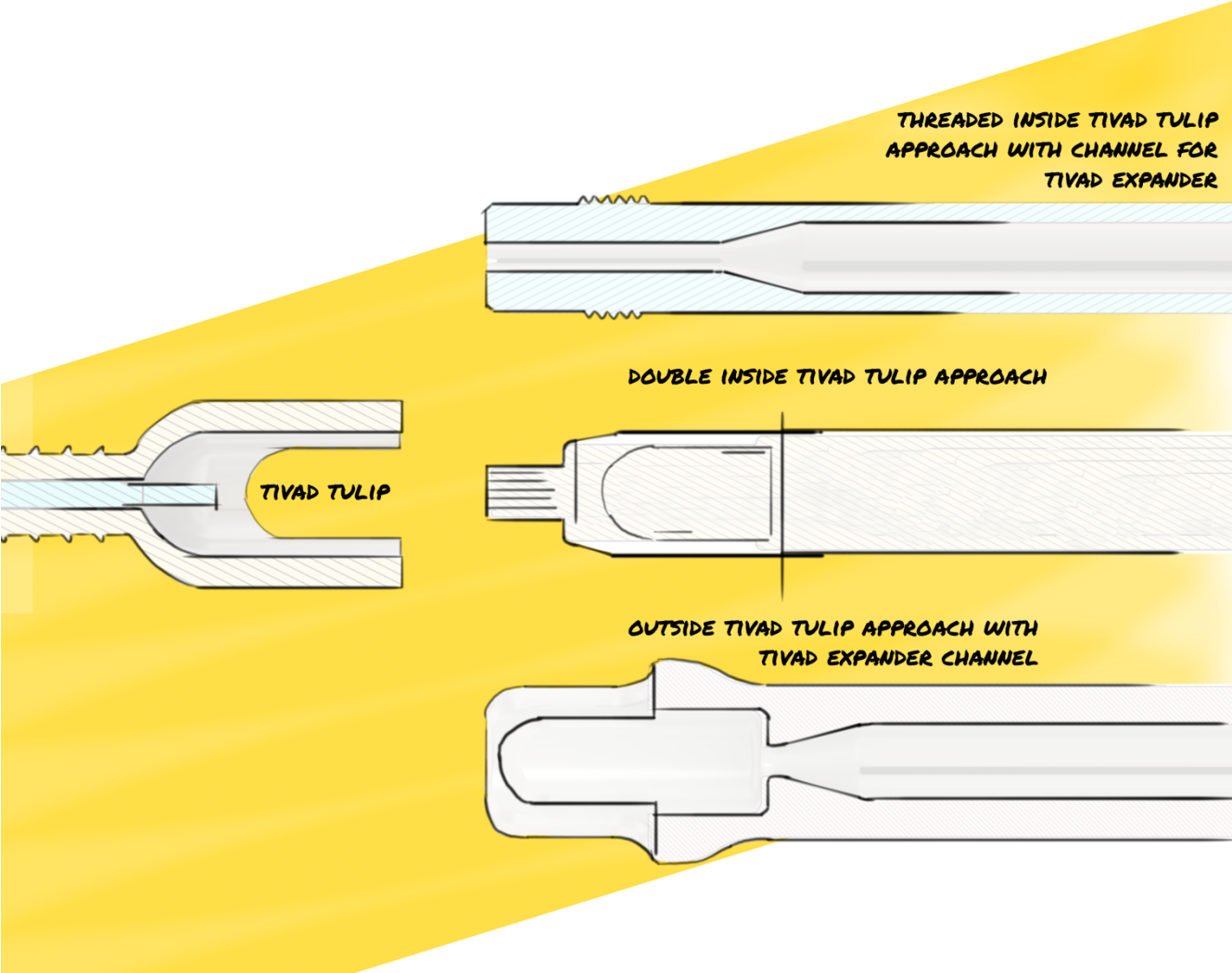


Figure 53 | TIVAD Inserter connection interface sketches

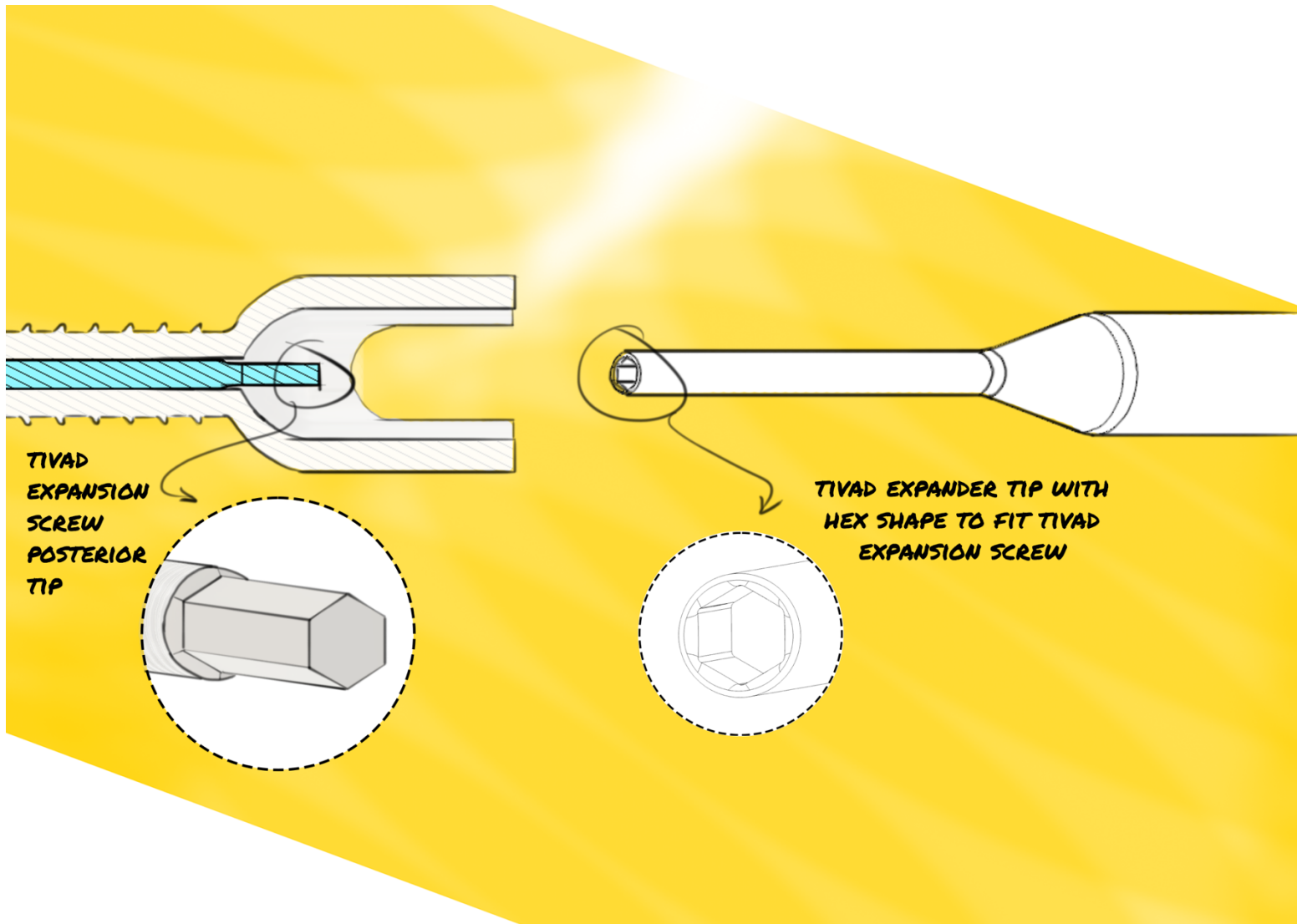


Figure 54 | TIVAD Expander connection interface

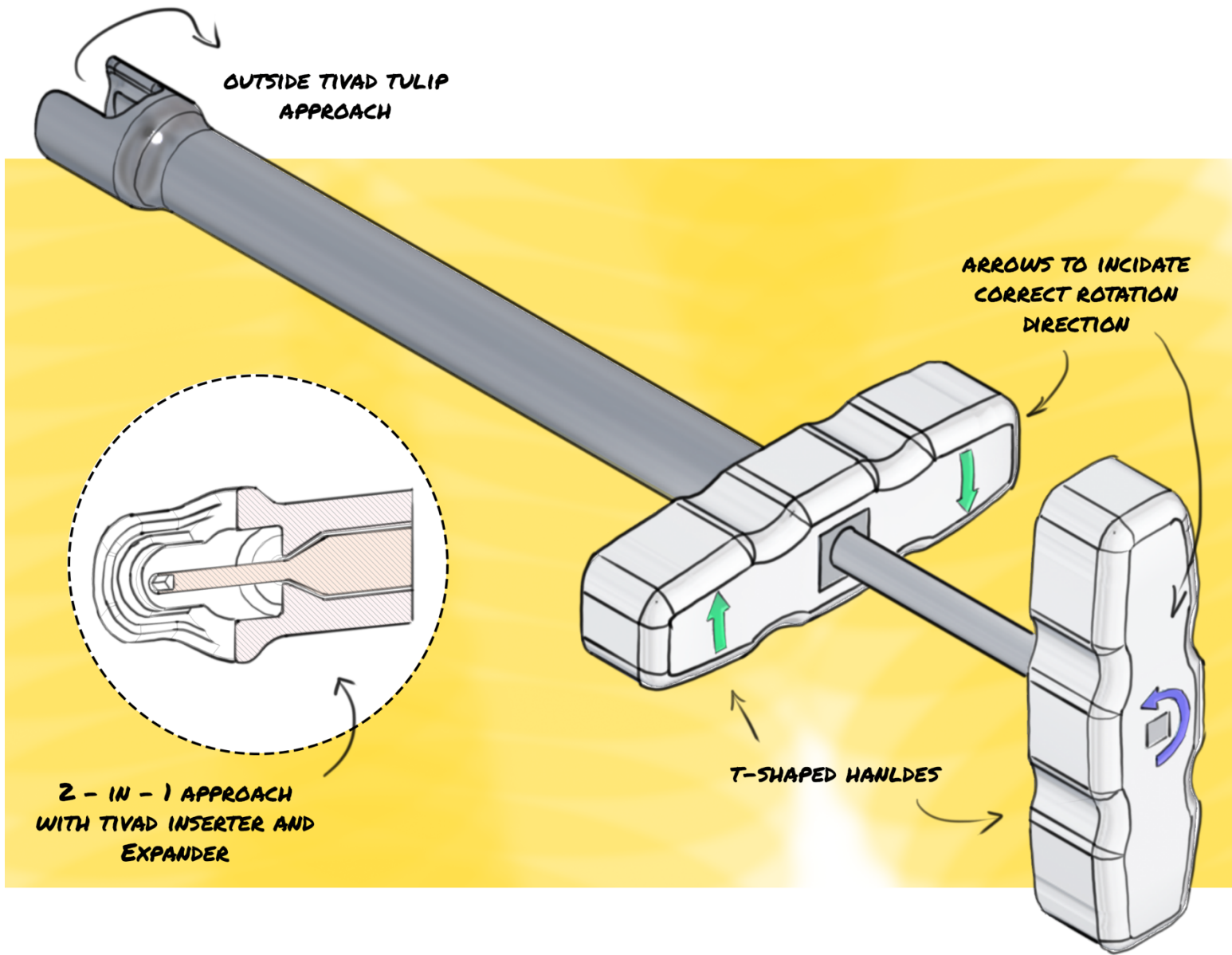
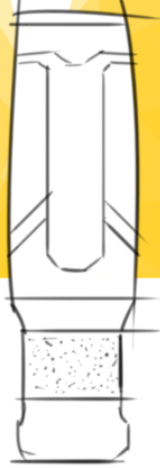


Figure 55 | TIVAD Inserter & Expander features sketch



STRAIGHT HANDLE IDEAS



T-SHAPE HANDLE IDEAS

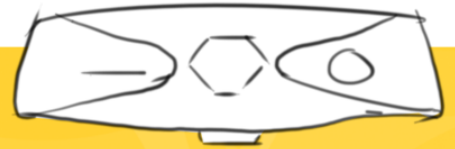
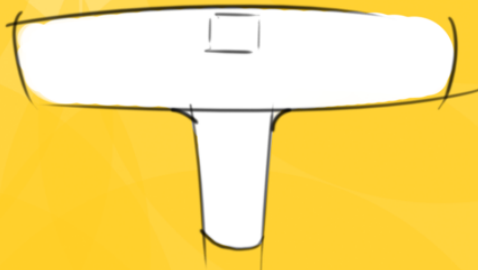


Figure 56 | TIVAD Inserter & Expander handle idea sketches

Appendix 8 – Physical ergonomics end user

Fig. 57 illustrates how much torque can be applied by a human being between the age group of 20-30 years old with two hands; the mean is 7Nm with a SD of 2. This information is used to have an indication with respect to the magnitude of the force that can be applied during the TIVAD insertion and expansion process with one hand: 3.5Nm (this is an assumption based on the 7Nm, which can be applied with two hands). Furthermore, Fig. 58 shows the instructions on how to measure a human hand.

The screenshot shows the DINED anthropometric database interface. On the left is a navigation menu with options: About Us, How it works (1D, 2D, 3D and 4D data), 1D Database, Ellipse, Mannequin, and Profiler. The main area has tabs for Introduction, Tool, and Help. Under the Tool tab, there are sections for Populations, a selection table, a table of measures, and a results table.

Populations

Dutch adults, dined2004			
Dutch adults, dined2003			
Dutch adults, dined1982			
Dutch elderly, geron1998			
Dutch children, kima1993			
Dutch elderly, gdvv1984			
Dutch Growth, growthdiagrams			
Dutch students, delstu2016			
Dutch students, delstu1986			
International, international			
Chilean children, chile2012			
CAESAR (NL), caesar			
CAESAR (USA), caesar-usa			
CAESAR (IT), caesar-it			
Chilean workers, chile2016-			

Dutch adults, dined2004 - more
select: female, male, mixed, none

	f	m	m+f
20-30	<input type="checkbox"/>	<input type="checkbox"/>	<input checked="" type="checkbox"/>
31-60	<input type="checkbox"/>	<input type="checkbox"/>	<input type="checkbox"/>
60+	<input type="checkbox"/>	<input type="checkbox"/>	<input type="checkbox"/>
20-60	<input type="checkbox"/>	<input type="checkbox"/>	<input type="checkbox"/>

Measures

Standing, length/depth
Standing, width/circumference
Sitting, length/width/depth
Head
Hand
Foot
Joint excursion
Force exercise
Other
combined measures
select: all, available, none

Table of Measures

57	60	58	59
----	----	----	----

hide selection panel

Results Table

populations	Dutch adults 20-30, mixed	
measures	mean	sd
Torque with two hands (Nm)	7	2

In this table the mean and standard deviation of the selected populations and measures can be compared. Use the top left button to switch the axis that display populations and measures. By clicking on a mean/standard deviation the corresponding population and measure will be shown in the 'single measurement' tab.

Figure 57 | DINED information on how much torque a human can apply with two hands

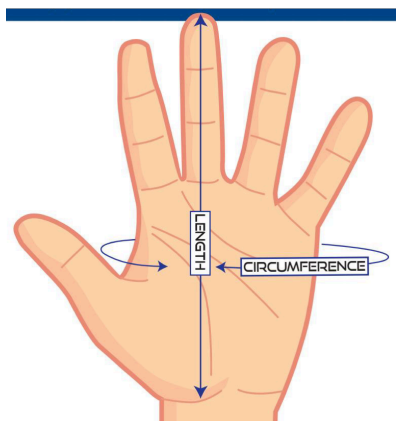


Figure 58 | Hand measurement instruction

Appendix 9 – Experimental tests (Torque measurements & usability)

The decision to test measure the insertional and expansion torque on synthetic bone and cadaveric bone is because the synthetic bone specimens can't be compressed – mimic a VCF - which means the expansion of the TIVAD implant can't be performed. Contrary to that, is it possible to do this with the cadaveric VBs. The torque sensor was fitted to the TIVAD inserter and expander with custom 3D printed adapters. As a result, we were able to measure the torque that was required for these two surgical processes.

9.1 Methods

9.1.1 Experimental tests setup

Table 15 | TIVAD Surgical procedure steps

Surgical step	Explanation
1. Patient positioning	1.1 Patient is positioned correctly on the spine table: in a prone position.
2. Implant positioning planning	2.1 FS images are made to capture the patient's spine position and locate the fractured VB. 2.2 Access path is determined that is used for the VB access step (5.1).
3. Skin incision	3.1 Once the access path is located, a skin incision will be made at the point of entry.
4. MIS dilator insertion	4.1 Once the incision of +/- 25mm is made, the dilator is pushed through the skin incision further down, passing the underlying soft tissues (back muscles and tendons) until it touches the pedicles.
5. VB access	5.1 Insertion of JamShidi Needle under FS guidance. When desired orientation is reached, the inner section is removed. 5.2 Insertion of K-wire into the hollow cavity of outer section JamShidi needle. Once K-wire is in place, the JamShidi needle's outer section will be removed,

	<p>leaving the K-wire in place. Pressure is applied on the k-wire to ensure it is not getting loose.</p>
6. Implant site preparation	<p>6.1 Fixated K-wire is used as directional guidance for the cannulated drill.</p> <p>6.2 Sliding process of a cannulated drill (6mm version) over the fixated K-wire until the exterior shell of VB is reached.</p> <p>6.3 Start drilling by rotating the drill clockwise until the desired depth is reached.</p> <p>6.4 Desired depth is determined by the length of the threaded part of the VCF device (TIVAD). Removal of Cannulated drill and K-wire to make space for TIVAD implant and TIVAD inserter.</p>
7. Implant insertion	<p>7.1 TIVAD implant is placed in the newly made cavity in the synthetic bone specimen/CVB.</p> <p>7.2 Once positioned correctly, the TIVAD implant is inserted using the TIVAD inserter.</p> <p>7.3 When the desired depth is reached, it is ready for expansion.</p>
8. Implant expansion	<p>8.1 Before the expansion, successful coupling of the TIVAD expander and the TIVAD's expansion screw is required through the TIVAD inserter.</p> <p>8.2 When coupled, TIVAD can be expanded using the expander and turning counter-clockwise until the desired height is achieved.</p>
9. Retraction of implant inserter & expander surgical instrument	<p>9.1 If the TIVAD is expanded successfully, the implant expander is decoupled and retracted.</p>

	<p>9.2 The dilator is pulled back</p> <p>9.3 The remaining wound/skin incision hole is closed with sutures</p>
--	--

Below, the specific procedure steps are explained for both the stage 1 and stage 2 tests.

NOTE: due to the setup of this test, which is ex-vivo, it is evident that there is no skin/soft tissue. Resulting in the fact that the creation of a hole in these tissues is not required, meaning that we can immediately start with the hole preparation through the vertebral body pedicle. This process starts at point 5.1.

Stage 1

For the stage 1 test, steps 6.3 till 7.2 are applicable; see Table 15. While following these steps the following two points will be assessed, observed, and measured:

1. Insertional torque on synthetic bone specimens (SBS - blocks), two insertions per block. As cadaveric vertebral bodies also have two pedicles per vertebral body.
2. Usability: handle ergonomics & force application

NOTE: at the point of stage 1's execution, there was no access to the JamShidi Needle, k-wire, and cannulated drill due to Covid-19. Therefore, the procedure started at step 6.3 with a solid drill rather than a cannulated one. This change had no impact on the rest of the stage 1 test.

Stage 2A

For the stage, 2a test steps 5.1 till 7.2 are applicable; see Table 15. While following these steps the following two points will be assessed, observed, and measured:

1. Insertional torque on cadaveric vertebral bodies (cadaver 1 & 6), two insertions per VB
2. Usability: handle ergonomics, force application, workflow with non-essential surgical instruments for TIVAD surgical procedure

Stage2B

For the stage 2b test, steps 5.1 till 8.2 are applicable; see Table 15. While following these steps the following two points will be assessed, observed, and measured:

1. Insertional torque on cadaveric vertebral bodies (cadaver 5 & 6), two insertions per VB
2. Expansion torque on cadaveric vertebral bodies, two expansions per VB
3. Usability: handle ergonomics, force application, workflow with non-essential surgical instruments for TIVAD surgical procedure

CVB Fracture creation

To be able to test the expansion mechanism of the TIVAD implant during the stage 2B test, a VCF has to be mimicked within the CVB. This is achieved by a cyclic loading cycle process, in which a vertical force is applied to the anterior upper endplate (Fig. 59). As a result, a fracture is created in the anterior CVB. This process is not possible with the SBS, and therefore, the TIVAD expansion torque is only measured in the CVB.

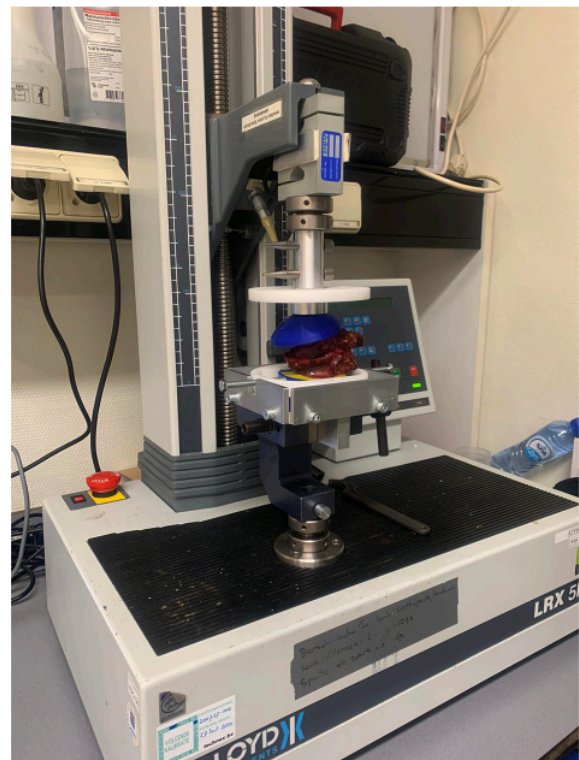
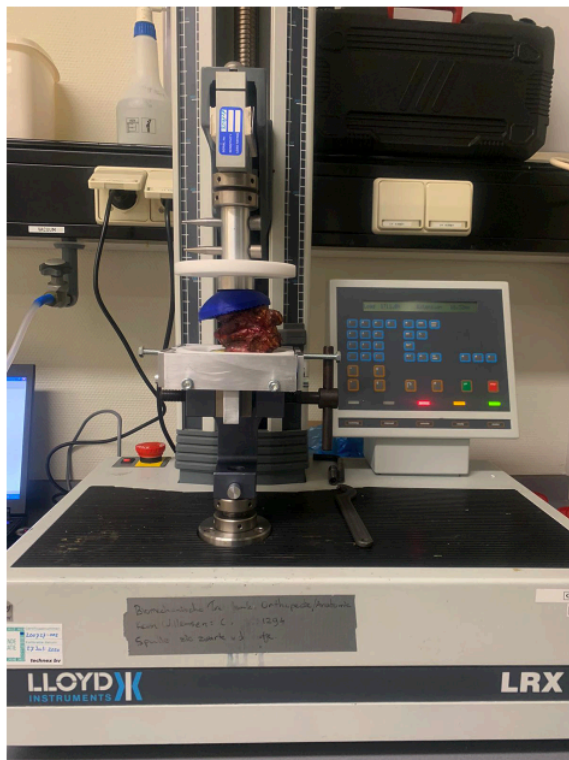


Figure 59 | CVB fracture creation process

9.1.2 Calibration Torque sensor

Table 16 shows the calibration values that are used to calibrate the torque sensor; this is also depicted in Fig. 60.

Table 16 | Torque sensor calibration

Volt [V]	Torque [Nm]	Mass [kg]	Arm [mm]
0	0	0	0
0,094	0,114777	0,1	117
1,02	1,262547	1,1	117
1,98	2,410317	2,1	117
2,95	3,558087	3,1	117

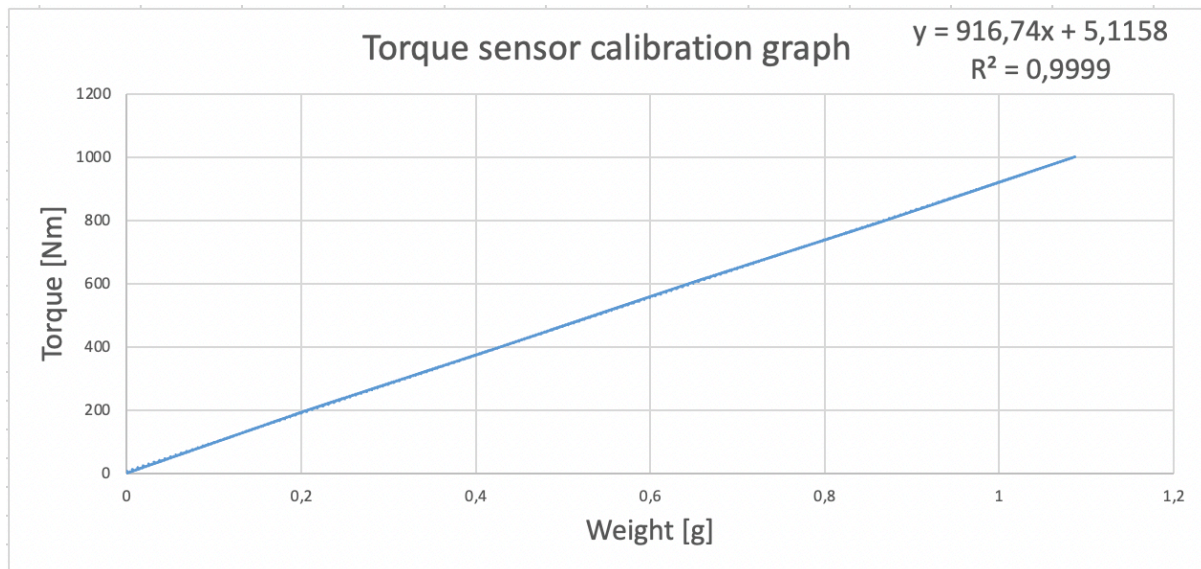


Figure 60 | Torque sensor calibration graph

9.2 Materials

9.2.1 Essential surgical instruments

For the stage 1, 2A & 2B tests, the TIVAD inserter and expander are used (Fig. 61)



Figure 61 | TIVAD Inserter (top), Expander (middle), 2-in-1 approach (bottom)

9.2.2 Non-essential surgical instruments (for stage 1)

Drill (Arthrex 5.0mm drill)

9.2.3 Non-essential surgical instruments (for stage 2a & 2b)

Two-part trocar (Medtronic BKP Instrument Set)

K-wire (Arthrex 2.5mm, threaded)

Drill (Arthrex 5.0mm cannulated drill)

9.2.4 Implants

TIVAD implant prototype (Fig. 62)

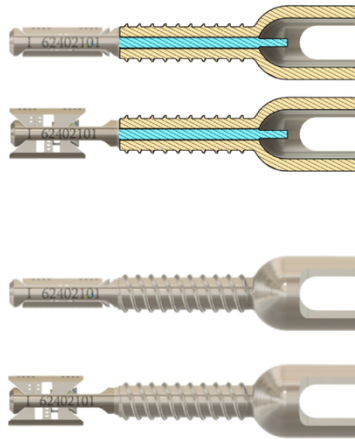


Figure 62 | TIVAD implant prototype

9.2.5 Torque sensor

Torque sensor system: this system features the torque sensor, DAQ module, voltage amplifier, LabView software & custom torque measurement program, and windows laptop

9.2.6 Samples/specimens

Table 17 shows the density properties of the SBS manufactured by Synbone.

Table 17 | Sawbone SBS density properties

PCF Value	Density [g/cm ³]
5	0.08
20	0.32
30	0.47

Appendix 10 – Experimental tests (Quantitative Image Analysis)

10.1 Methods

1. Capture microCT image of VB with microCT machine (Fig. 63)
2. Save microCT sequence in DICOM file format
3. Import DICOM sequence into scanIP software
4. Crop image according to ROI
5. Determine threshold (Fig. 64)
6. Create mask (Fig. 65)
7. Create a new FE model to find density related information
8. Determine material
9. Insert greyscale/density information from calibrated phantom (Table 18)
10. Based on the calibrated phantom, these corresponding greyscales can be read from the image. Thereafter, a calibration graph is made with this information (Fig. 66 and Fig. 67).

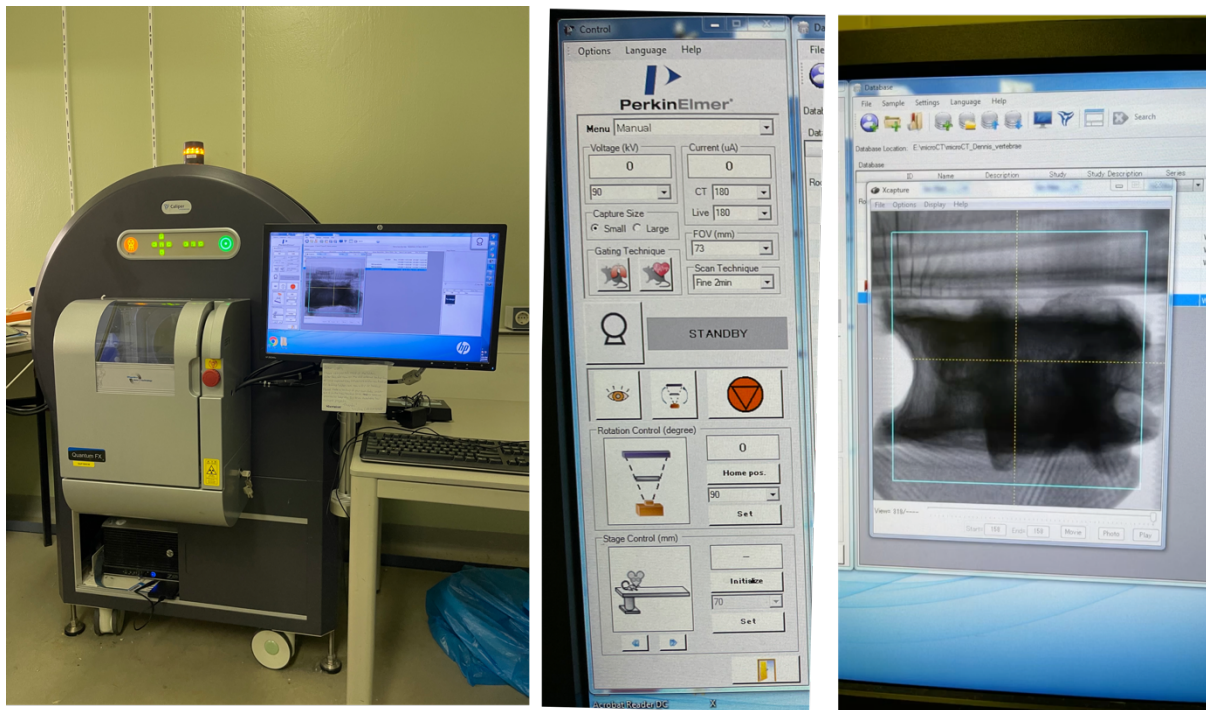


Figure 63 | microCT machine (left), microCT settings (middle), microCT preview (right)

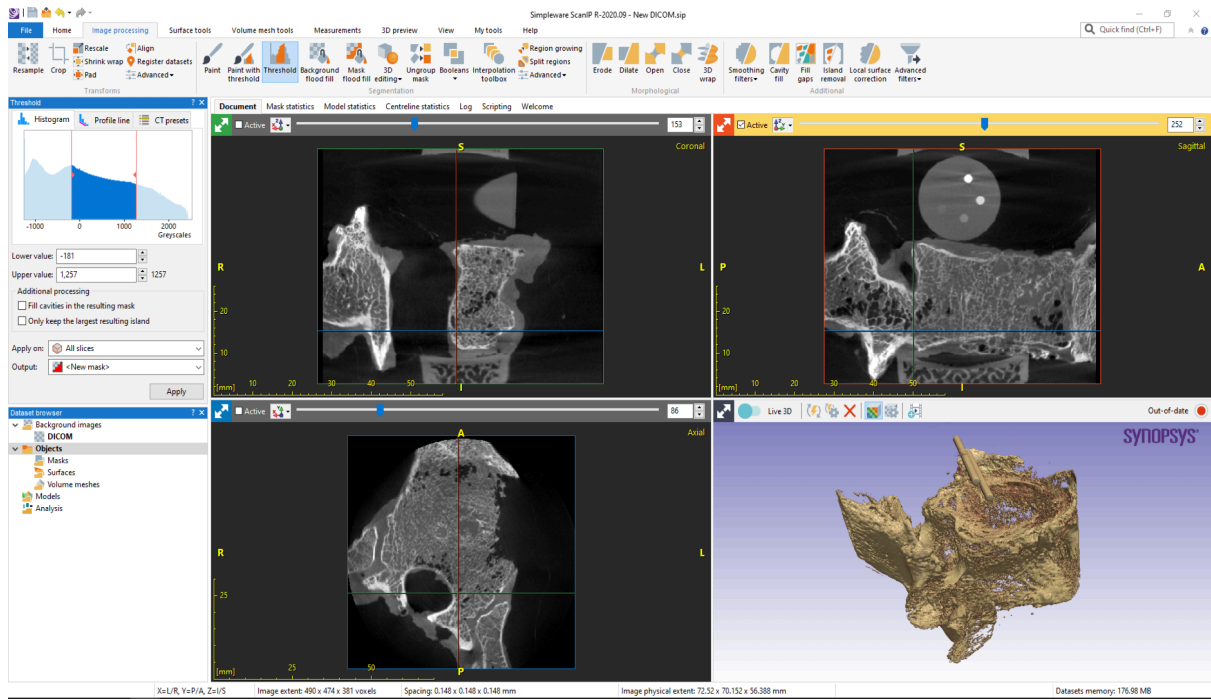


Figure 64 | scanIP threshold setup

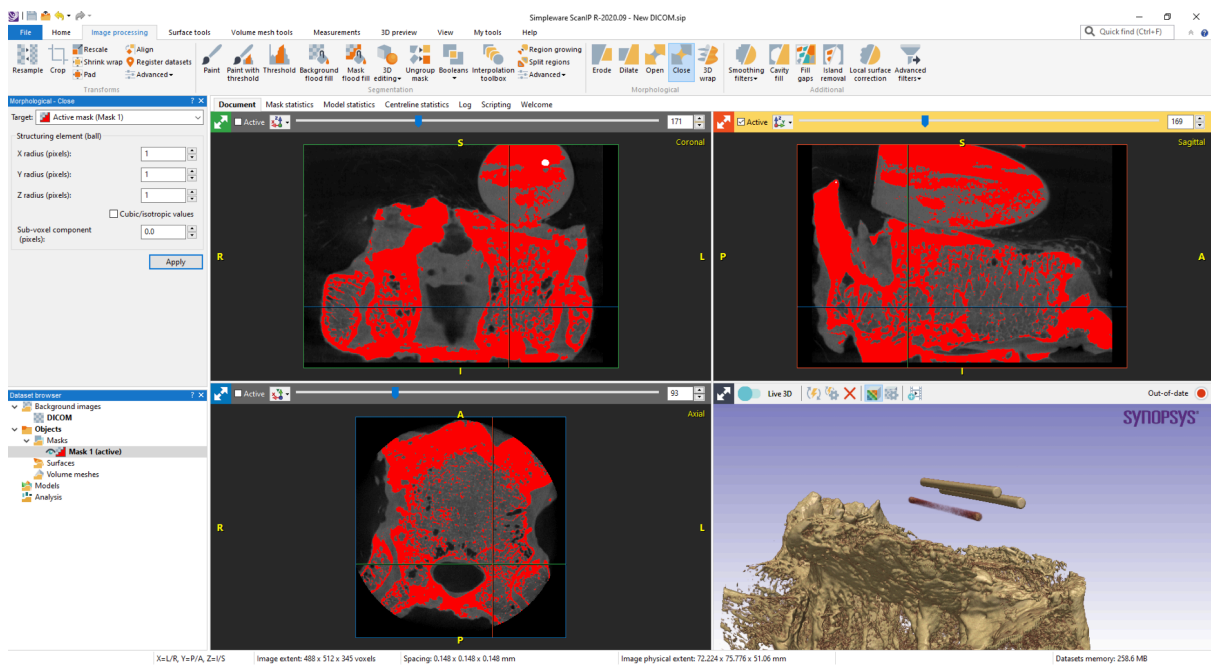


Figure 65 | scanIP mask creation

Table 18 | HA Phantom properties

Specified HA	Diameter insert	Density	Base (EP)	HA	Calibrated HA
HA 0	2.0 +- 0.1mm	1.13 g/cm ³	100.00%	0.00%	0.0 mg HA / cm ³
HA 50	2.0 +- 0.1mm	1.17 g/cm ³	95.72%	4.28%	49.7 mg HA / cm ³
HA 200	2.0 +- 0.1mm	1.26 g/cm ³	84.14%	15.86%	199.8 mg HA / cm ³
HA 800	2.0 +- 0.1mm	1.65 g/cm ³	51.20%	48.80%	802.2 mg HA / cm ³
HA 1200	2.0 +- 0.1mm	1.90 g/cm ³	36.51%	63.49%	1205.2 mg HA / cm ³

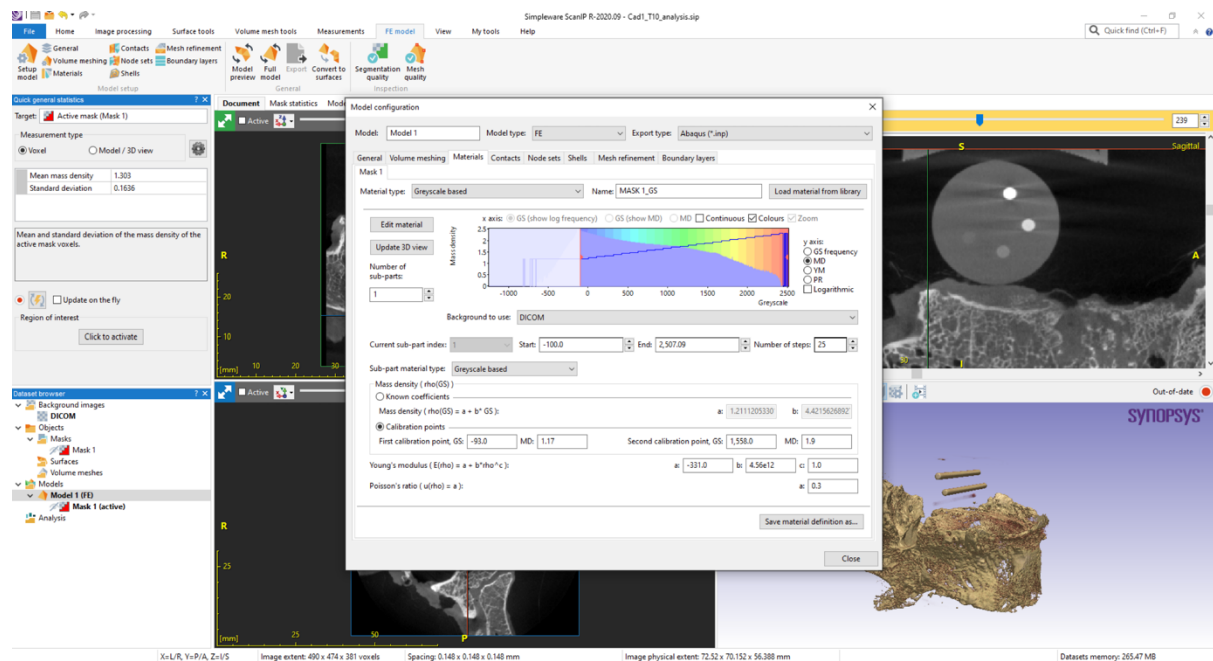


Figure 66 | scanIP HA Phantom properties setup

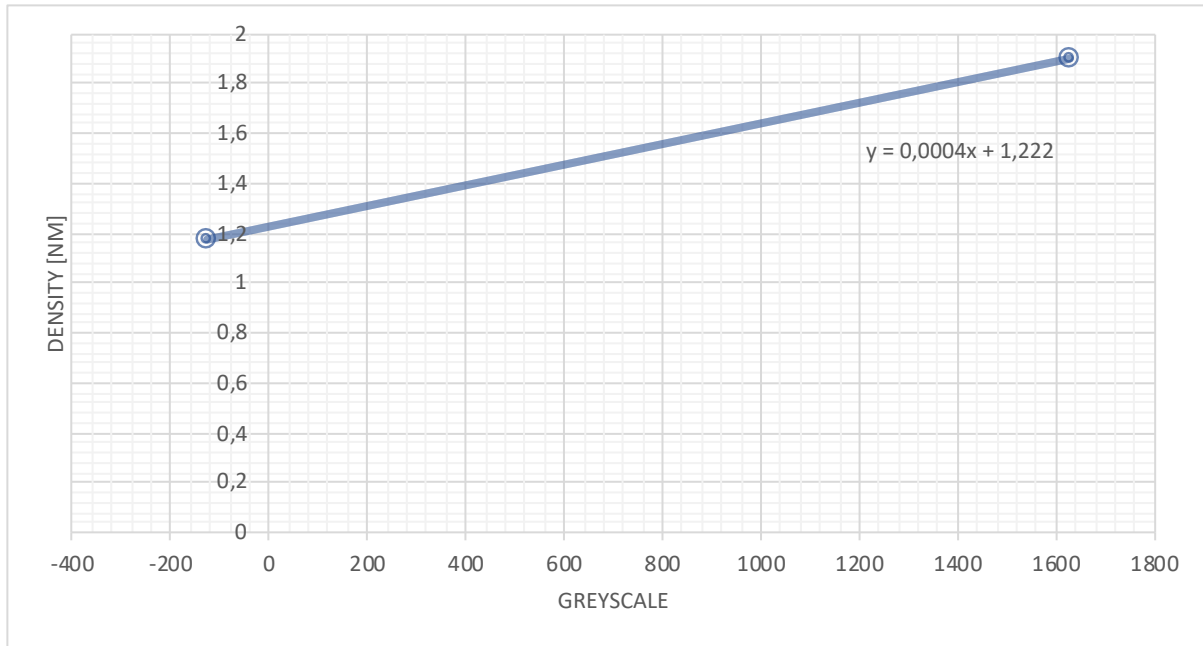


Figure 67 | Calibration graph phantom

10.2 QIA Calibration

With the help of the scanIP software, the greyscale of the phantom that was attached to each individual VB while it was scanned in the microCT machine was determined (Table 19). It is clearly visible that for the same HA values of the phantom different greyscales are provided by the DICOM³ image for each of the three VBs (T10/T11/T12), with the mean values and SD attached in the green columns on the right of Table 5. The difference in greyscale can be explained by the fact that the microCT machine does not always act linearly, which means that it adapts its highest greyscale value to the densest part of the specific microCT scan. With the results of Table 5, the three figures for T10/T11/T12 in Fig. 68 were made.

Table 19 | BMD-Greyscale calibration table of CVB T10/T11/T12

	T10		T11		T12			
HA VALUE	DENSITY	GREYSCALE	DENSITY	GREYSCALE	DENSITY	GREYSCALE	MEAN	SD
HA50	1.17	-65	1.17	-60	1.17	-120	-81.67	33.2916406
HA200	1.26	210	1.26	265	1.26	300	258.33	45.3688586
HA800	1.65	1530	1.65	1450	1.65	1200	1393.33	172.143351
HA1200	1.9	2260	1.9	1900	1.9	1600	1920.00	330.454233

³ The Digital Imaging and Communications in Medicine (DICOM) Standard specifies a non-proprietary data interchange protocol, digital image format, and file structure for biomedical images and image-related information (Bidgood et al., 1997)

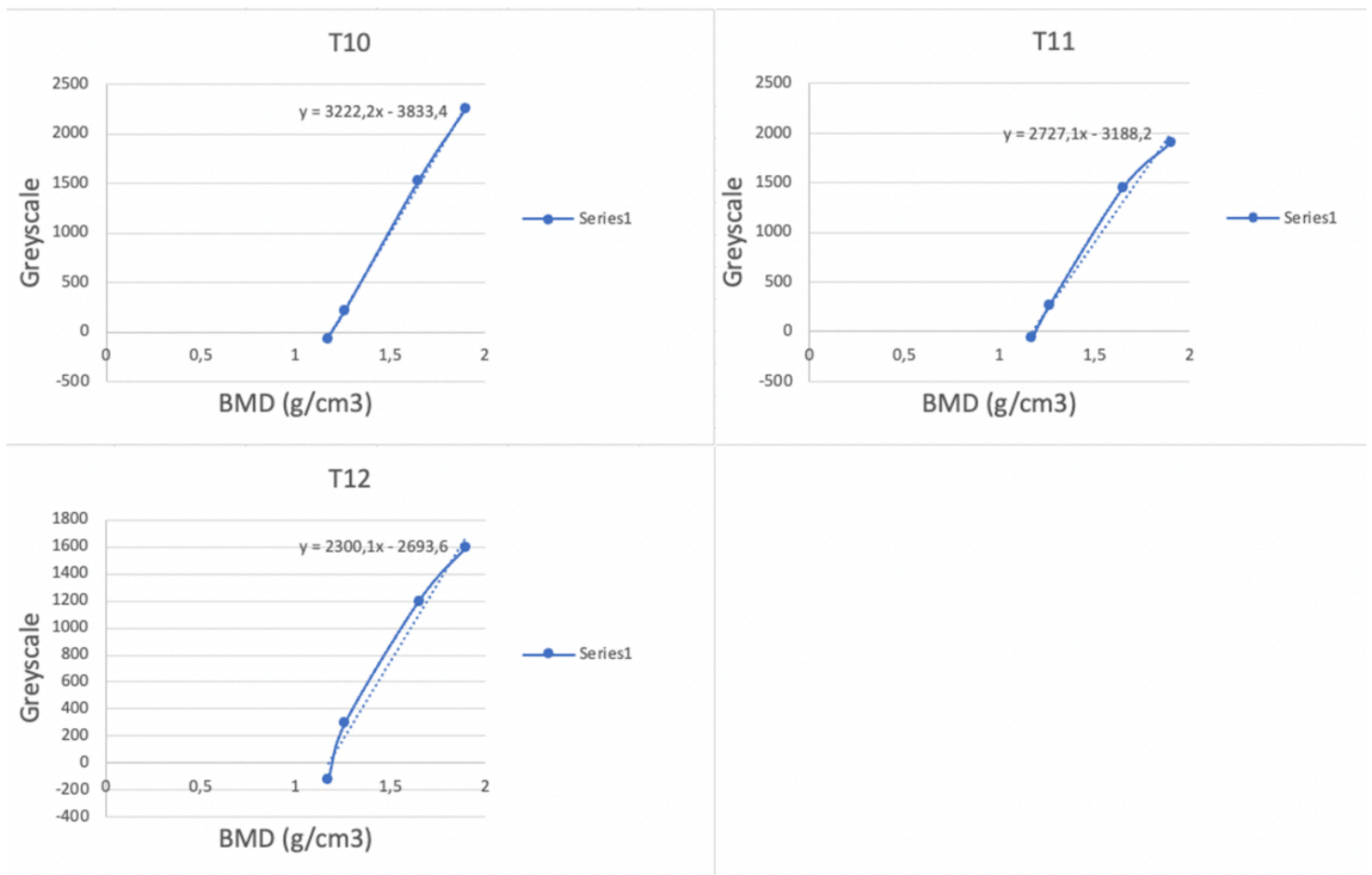


Figure 68 | Phantom calibration graphs

10.3 Materials

MicroCT machine @ UMC Utrecht

VB adapter to fixate VBs inside microCT machine

scanIP software (to perform QIA)

Calibrated phantom (Fig. 69, Datasheet: Table 20)

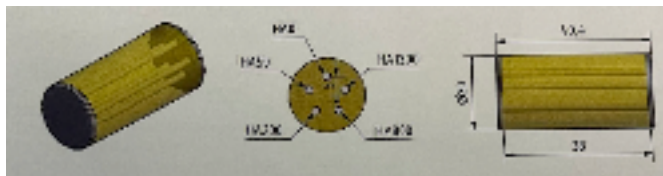


Figure 69 | HA Phantom

Table 20 | Datasheet Synthetic Bone Specimens

Description	Density [g/cm ³] (ISO 1183)	Density [PCF] (ASTM 1622)	Compressive strength [MPa] (ISO604) (ASTM-D 685)	Flexural strength [MPa] (ISO 178) (ASTM-D 790)
PCF 5	0,08	5	0,7	N/A
PCF 20	0,35	20	8-12	8-12
PCF 30	0,47	30	10-15	10-15

Appendix 11 – Risk assessment (general)

Table 21 | Risk Analysis - General

Identified hazards	Foreseeable events	Hazardous situation	Risk factor	How to mitigate the risk?
Composition of TIVAD inserter and expander: 316 SS for shafts & PLA for handles	Allergic reactions	Post-operative complications	2C	Questionnaire for the patient before the surgery with respect to allergies Evaluation of the Datasheet of the SIS by the clinical staff Adverse event reporting by the clinical staff
moving – connecting parts/components of the SIS	Remaining parts in the body of the patient Harm/injury to the patient	Safety risk for the patient	1C	No off-label use: Use according to the IFU Technical evaluation of the SIS as part of the specification of the manufacturer – complaint handling
usability-terms of use: reprocess of single-use SIS - malpractice (Cancel, 2016)	Safety of the patient	Cross-contamination between patients - infection - Safety risk for the patient if the one-way SIS is used twice too, e.g., minimize costs of surgery which is a huge cost factor of a hospital (budget) – post-operative complications	2C	Implement the one-way use of disposables into the management policy of hospitals Training of the surgery team Enhance organizational and Managerial processes (Rezaei et al., 2015) Labeling: to mention the single-use on the front page of the packaging in bold and capital letters IFU: single-use should be

				<p>stated in Capital letters, and the risks of multi-use should be disclosed to the IFU</p> <p>Complaint handling</p>
Harm to the SIS by abrasive sterilization	In compliance with the SIS	<p>Destruction/damage of the SIS surface by abrasive sterilization methods like the use of, e.g., glutaraldehyde or Chlorine dioxide gas, which is a strong oxidative gas that may corrode some materials (microstructural changes or corrosion of the surface and original feature/corrosion (Giai et al., 2016) and (Lerouge & Simmons, 2012)</p> <p>SIS mal-function and, in a worst-case scenario, failure of the surgery due to product interaction with the implant</p> <p>incorrect performance of the SIS this means failure of the SIS to perform its intended use (Rezaei et al., 2015)</p>	3C	<p>Implement the one-way use of disposables into the management policy of hospitals</p> <p>Enhance inter-departmental communication and teamworking</p> <p>Training of the Sterile department of the hospital and the surgery team - clinical staff (Rezaei et al., 2015)</p> <p>Labeling: mention on the front side of the packaging: Not to be sterilized-Single Use only” in bold and capital letters</p> <p>IFU: single-use should be stated in Capital letters</p>

Table 22 | Risk Factor Overview

Risk probability	Risk severity				
	Catastrophic A	Hazardous B	Major C	Minor D	Negligible E
Frequent (5)	5A	5B	5C	5D	5E
Occasional (4)	4A	4B	4C	4D	4E
Remote (3)	3A	3B	3C	3D	3E
Improbable (2)	2A	2B	2C	2D	2E
Extremely improbable (1)	1A	1B	1C	1D	1E

In Table 22, the three colors represent the following risks:

Green: acceptable risk

Yellow: tolerable risk

Red: intolerable risk

Table 23 | Risk factor frequency

Risk factor	Frequency
1B	4x
1C	1x
1D	1x
2B	1x
2C	4x
2D	5x
2E	1x
3C	1x
3D	2x
3E	2x

Appendix 12 – CES Edupack engineering solver plug-in

Engineering Solver

Shaft in torsion

Change situation



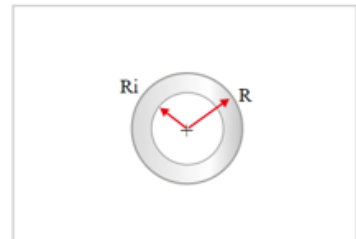
Estimates the minimum strength and stiffness values required for a shaft with the specified geometry and load conditions.

Assumptions:

- Material is homogeneous
- Shaft is straight and has uniform cross section
- Shaft is only loaded by equal & opposite twisting forces applied at its ends
- End sections are free to distort (i.e. not constrained)

Geometry

Cross-section:	Circle, hollow
Radius (R):	6 mm
Inner radius (Ri):	2.95 mm
Length (l):	150 mm



Design parameters

Torque:	4 N m
Safety factor:	2
Angle of twist:	1 deg

Results

Shear modulus	Yield strength
35.9 GPa	50.1 MPa

Figure 70 | CES Edupack Engineering plug-in, TIVAD inserter shaft

Shaft in torsion

Change situation



Estimates the minimum strength and stiffness values required for a shaft with the specified geometry and load conditions.

Assumptions:

- Material is homogeneous
- Shaft is straight and has uniform cross section
- Shaft is only loaded by equal & opposite twisting forces applied at its ends
- End sections are free to distort (i.e. not constrained)

Geometry

Cross-section:

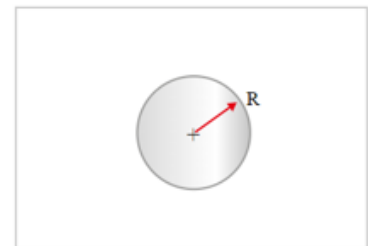
Circle ▼

Radius (R):

3 mm ▼

Length (l):

150 mm ▼

**Design parameters**

Torque:

1.5 N m ▼

Safety factor:

2

Angle of twist:

3 deg ▼

Results

Shear modulus

67.5 GPa ▼

Yield strength

141 MPa ▼

Figure 71 | CES Edupack Engineering plug-in, TIVAD expander shaft

Appendix 13 – Cost price

Table 24 | Cost price calculation (estimation)

Part	Machine costs / part	Labour costs / part	Material costs / part	Profit for Amber Implants (%)	Total cost price per part (€)
TIVAD inserter shaft	Machine costs per hour = €32 Time per part = 15 minutes $€32/4=€8$ machine costs per part	Labor costs per hour = €28 Time per part = 15 minutes $€28/4=€7$ labor costs per part	316 Stainless steel = €3,31/kg 238g * $€0,00331=€0,78$	20%	€18,94
TIVAD expander shaft	Machine costs per hour = €32 Time per part = 15 minutes $€32/4=€8$ machine costs per part	Labor costs per hour = €28 Time per part = 15 minutes $€28/4=€7$ labor costs per part	316 Stainless steel = €3,31/kg 50g * $€0,00331=€0,16$	20%	€18,94
TIVAD inserter handle	Machine costs per hour = €0,52 Print time = 7 hours $7 \times €0,52 = €3,74$	Labour costs per print = €3,00 Labor for 3D printing is only loading 3D print information to a 3D printer and starting the 3D print. During the	€21/kg $€0,03/g$ Handle = 22g $22g \times €0,03 = €0,66 / \text{handle}$	20%	€9,00

		print process, no labor is required			
TIVAD expander handle	Machine costs per hour = €0,52 Print time = 7 hours 7 x €0,52 = €3,74	Labour costs per print = €3,00 Labor for 3D printing is only loading 3D print information to 3D printers and starting the 3D print. During the print process, no labor is required	€21/kg €0,03/g Handle = 22g 22g x €0,03 = €0,66 / handle	20%	€9,00

Appendix 14 – Technical drawings

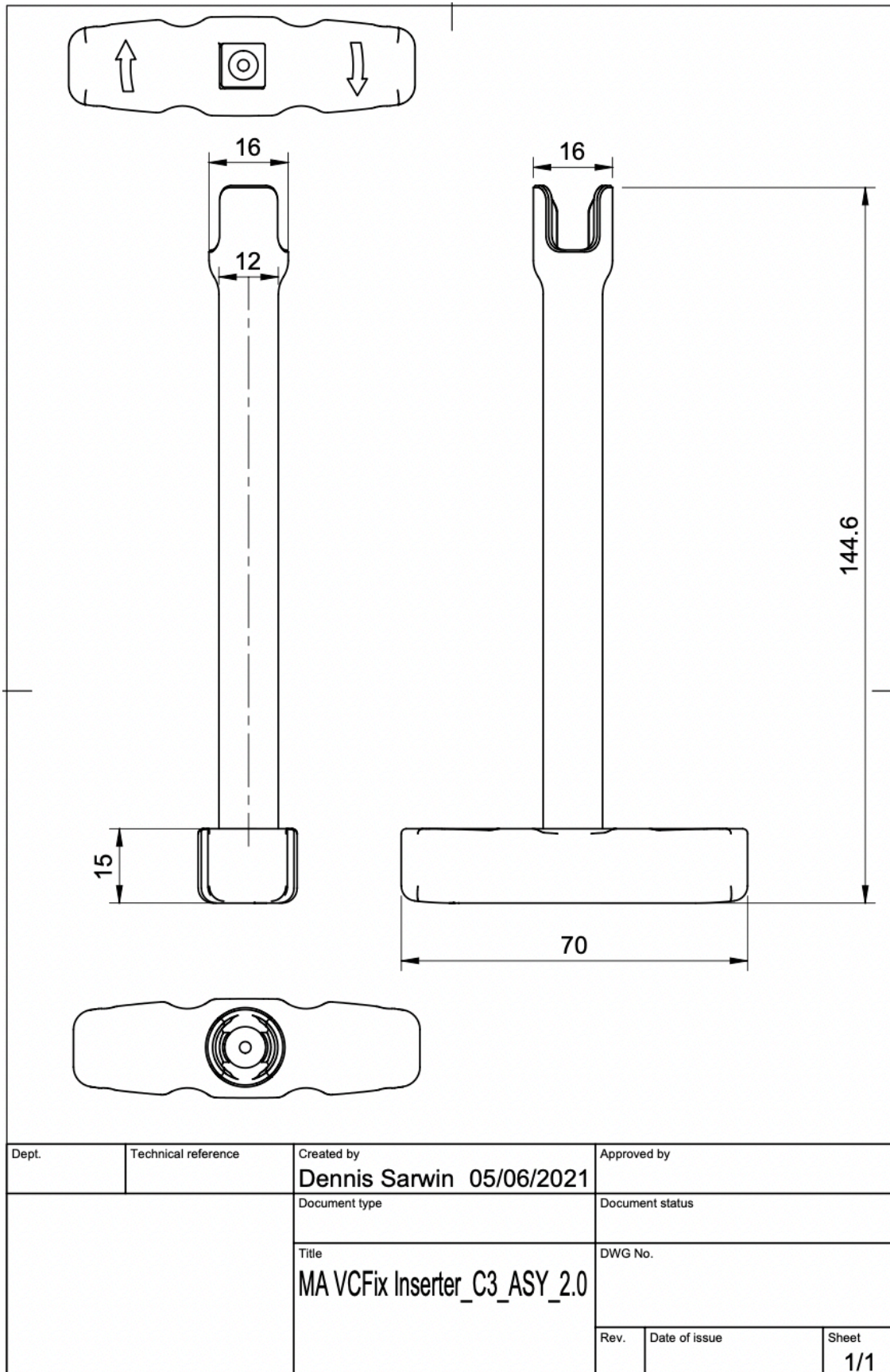


Figure 72 | TIVAD Inserter technical drawing

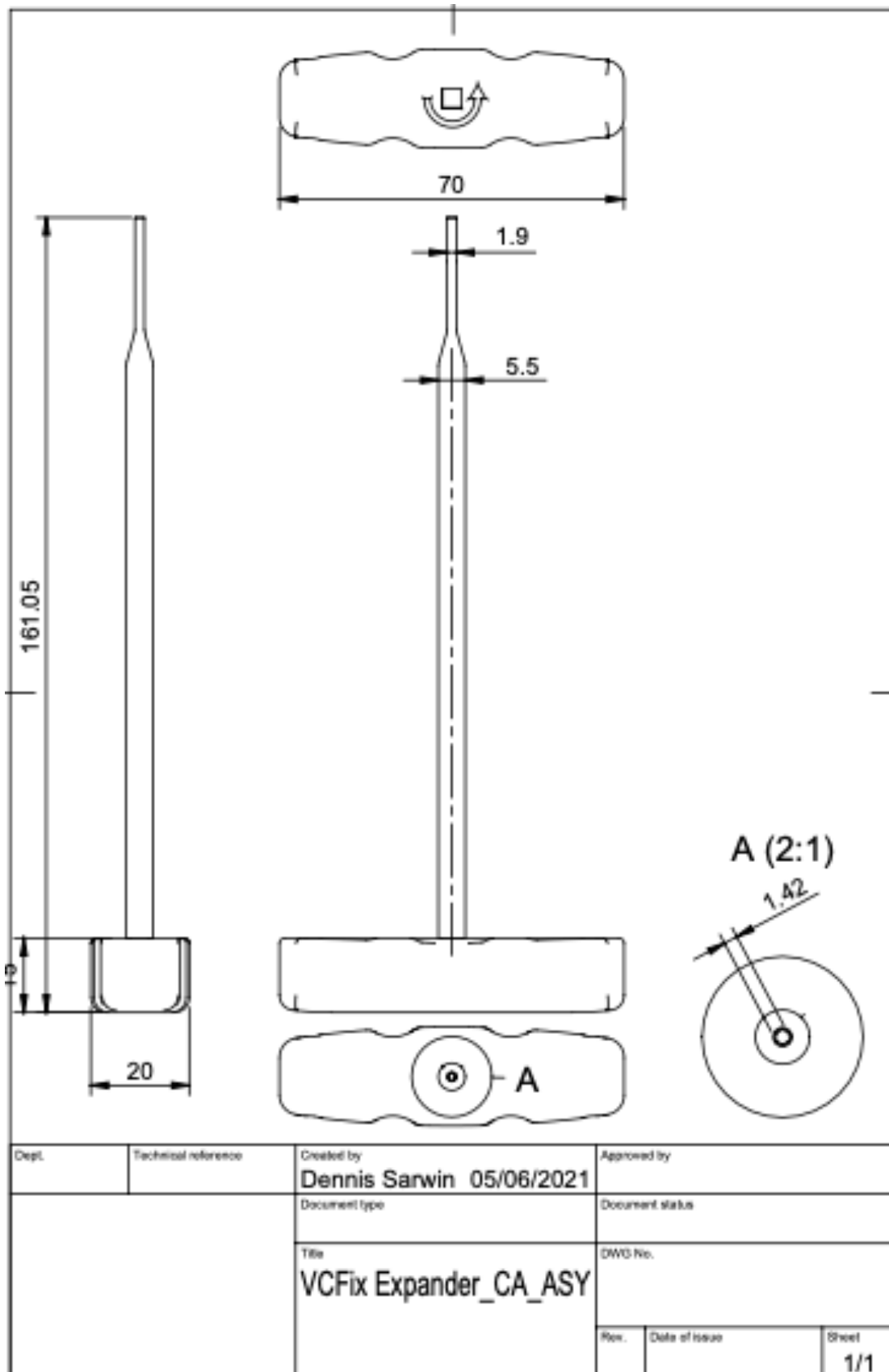
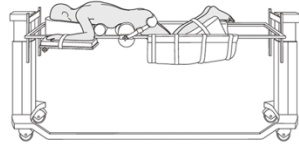


Figure 73 | TIVAD Expander technical drawing

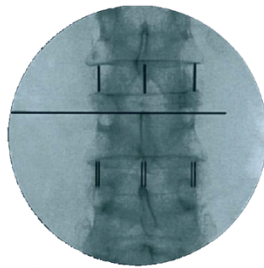
Appendix 15 – Surgical technique

1. PATIENT POSITIONING

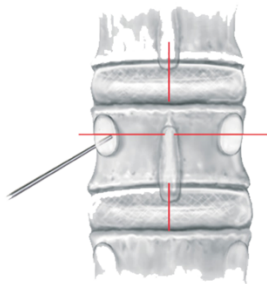


1a) Position the patient in the prone position. A/P and lateral fluoroscopy should be used to provide proper imaging.

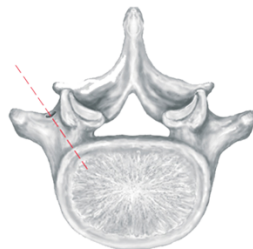
2. APPROACH



2a) Attain an A/P fluoroscopy image with spinous process aligned and end plates parallel to each other.

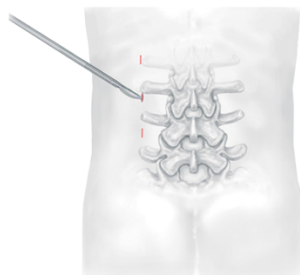


2b) Verify the lateral edge of the pedicle ovals are close to the lateral edge of the vertebral body.



2c) The top of the ovals for both pedicles should be parallel and equidistant from the end plate.

3. ACCESS



3a) Locate and make the first incision as defined in the incision planning step. The incision is approximately 15mm in length to match the diameter of the MIS Dilator.

4. MIS DILATOR INSERTION



4a) Insert MIS Dilator through the incision in the skin carefully through the soft tissues all the way till the tip of the MIS Dilator touches the posterior surface of the pedicle at the lateral edge of the pedicle ovals where the cavity for the TIVADt will be made.

5. CREATE VB ACCESS



5a) Insert assembled two-part Jam-Shidi needle into 1/3 of VB.



5b) Remove inner Jam-Shidi needle part.



5c) Insert K-wire into hollow outer Jam-Shidi needle up to 1/2 of VB.



5d) Remove outer Jam-Shidi needle. Repeat step 5a till 5e for the second TIVAD in the other pedicle.

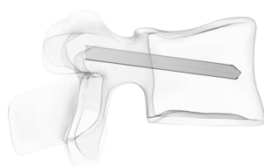
6. CREATE TIVAD CAVITY



6a) Slide cannulated drill over the K-wire to start the drill process into the vertebral body.



6b) Drill until maximum TIVAD depth is reached, be cautious that anterior VB wall is not penetrated.



6c) Once the desired depth is reached the drill and the K-wire can be retracted, leaving the clean cavity for the next step: the TIVAD insertion. Repeat step 6a till 6b for the second TIVAD in the other pedicle.

7. TIVAD INSERTION

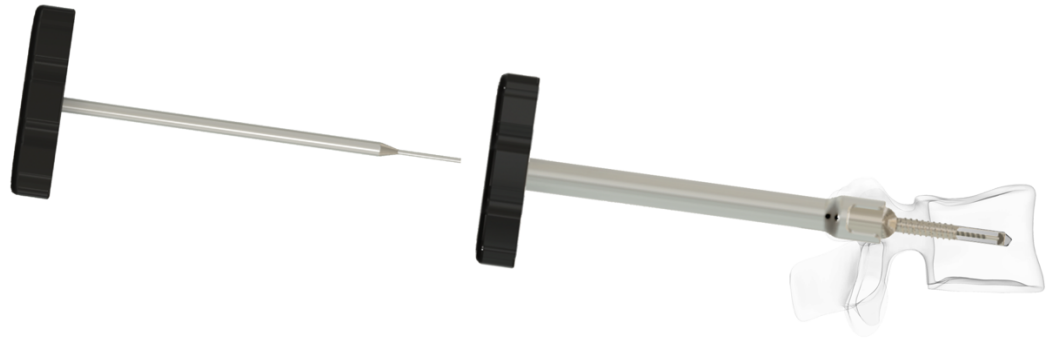


7a) Insert TIVAD inserter with TIVAD into cavity until threaded part touches trabecular bone.



7b) Rotate TIVAD inserter clockwise until desired depth is reached with TIVAD inside fractured VB, monitor insertion process with fluoroscopy.

8. TIVAD EXPANSION



8a) Once desired depth is reached, insert the TIVAD expander through the TIVAD inserter's channel. Push all the way forward until successfully attached to TIVAD's expansion screw.



8b) After successful attachment, rotate TIVAD expander counter-clockwise until desired TIVAD expansion is reached. Monitor expansion process via fluoroscopy.

9. REMOVAL OF TIVAD INSERTER & EXPANDER



9a) After successful TIVAD expansion, detach and retract both the TIVAD expander and then the TIVAD inserter from the TIVAD. Ultimately, retract the MIS dilator.

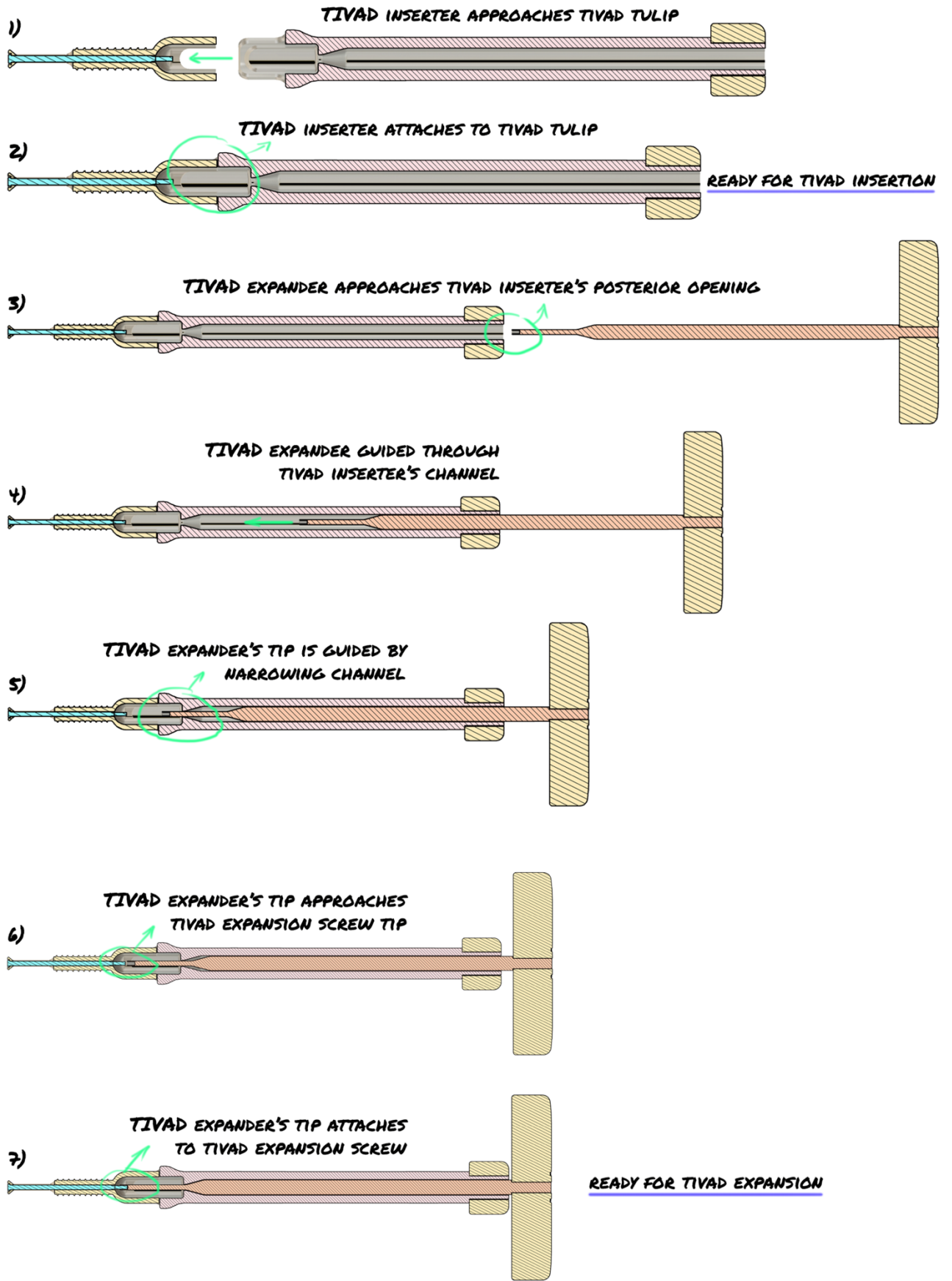


Figure 74 | TIVAD inserter & expander workflow